Master Degree Program of Biomedicine

May 2018

High fat diet exposure during different life stages in mice and consequences for metabolic programming in the liver

Laila Høydalsvik

Faculty of Health Sciences

Department of Life Sciences and Health

OsloMet – Oslo Metropolitan University

Laila Høydalsvik

High fat diet exposure during different life stages in mice and consequences for metabolic programming in the liver

Master Degree Program of Biomedicine

Faculty of Health Sciences

Department of Life Sciences and Health

OsloMet – Oslo Metropolitan University

Performed at

Norwegian Institute of Public Health

Department of Toxicology and Risk Assessment

Advisors: Birgitte Lindeman, Nur Duale and Inger-Lise Steffensen

Thesis submitted for Master Degree, 60 ECTS

May 2018

Acknowledgement

The work presented in this master thesis was performed at the Norwegian Institute of Public Health (NIPH) from March 1 2017 until May 21 2018. The gene expression and Luminex analysis were performed in the laboratory of Department of Toxicology and Risk Assessment at NIPH. The lipid class analysis was performed by Vitas AS, Oslo, Norway. The project has been part of the master degree program in biomedicine. My main advisors were Dr. Birgitte Lindeman and Dr. Nur Duale, and Dr. Inger-Lise Steffensen was my co-advisor. Maria Amberger trained me to get started in the gene expression work-flow, and Else-Carin Groeng assisted me in performing the Luminex analysis.

First of all I want to thank the totally wonderful people Birgitte, Nur and Inger-Lise for giving me the opportunity to do my thesis in their department, while I have also been working. They have organized time and work to make this possible for me, so I am forever grateful that you made it possible for me to complete my master degree. Secondly I want to thank them for sharing their knowledge and brilliant expertise with me in the most pleasant and caring way, and patiently answered my strange and numerous e-mails during the whole process.

A warm thank to Maria and Else-Carin for showing me around in the lab. I also want to thank everyone at NIPH for always making me feel welcome.

My employer has also given me the opportunity to study while working, and I am very grateful for this opportunity.

Finally I want to thank my children and parents; for each and one in their different ways have supported me this year. Thanks to friends, and especially thank you to Gro, Berit, Kristin, Ole Anders, Inger and little brother Espen for supporting me in ways that were needed at the time.

Abstract

Non-alcoholic fatty liver disease (NAFLD) is the most common chronic liver disease in the world, and is the hepatic manifestation of the metabolic syndrome. Obesity is closely associated with NAFLD. The concept of fetal programming, known through Barker's hypothesis and the Developmental Origins of Health and Disease (DOHaD) approach, suggests that early life environment has consequences for adult health. The contribution of maternal and early life influences on development of NAFLD is less understood, and would be of importance to be able to point to intervention measures to improve public health. The main objective of this master thesis was to assess which NAFLD-related signaling pathways are affected after exposure to a HFD during five different life stages in liver of adult mice. The animal material used in this thesis originated from a mouse obesity study conducted at the Norwegian Institute of Public Health in 2014. The mice were divided in five HFD exposed groups fed a 45% fat diet (45% kcal from fat); *in utero* (IU), during lactation (LA), *in utero* and lactation (IU+LA), during whole life from *in utero* to adulthood (WL) and only as adult (AD). The results were compared with control group on normal 10% fat diet (CTL). In mice livers, four lipid classes to assess lipid accumulation were measured by high pressure liquid chromatography, and a Luminex assay was applied to measure insulin-like growth factor 1 (IGF-1) protein expression in serum samples. Further; liver samples were used to analyze the relative expression of 69 genes involved in NAFLD signaling pathways through RT-qPCR. Mild liver steatosis (TAG above 5%) was observed in 38% of the animals in the IU+LA and WL groups compared to none in the CTL and IU groups and 8% in LA and AD groups. An increase of serum IGF-1 protein expression was suggested in the IU and WL groups; indicating implication of organ growth for these groups. The gene expression analysis gave three genes with significantly higher ($p<0.05$), *Il10*, *Pparδ and Slc2a2*, and four genes with borderline significantly higher ($p<0.1$), *Hnf4a*, *Insr*, *Tnfrsf1a* and *Nfe2l2* expression compared to the CTL group. These genes act in several signaling pathways related to NAFLD, and are involved in lipid metabolism, oxidative stress, insulin and glucose regulation, inflammation and organ developments. Thus, this study suggests a modification of several of the major NAFLD signaling pathways in one or more of the HFD exposed groups. The results also propose that the early life period is a phase of increased susceptibility for the risk of development of liver steatosis and NAFLD, in line with the DOHaD hypothesis.

Sammendrag

Non-alkoholisk fettlever (NAFLD) er den mest utbredte kroniske leversykdom i verden, og er den hepatiske manifestasjonen av det metabolske syndromet. Fedme er nært knyttet til NAFLD. Konseptet om føtal programmering, kjent under Barker-hypotesen og senere Developmental Origins of Health and Disease (DOHaD) foreslår at miljøet under fosterlivet og tidlig post-natal fase har konsekvens for helsen som voksen. Hvilken påvirkning miljøet har for foster og tidlig i livet med tanke på utvikling av NAFLD er uklart, og det vil være viktig å kunne gjøre tiltak for å forbedre befolkningens helse. Hovedmålet i denne masteroppgaven var å evaluere hvilke NAFLD-relaterte signalveier i leveren som påvirkes etter eksponering av fettholdig diett i fem ulike livsstadier i mus. Dyrematerialet som ble brukt i denne oppgaven stammer fra et musefedme-studie utført ved Folkehelseinsituttet i 2014. Musene ble delt opp i fem grupper som så ble eksponert for 45% fettholdig diett (45% kalorier fra fett); i uterus (IU), under amming (LA), i uterus og amming (IU+LA), gjennom hele livet (WL) og kun som voksen (AD). Resultatene ble sammenlignet med en kontrollgruppe som fikk normal diet med 10% kalorier fra fett (CTL). I muselever ble fire lipid grupper analysert for evaluering av fettinhold i lever ved hjelp av væskekromatografi, og Luminex-analyse ble benyttet til å måle insulin-like growth factor 1 (IGF-1) protein ekspresjon i serumprøver. Videre ble den relative gen ekspresjonen for 69 gener involvert i NAFLD signalveier analysert i leverprøver ved RT-qPCR. Mild leversteatose (TG over 5%) ble observert i 38% av musene i IU+LA og WL gruppene sammenlignet med ingen i CTL og IU gruppene og 8% i LA og AD gruppene. En økning av serum IGF-1 protein ekspresjon ble foreslått i IU og WL gruppene. Funnet indikerer implikasjoner av organvekst for disse gruppene. Gen ekspresjon analysene ga tre gener (*Il10*, *Pparδ* og Slc2a2) med signifikant høyere ($p<0.05$) og fire gener (*Hnf4α*, *Insr*, *Tnfrsf1a* og *Nfe2l2*) med grensesignifikant høyere ($p<0.1$) ekspresjon sammenlignet med CTL. Disse genene bidrar i flere signalveier relatert til NAFLD, og er involvert i lipid metabolisme, oksidativt stress, insulin og glukose regulering, betennelse og utvikling av organer. Derav foreslår dette studiet en modifisering av flere viktige NAFLD signalveier i en eller flere av gruppene eksponert for fetthold diett. Resultatene antyder også at eksponering i tidlige livsfaser øker disposisjonen for risiko for utvikling av leversteatose eller NAFLD; som også er i tråd med konseptet om føtal programmering og DOHaD.

Abbreviations

AD	Adult
ALW	Absolute liver weight
ANOVA	Analysis of variance
AOP	Adverse outcome pathway
APC	Adenomatous polyposis coli
BAT	Brown adipose tissue
BMI	Body mass index
CAT	Catalase
cDNA	Complementary DNA
CE	Cholesterol esters
Cq	Quantification cycle
CT	Cycle threshold
CTL	Control
CV%	Coefficient of variation in %
DAG	Diacylglycerol
DIO	Diet-induced obesity
DNA	Deoxyribonucleic acid
dNTPs	Deoxynucleotides triphosphates
DOHaD	Developmental Origins of Health and Disease
dT	Deoxythymine
E	PCR efficiency
ELISA	Enzyme-linked immunosorbent assay
ELSD	Evaporative light scattering detector
FABP4/A	Fatty acid binding protein 4/A
FC	Free cholesterol
FD	Fold difference
FFA	Free fatty acids
GH	Growth hormone
HDL	High density lipoproteins
HFD	High fat diet

HNF4α	Hepatocyte nuclear factor 4 alpha
IGF-1	Insulin-like growth factor 1
IGF-2	Insulin-like growth factor 2
IR	Insulin resistance
IU	*In utero*
IVC	Individually ventilated cages
KEGG	Kyoto Encyclopedia of Genes and Genomes
LA	Lactation
LDL	Low density lipoprotein
LOD	Limit of detection
mRNA	Messenger ribonucleic acid
NAFLD	Non-alcoholic fatty liver disease
NASH	Non-alcoholic steatohepatitis
Nfe2l2	Nuclear factor, erythroid derived 2, like 2
NF-κB	Nuclear Factor-Kappa B
NGS	Next generation sequencing
NIPH	Norwegian Institute of Public Health
NP-HPLC	Normal phase high-performance liquid chromatography
NRT	Reverse transcriptase control
NTC	No template control
OECD	Organization for Economic Co-operation and Development
PAI-1/Serpin E1	Plasminogen activator inhibitor-1/Serpin E1
PDGF-BB	Platelet derived growth factor-BB
PPAR	Peroxisome proliferator activated receptor
qPCR	Quantitative polymerase chain reaction
RFU	Relative fluorescence units
RIN	Ribonucleic acid integrity number
RLW	Relative liver weight
RNA	Ribonucleic acid
RNase	Ribonuclease
ROS	Reactive oxygen species
rRNA	Ribosomal RNA

RT	Reverse transcriptase (enzyme)
RT-qPCR	Reverse-transcription quantitative polymerase chain reaction
RXRα	Retinoid X receptor alpha
SE	Standard error
SOD	Superoxide dismutase family
TAG	Triacylglyceride
TBW	Terminal body weight
TE	Tris-EDTA
Tm	Melting temperature
TNFα	Tumor necrosis factor alpha
VAT	Visceral adipose tissue
VLDL	Very low density lipoprotein
WAT	White adipose tissue
WHO	World Health Organization
WL	Whole life

See primer list in Appendix A4 Table A.1 for full gene names

Contents

Table of Contents

1. Introduction

Non-alcoholic fatty liver disease (NAFLD) is the most common liver disease in the world. The incidence of NAFLD is increasing worldwide and is considered the hepatic manifestation of obesity and metabolic syndrome (1, 2). This master project is an extended study of high fat diet (HFD) effects on mice performed at the Norwegian Institute of Public Health (NIPH) in 2014 (3). The study examines the effect of HFD exposure during different life stages in mice to see if and what repercussions this might have on metabolic programming of signaling pathways involved in NAFLD later in life.

1.1 Overweight and obesity

1.1.1 Prevalence and definitions of obesity

NAFLD is closely associated with obesity and was first described in 1980 by the Mayo Clinc (4, 5). The current prevalence of overweight and obesity are increasing all over the world and harms the life quality and health of people (6). The rate of obesity has more than doubled over the past 20 years in most OECD countries (countries member of the Organization for Economic Co-operation and Development forum) (7). NIPH communicates through their website that today about 25% of young people in Norway are overweight or obese, and about 25% of men and 20% of women between 40-45 years are obese (8). Studies have suggested obesity to be defined as an excess accumulation of adipose tissue, and obesity have been connected to increased morbidity and mortality due to increased risk of diabetes mellitus type 2, cardiovascular disease, chronic kidney disease, musculoskeletal disorders and cancers (9, 10). Obesity is an important element in development of the metabolic syndrome, which can be defined as coexistence of several factors in the same individual, such as hyperglycemia, dyslipidemia, and hypertension (11, 12). Obesity is most commonly defined by body mass index (BMI) which equals the ratio of weight in kilograms divided by height in meters squared (kg/m^2). The classes of BMI advised by World Health Organization (WHO) are: 18.5-24.9 kg/m^2 for normal, 25.0-29.9 kg/m^2 for overweight and >30 kg/m^2 for obesity (13).

1.1.2 Obesity risk factors

A review of publications from 1976 to 2016 from the Nurses' Health Study in USA with focus on obesity, proposed that determinants of obesity included dietary factors (especially energy dense diets due to e.g. high intake of, sugar-sweetened beverages/fruit juices, saturated fat and trans fat), low physical activity (<30 minutes per day) and short sleep duration (<7-8 hours per night) (14). Several studies in humans have shown that during early development the response to maternal obesity established an early-life programming in the offspring, that increased the risk of metabolic disorders such as obesity later in life (15, 16). Eleven years of genome-wide association studies have provided data to investigate the connections between genetic variants to prediction of diseases such as obesity. These studies are still ongoing (17, 18). The challenge lies in understanding if the cause is due to nature or nurture. Some human studies suggested that heritable factors might predetermine body fat distribution and that differences in BMI in adult life were to a high degree inherited (19, 20). Obesity stands out as the dominant disorder in children all over the world, and predisposes children to diabetes, hypertension, hyperlipidemia, cardiovascular disease and liver disorders (21). Development of obesity among children can be caused by many factors in their life, such as heritage, genetic factors, lifestyle and availability to a healthy environment (21). Figure 1.1 shows an overview of suggestions of possible elements that might have effect on development of obesity

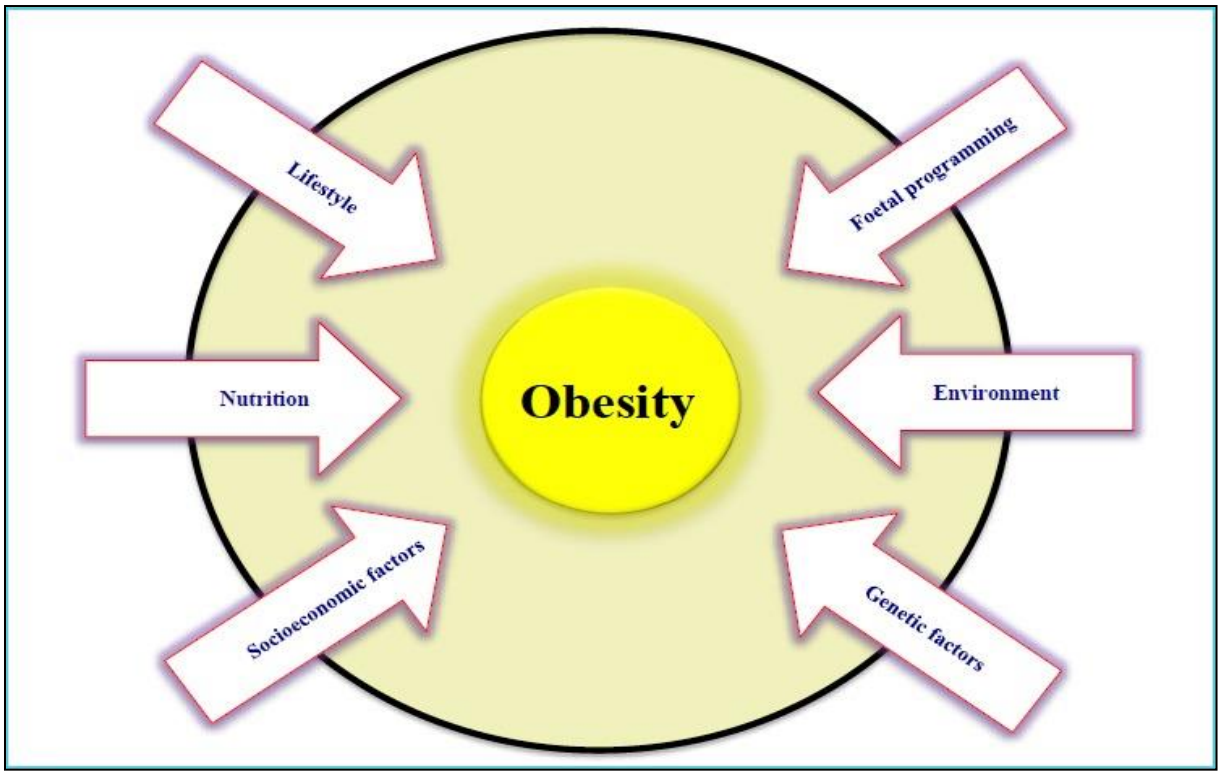

Figure 1.1: Risk factors for development of obesity in children. Figure used with permission from Levy et al. 2017(21).

There is a clear focus from WHO to reduce obesity in children because obese children are at higher risk of being obese as adults with increased risk diseases in adulthood (22). A review proposed that several studies have linked high childhood BMI with diabetes, coronary heart disease and some types of cancers as adults. When assessing the risk of adult morbidity there were only moderate risks, and it seemed like most of the adult obesity-related morbidity appeared also in patients that were of healthy weight in early life (23). In this master thesis, the effects of HFD during early life stages as a risk factor for NAFLD, as a metabolic dysregulation, have been studied

1.2 Non-alcoholic fatty liver disease (NAFLD)

1.2.1 The pathogenesis of NAFLD

NAFLD is the most common type of chronic liver disease, and is found in 17-30% of the Western population and 2-4% of the worldwide population (24). For children from a general population, a review suggested that the pooled mean prevalence was approximately 8-34% (25). A study found that even non-obese humans also had developed NAFLD, and that the paradigm of NAFLD regarded as the hepatic manifestation of metabolic syndrome can prove to be outdated (26).

NAFLD is a spectrum of disorders from simple steatosis to non-alcoholic steatohepatitis (NASH) to cirrhosis. Liver steatosis can be defined as the accumulation of triacylglycerides (TAG) within hepatocytes that exceeds 5% of liver weight in the absence of excessive significant alcohol consumption, other liver diseases or the consumption of steatogenic drugs (24, 27-29). A study found that in some cases the patients with simple steatosis progressed into NASH, which is characterized by hepatocyte necrosis and inflammation. Further they found that the liver disease may further progress to liver cirrhosis (27). In 2015 Ahmed outlined in an article the following classification and grading of NAFLD showed in Table 1.1 (30).

Table 1.1: NAFLD as a spectrum of disorders. NAFLD can be classified by severity according to amount of fat deposition and hepatocyte expression in liver biopsy. Table modified from Ahmed 2015 (30).

NAFLD classification type	
Type 1	Simple steatosis
Type 2	Steatosis + inflammation (lobular and portal)
Type 3	Steatosis + ballooned hepatocytes – NASH
Type 4	Steatosis + fibrosis – NASH
Grades of hepatic steatosis	
Normal	Less than 5% of hepatocytes are affected
Grade 1 (mild)	5 to 33% of hepatocytes are affected
Grade 2 (moderate)	34% to 66% of hepatocytes are affected
Grade 3 (severe)3	More than 66% of hepatocytes are affected

There have been many discussions in the field about what developmental model of NAFLD to agree upon. The two-hit hypothesis has been the traditionally agreed model launched by Day and James in 1998 (31, 32). The first hit was viewed as the accumulation of TAG in hepatocytes which made the liver vulnerable to further disturbances, and the second hit lead to steatohepatitis by factors such as oxidative stress, lipid peroxidation, decreased mitochondrial function, gut-derived endotoxins and inflammation (31, 33, 34).The multi-hit hypothesis was a newer model suggested in 2010 (34). This model proposed that many factors could hit at the same time and create a harmful road that led to NASH. The factors could be insulin resistance (IR), lipotoxicity from free fatty acids (FFA) and cholesterol, gut-derived signals, adipose tissue derived signals, genetic background of the patient and HFD (33-35). A review looked at numerous studies from both animal models and humans about

connections of IR, adipocytokines and adipose tissue inflammation, and proposes that multiple factors hit at the same time from adipose tissue and the gut promotes liver inflammation (35). Figure 1.2 shows NAFLD viewed as a pathogenic disease depending on a number of factors or causes (35).

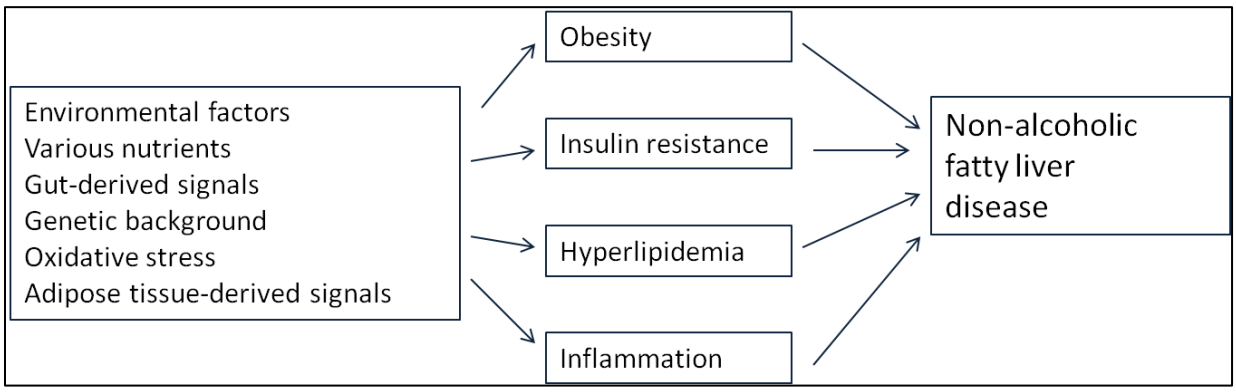

Figure 1.2: Multi-hit hypothesis for development of NAFLD. Overview of possible interactions between factors in the development of non-alcoholic fatty liver disease (NAFLD). Figure modified from Alam et al. 2016 (35).

1.2.2 Fetal programming of NAFLD

A study pointed out the concern of the prevalence of NAFLD increasing among children and adults, and that the patients were being diagnosed at younger ages (36). The contributions of gestational and early life influences on development of NAFLD are less understood (37). In a human study the results indicated that the fetus experienced a critical period of plasticity during pregnancy and the fetus might have been significantly influenced by environmental factors such as maternal nutrients (38). The concept of fetal programming is well founded in the literature through the famine during the Dutch Hunger Winter, known as the Barker hypothesis (39). The offspring of mothers who were exposed to famine gave birth to babies with lower birth weight. As also confirmed by another study they were subsequently at increased risk of cardiovascular diseases and other health issues such as increased BMI and prevalence of type 2 diabetes mellitus in adulthood (39, 40). While the Barker study disclosed fetal programming by undernutrition, later studies have shown that maternal HFD also give similar long-term programming of offspring disease risk (41). The Barker hypothesis laid the foundation of the Developmental Origins of Health and Disease (DOHaD) hypothesis. Newer studies have also identified other diseases that can originate from fetal under- or overnutrition such as mental health, immunological and reproductive illnesses (42). Epigenetics has been found to be a part of fetal programming (43). There is evidence that epigenetics might, through different responses to diet, cause development of chronic

diseases later in life (44). The fetus may be vulnerable to liver steatosis because the immature fetal adipose depots are not able to buffer excess transplacental lipid delivery in maternal obesity (45). Studies in mice demonstrated that offspring from dams fed obesogenic diet during pregnancy and lactation were prone to develop hepatic steatosis (46). Furthermore, another study showed that offspring of diet-induced obese dams had disrupted liver metabolism and developed NAFLD prior to any differences in body weight or body composition (47). It is thus important to investigate the molecular alterations in the liver of adult offspring to elucidate the effects of developmental overnutrition on metabolic programming of liver metabolism (46).

1.3 The role of HFD and diet-induced obesity models

Diet-induced obesity (DIO) has become one of the most used models in rodents for understanding what effects obesity could have for metabolic diseases (48). The mouse model of DIO was used in this study. The DIO model provides crucial information regarding causalities between HFD/obesity and risk of disease. Uses of mice in medical science have proven useful because like humans, mice are mammals, with important similarities in immune responses and hormone (endocrine) systems as humans. They are also one of the first species – along with humans, to have their complete genome sequenced. From this we have learned that they share approximately 80% of their genes with us (49). The mouse provides a rich resource of genetic diversity combined with possibilities for genome manipulation, and is therefore a powerful application for modeling human diseases and processes (50). Mice have short pregnancies and large litter sizes that facilitate the opportunity to create own modified mice. C57BL/6J is the most widely used inbred strain of mice and the first to have its genome sequenced. It is a permissive background for maximal expression of most mutations. The C57BL/6J mice are susceptible to DIO and a commonly used DIO model (51).

The phenomenon known as “early-life programming” acknowledges that *in utero* milieu has long term repercussions on risks of disease later in life (52). Obese pregnant mothers may transmit their metabolic phenotype to their offspring, leading to obesity and diabetes over generations. Dams fed a HFD have shown significantly changed hepatic lipid levels and messenger ribonucleic acid (mRNA) levels of genes involved in lipid metabolism (53). A study indicated that early overnutrition program offspring to more harmful response to HFD later

in life (54). A study showed greater weight gain, higher adiposity and higher food intake in mice offspring from obese dams compared to control dams fed standard chow. The mice also showed impairment on insulin signaling in central and peripheral tissues (55). Another study showed that unbalanced maternal diet, such as HFD during fetal development, is likely to induce metabolic abnormalities in offspring (56). HFD *in utero* and early life has been suggested to impact the development of NAFLD in offspring; and a study have shown that obesogenic diets during pregnancy and lactation were associated with the development of fatty liver in offspring (57). A human study showed that cells from umbilical cord had alterations in gene expression that may promote inflammation and development of metabolic disease in offspring (58). Convincing evidence supported by a large number of animal studies shows that HFD during pregnancy builds a pro-inflammatory intrauterine environment (59). Figure 1.3 visualizes how the transfer of energy, hormones, central molecules as cytokines and altered blood supply can lead to disturbed fetal development and growth (59).

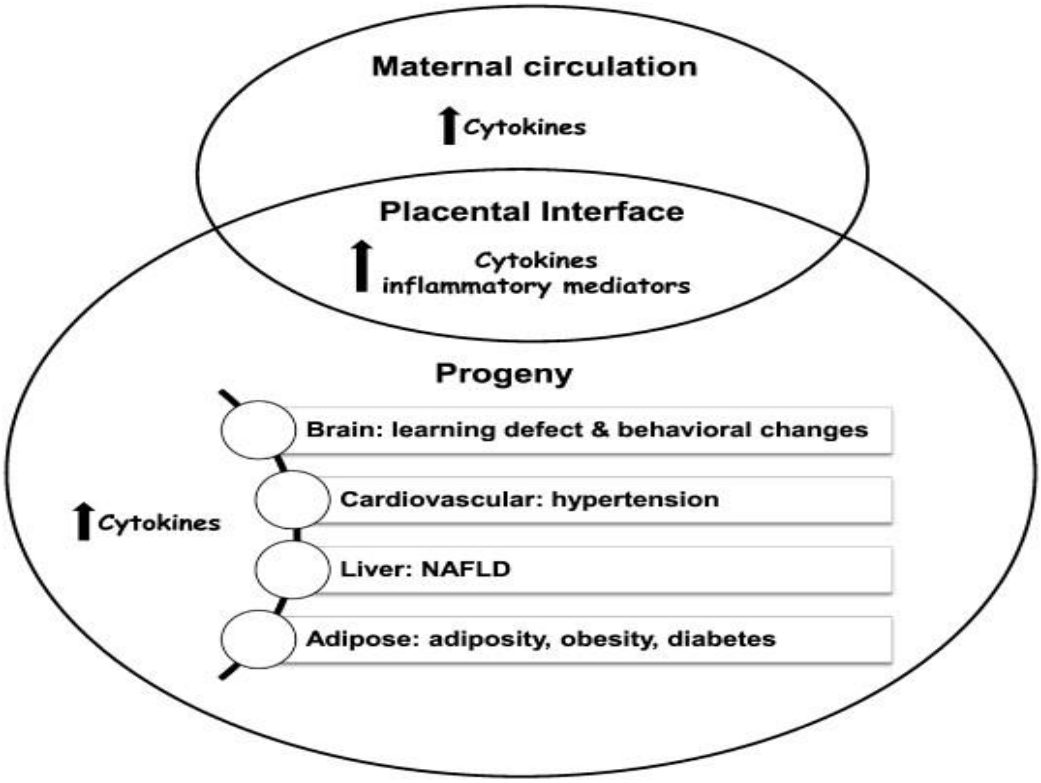

Figure 1.3*: In utero* exposure to high-fat diet (HFD) programs the increased susceptibility to chronic diseases during development and growth. Figure reprinted from Journal of Nutritional Biochemistry, 26 /2015, Zhou D, Pan YX, Pathophysiological basis for compromised health beyond generations. Role of maternal high-fat diet and low-grade chronic inflammation / Transgenerational epigenetic experiences, 1-8, Copyright (2015), with permission from Elsevier (59).

A recent study in mice suggested that HFD during lactation altered the milk composition and was related to development of metabolic disturbance in the offspring. The pups also weighed significantly more than the pups from the control group fed normal diet (60). Another study observed that dams fed HFD during lactation had a decreased prolactin level in milk and increased body weight and adiposity, development of fatty liver and hyperinsulinemia, and their offspring showed IR during weaning. Prolactin treatment, either by the HFD-fed mothers or directly in the pups, reduced visceral adiposity, improved the fatty liver and ameliorated insulin sensitivity in the offspring (61). The uses of animal models in studies are viewed as necessary tools to get new insight in research areas. In later years, laws to prevent overuse of animals and to protect animals from painful and unnecessary trials have been strengthened (European Convention for the Protection of Vertebrate Animals used for Experimental and other Scientific Purposes, ETS No. 123). The researchers are constantly mindful of the three R`s (replace, reduce and refine) when planning new studies that require results from animals. In this master thesis, it was avoided to use new animals because liver tissue and serum from adult male C57BL/6J-Apc^{+}/$^{+}$ (adenomatous polyposis coli) mice provided from an existing mouse obesity study at NIPH were utilized for further experiments (3).

1.4 Contribution of dyslipidemia to NAFLD

White adipose tissue (WAT) is the main energy storage depot of lipids in form of TAG, and is widely distributed through the whole body in subcutaneous regions and around internal organs (visceral adipose tissue, VAT). TAG is mobilized via lipolysis when energy is needed. Brown adipose tissue (BAT) is responsible for energy dissipation during cold-exposure. Beige adipose tissue is WAT adapting to a phenotype similar to BAT when the body is exposed to cold in a process called browning (62). Adipose tissue is crucial for maintaining metabolic homeostasis (63). Imbalance in energy homeostasis leads to excessive fat buildup in the adipose tissue and is disturbing the normal function of adipocytes. Lipid overload may lead to accumulation of TAG within the skeletal muscle and liver as ectopic fat. Ectopic lipid, together with the increasing amount of circulating FFA, may cause IR in various tissues, and thereby disrupt glucose homeostasis. IR can be defined as a condition where higher than normal insulin concentrations are needed to achieve normal metabolic responses, or normal insulin concentrations fail to achieve a normal metabolic response (64). The regulatory

systems that control body weight homeostasis can promote positive energy balance, which might contribute to weight gain and fat accumulation in obese individuals. A review proposed that while a robust biological response was activated to restore homeostasis when body fat stores were at risk (for example under starvation), excess of adiposity was associated with absence of significant response due to a dysfunctional regulatory pathway controlling energy balance (65). Two important components of the metabolic syndrome, glucose and TAG, are overproduced by the fatty liver. The liver is therefore a key determinant for metabolic abnormalities (66). The liver has a key function in lipid metabolism. It imports FFA, rearrange, store and export lipids by cooperation with lipoproteins such as chylomicrons, low density lipoproteins (LDL), very low density lipoproteins (VLDL) and high density lipoproteins (HDL). Changes in any of these processes can lead to development of NAFLD (67). Figure 1.4 shows an overview of suggested dysfunctional mechanisms in hepatic steatosis.

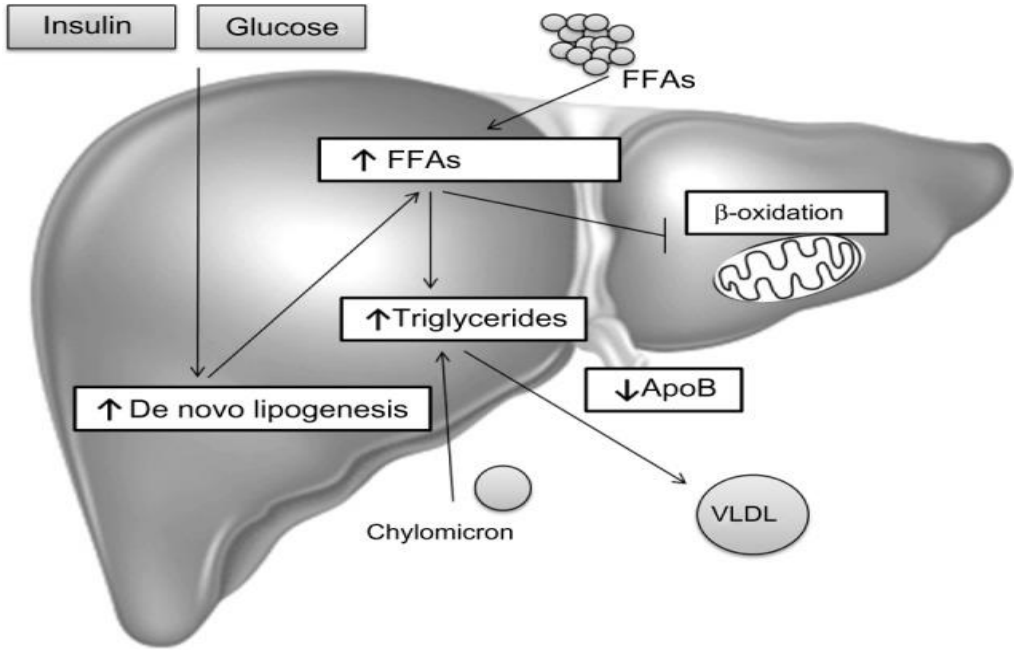

Figure 1.4: Hepatic steatosis. The first hit of NAFLD is triacylglyceride (TAG) accumulation in the cytoplasm of hepatocytes due to imbalance between lipid input and output: 1) an increase in free fatty acids (FFA) uptake derived from the bloodstream due to increased lipolysis from insulin resistant adipose tissue and/or from the diet transported as chylomicrons; 2) an increase in glucose and insulin levels in response to carbohydrate intake that enhances de novo lipogenesis; 3) a decrease in FFA mitochondrial oxidation; 4) a decrease in TAG hepatic secretion by reduced packaging with ApoB into VLDLs. Figure used with permission from Berlanga et al. 2014 (67).

FFAs are involved in many important cellular events, and chronically raised FFA can disturb different metabolic pathways, and induce IR in many organs. Hence, hepatic fat

accumulation has been strongly linked to IR (68). TAG accumulation in the cytoplasm of the hepatocytes, as the hallmark of NAFLD, emerges from a disturbance between FFAs uptake, *de novo* lipogenesis and removal of lipids (67). Regardless of the source of FFA that hepatocytes uses in production of TAG it is usually packaged into lipoproteins in the hepatocyte endoplasmatic reticulum and then exported to adipose tissue for storage. Therefore, accumulation of fat in the liver is caused by an excessive delivery of FFAs from VAT into the liver, increased *de novo* lipogenesis by high glucose level, disturbed oxidation of FFA in the mitochondrial system or decreased output of TAG due to inadequate production of VLDLs (69). Despite TAG being the main lipids stored in the liver of NAFLD patients, studies have suggested that they might exert protective functions (34, 70, 71). TAG synthesis seems to be an adaptive beneficial response in situations where hepatocytes are exposed to potentially toxic TAG metabolites. FFA and cholesterol, especially when accumulated in mitochondria, are considered the "aggressive" lipids leading to tumor necrosis factor (TNF-α)-mediated liver damage and reactive oxygen species (ROS) (34). Cholesterol is transported into the liver via mainly the lipoprotein chylomicron. Increased *de novo* lipogenesis in the liver linked to excess adiposity results in increase in harmful lipid intermediates including diacylglycerol (DAG), ceramide and free cholesterol (FC). Their lipotoxic effect promotes inflammation through several pathways (72). A review proposed that dietary cholesterol intake served as a factor related to higher risk and severity of NAFLD (71). To be able to monitor the progression of NAFLD it would be of great importance to understand the underlying mechanisms of lipid accumulation in the liver and the developmentally programmed changes associated with early life overnutrition (67).

1.5 Insulin-like growth factor-1 (IGF-1) system and NAFLD

Liver is the main site of synthesis of endocrine factors involved in whole-body metabolism, such as the insulin-like growth factor 1 (IGF-1) (73). IGF-1 and insulin-like growth factor 2 (IGF-2) proteins are released by the liver in response to growth hormone (GH) stimulation (74). Function of IGF-1 is to promote growth and development during fetal and postnatal life. There is increasing evidence supporting that GH and IGF-1 is likely to have roles in the development and progression of NAFLD in humans and mice (74, 75). A human study suggested that IGF-1 had anti-inflammatory effect on hepatocytes. Patients with progressed NAFLD had a low level of IGF-1 caused by inflammatory cytokines (76). A mice study

proposed the protective effect IGF-1 can have on liver function (77). IGF-1 is also important for maintaining normal insulin sensitivity, and disturbance in IGF-1 secretion increases IR (78).

1.6 NAFLD signaling pathways

Recent studies have focused their attention on molecular mediators that may be implicated in NAFLD (68). In this master project, expressions of NAFLD-associated genes were analyzed in livers from HFD exposed mice in different life stages in order to identify potential changes in signaling pathways. Adverse outcome pathway (AOP) is a conceptual model that structures existing knowledge regarding biologically credible and empirically supported links between molecular-level disturbance of a biological system and an adverse outcome at a level of biological organization of regulatory relevance. AOP frameworks have potential to impact regulatory decision-making through an effective and accurate use of mechanistic data (79). On the other hand, use of biological pathway databases gives easy access to the myriad of interactions underlying biological processes for researchers and scientists. Pathway databases are used to analyze experimental data by research groups in many fields (80). There are many databases worldwide, and their popularity depends on researchers loading their findings in the databases and using the database for their research, and thereby updating the database with the newest results and information. Some popular databases are Reactome, Wikipaths and Kyoto Encyclopedia of Genes and Genomes (KEGG). KEGG is among many scientists seen as the standard of databases (80, 81). Both AOP concerning hepatic steatosis and KEGG pathway for NAFLD for mice were used for choosing feasible biomarkers for this thesis.

1.7 Gene expression measurements

1.7.1 Choices of technology for gene expression measurements

The flow of genetic information from deoxyribonucleic acid (DNA) to mRNA to protein/gene product is the fundamental principle of molecular biology. The genetic information contained by DNA is transcribed into mRNA. mRNA molecules are translated into proteins within individual cells. Proteins in turn are directly responsible for cell organization and function and for the regulation and synthesis of other types of molecules. Gene expression is a highly regulated mechanism that controls the function and adaptability of all living cells,

and different factors contribute to the expression of genes (82). Different technologies exist for investigation and quantification of gene expression. Some techniques are well established and others are newer and complex procedures, and they can also be divided into low, medium and high throughput methods. The choice for appropriate technology and instrumentation involves reflections on for example type and volume of sample materials available, accessibility of instrumentation, the in house competence for the assay technology and bioinformatics, time spent for performing analysis (manual versus automated work-flows) and cost-benefit evaluations. Two gene expression profiling methods have proven useful as complementary techniques besides reverse-transcription quantitative polymerase chain reaction (RT-qPCR) assays. These are gene expression microarrays and Next Generation Sequencing (NGS) for ribonucleic acid (RNA) sequencing (83). Microarrays utilize target-oriented nucleic acid probes covalently bound to a solid phase such as glass microscope slides (84). The target sequences are labeled with fluorescent dye(s) and are applied to the slide where the target RNA hybridizes with its probe. The fluorescence intensity is measured by image analysis, and enables the quantification of gene expression. The advantages of microarrays are the large scale analyzing all targets of interest (often whole genome) (83). Often, a whole-genome discovery is not needed. Due to logistics, sensitivity, costs of whole-genome microarrays and because a known gene or pathway exists the gene expression analyses can be executed by quantitative polymerase chain reaction (qPCR) (85). In gene expression studies, sequence-based methods have come forward as more common methods to use due to development of more easy-to-use protocols. Sequencing technologies involve template preparation, sequencing and imaging, and are completed with data analysis that requires bioinformatics tools (86). NGS is able to recognize and quantify infrequent transcripts without any knowledge of the gene in question, and can also provide information about alternative splicing and sequence variation in identified genes (86). NGS can achieve higher resolution of differentially expressed genes and has a much lower limit of detection (LOD) than a standard whole genome microarray. The NGS is a new and evolving field, and cost, data collection tools and available bioinformatics personnel, are conditions to consider when making choices for study designs.

Both microarrays and RNA sequencing are methods that give broad insights in genes expressed in one sample. However, it is a common procedure to verify the findings by

another technology. Validation of differentially expressed genes is often achieved by qPCR, and especially for verification of microarrays the RT-qPCR remains the gold standard (83, 85). By using RT-qPCR, small sample sizes can be used in the quantification of mRNA, and RT-qPCR is in theory capable of identifying a single mRNA molecule. The results give information on mRNA present in the cell at the time of analyzing and RT-qPCR is considered as the gold standard for accurate, sensitive and fast measurement of gene expression (87).

1.7.2 Gene expression analysis by RT-qPCR assay

In this master project the RT-qPCR methodology was chosen for gene expression analysis. The main reason was that a targeted gene strategy was considered appropriate in relation to the project main aim. Also the procedures and instrumentation were available in the lab, and the technology was considered time- and cost effective. To secure accurate, high quality and meaningful results when working with molecular assays and RNA in particular, it is crucial to follow good and standardized methodological procedures. RNA is susceptible to digestion by the ribonuclease enzyme (RNase). These RNases are present naturally both in the cells and outside on almost everything that comes into contact with humans and extreme care must be in place to avoid sample contamination and degradation. The goal is to create a RNase-free environment, and the procedures include freezing of samples quickly for storage at -80°C, wearing gloves all the time and frequently change them, dedicate lab equipment for separate work to keep control on usage of the devices, decontaminate all equipment, instruments, cabinets and benches with RNase inhibitors to inhibit any RNases present. The overall objective for the strict instructions is to keep the mRNA of the samples intact for downstream applications in order to create meaningful data. A RT-qPCR analysis of mRNA starts with converting isolated mRNA to complementary DNA (cDNA) by reverse transcription; hence the name reverse transcriptase quantitative PCR. A requirement for the relative quantification of cDNA is that the reverse transcriptase reaction generates products in a way directly dependent on the amount of input RNA template. The RT-qPCR assay amplifies specific DNA molecules by DNA polymerase and specific primer sequences that are complementary to a chosen region in the target. The qPCR technique measures the amplification of target sequences at every cycle by fluorescence. The point where the fluorescence shows an exponential increase is the cycle value to use for quantification of the gene of interest.

1.7.3 Relative gene expression analysis

Absolute quantification and relative quantification are two commonly used methods to measure the level of gene expression (88). Absolute quantification determines the input copy number by comparing the PCR signal to a standard curve. Relative quantification indicates the relative difference between two samples; for example a sample from a group fed HFD compared to a sample from a control group fed normal diet. qPCR methods measuring relative quantification need to be controlled for several variables such as amount of starting material, enzymatic efficiencies, and differences between tissues in overall transcriptional activity (89). To date this is commonly solved by applying internal control genes (reference genes) for normalization of the mRNA fraction (89). In this way the non-biological variation between samples will be corrected and differences in gene expression will be due to true biological levels of expression for the target of interest. Normalization uses reference genes by the assumption that their expression is similar between all samples in a study, resistant to the experimental treatment and undergoes all steps of the qPCR with the same kinetics as the target gene (85). A study suggested the advantage of using several reference genes and calculating the geometric mean instead of average of the chosen reference genes for calculating the cycle threshold (C_T) reference gene value (89). The reason given was that the geometric mean better controls for outlying values and abundance differences between the different genes.

In this master project the mouse liver is the tissue of interest. The liver is a gland organ with many tasks for enabling the body to function. The different processes involve a complex and well organized change in the gene expression profile. It is therefore very important to use reference genes for internal control that are uniformly expressed (90). Sometimes it can be difficult to find reference genes that are not impacted to a certain degree by the treatment the samples undergo during an experiment and in these cases geometric mean of multiple reference genes can be applied. This approach minimizes the influence of treatment effects on the internal control set and increases the quality of resultant data (85). For decision of which reference genes to use in a qPCR study, the stability across treatment of the genes can be statistic calculated by mathematical algorithms such as geNorm and NormFinder to find the best fit for one specific experiment.

The Livak-method, also called comparative quantification cycle (C_q) method (91) or $2^{-\Delta\Delta Cq}$ method (88), is the most common method for relative quantification (85). This method takes into account two assumptions. The first assumption is that with each cycle of PCR the product doubles; giving 100% efficiency. This expectation requires setting of the C_q at the earliest cycle possible in the exponential phase of the PCR curve. The second assumption of the $2^{-\Delta\Delta Cq}$ method is for the reference genes to be expressed at a constant level between the samples (85). The raw C_q values are first normalized by subtracting the geometric mean of four stably expressed reference genes (used in this thesis) from the C_q value of the target genes to make the ΔC_q value of the samples. Thereafter the difference in expression between treatment group and control group can be calculated by the difference between these ($\Delta\Delta C_q$). The difference is in log2-format and is converted to fold difference (FD); the relative difference between the treatment group and the control group. If expression of mRNA is the same for both groups, the $\Delta\Delta C_q$ will be 0 and FD will be 1 (91, 92).

The relative expression is presented as how many times the target gene is up- or down-regulated compared to the control group given in the following formula:

$$\Delta Cq = Cq_{\text{target mRNA}} - Cq_{\text{geometric mean of reference genes}}$$

$$\Delta\Delta Cq = \Delta Cq_{\text{sample from treated group}} - \Delta Cq_{\text{sample from control group}}$$

$$\text{Fold difference} = 2^{-\Delta\Delta Cq}$$

1.7.4 Choice of relevant genes

This master thesis evaluated if the expression of genes involved in NAFLD was changed due to HFD in different life stages. Based on the KEGG pathway for NAFLD, as described in chapter 1.6, and on NAFLD literature reviews, in total sixty-nine genes involved in hepatic lipid metabolism, insulin response, glucose regulation, inflammation and oxidative stress were selected for gene expression analysis. Several reviews have suggested that IR occur before lipid accumulation in the process of developing NAFLD, and increased adipose tissue lipolysis generates increased supply of FFA in the blood (67, 93). FFA uptake into liver and muscle is closely connected to development of IR in these tissues. Reviews proposed that IR caused increased hepatic glucose output that again leads to increased insulin secretion, hence the threesome of IR: hyperglycemia, hyperinsulinemia and increased serum FFA (67,

72). Furthermore, if NAFLD progressed from simple steatosis to NASH, the lipid accumulation and IR appeared to be followed by a “second hit” were pro-inflammatory mediators gave rise to inflammation or oxidative stress that lead to hepatocellular injury (67, 93). A review article by Williams and co-workers from 2013 focused on the programming effects of maternal HFD in offspring, and indicated that the liver-specific injuries by exposure to maternal HFD gave disturbances such as reduced mitochondrial function, increased levels of pro-inflammatory cytokines and changed lipogenic gene expression (94).

A range of genes representative in signaling pathways such as the peroxisome proliferator-activated receptor (PPAR), tumor necrosis factor (TNFα), insulin and adipokine were analyzed. A group of genes related to oxidative stress were also included in the gene expression analysis due to earlier studies suggesting oxidative stress response genes being up-regulated in livers from mice fed HFD (95, 96). See Appendix A4 Table A.1 for a complete overview of analyzed genes.

2 Hypothesis and aims of study

Researchers at Norwegian Institute of Public Health (NIPH) have previously shown that the intrauterine and lactation periods are susceptible life stages for the development of HFD-induced obesity and intestinal tumorigenesis in adult C57BL/6J-Min (multiple intestinal neoplasia/+ mice (3). The outcome was increased body weights in young adults and increased numbers of tumors in the small intestine in the Min/+ mice. In the same study, impaired glucose tolerance was observed for wild-type mice fed obesogenic diet as adults or throughout life. A further study (personal communication) at the institute has focused on miRNA expression levels in VAT from adult male mice in the study by Ngo and co-workers (3).

This master project extends these two former studies by analyses of potential consequences of HFD during various life stages for metabolic programming in the liver of wilt type male mice. The study focuses on liver lipid accumulation and on signaling pathways related to liver steatosis/NAFLD.

Main objective: To determine potential changes in signaling pathways involved in development of NAFLD after exposure to a HFD during five different life stages in the adult offspring.

This master project states the following hypotheses:

1) HFD exposure during different life stages predisposes to increase of liver lipid accumulation in the adult

2) HFD exposure during different life stages affects hepatic secretion of IGF-1

3) HFD exposure during different life stages changes the expression of genes in signaling pathways related to NAFLD

4) Early-life exposure to HFD has more serious consequences than exposure later in life for risk of developing NAFLD

In order to test these hypotheses, the master project had the following objectives:

1) To determine the level of lipid accumulation in the livers of mice exposed to HFD in different life stages

2) To determine changes in serum IGF-1 in mice exposed to HFD in different life stages

3) To determine changes in the expression of genes in signaling pathways associated with NAFLD in mice exposed to HFD in different life stages

4) To determine potential differences in susceptibility for liver lipid accumulation and signaling pathways dependent on different life stages of exposure to a HFD

3. Materials and Methods

3.1 Diet induced obesity model (DIO model)

Liver tissues and serum samples from mice used in this thesis project originated from a published mouse obesity study conducted at NIPH in 2014 (3). The harvested liver tissue samples were used for gene expression and lipid class analysis, while the serum samples were used for determination of protein expression level.

Ngo and co-workers mated female C57BL/6J-Apc$^{+/+}$ (wild-type) mice with C57BL/6J-Apc$^{Min/+}$ males. The Min/+ mouse is heterozygous for a germline non-sense mutation in the tumor suppressor gene adenomatous polyposis coli (*Apc*) leading to a truncated nonfunctional APC protein. This change in the APC protein leads to development of multiple adenomas in the small intestine and to lesser extent in the colon. Proven breeders having had a litter on a regular breeding diet (2018 Teklad Global 18% Protein Rodent Diet from Harlan Industries Inc., Indianapolis, IN, USA) where used before the experimental litters on special diets with 10% or 45% fat were obtained (described below). Both females and males were bred at NIPH, Oslo, Norway. C57BL/6J-Apc$^{Min/+}$ males were originally purchased from the Jackson Laboratory (Bar Harbour, ME, USA). To minimize the genetic drift from the colony at the Jackson Laboratory, both females and males in the breeding stock at NIPH were regularly replaced.

Genotyping of the offspring for the *Apc* gene was performed with allele-specific PCR using DNA extracted from ~ 2 mm^2 ear puncture samples obtained during identification of individual mice at weaning. In this thesis, only the adult male wild-type C57BL/6J-Apc $^{+/+}$ mice where used.

The mice were housed in air flow individually ventilated cages (IVC) racks (Innovive Inc., San Diego, CA, USA) in 100% PET plastic disposable cages on Nestpak Aspen 4HK bedding (Datasand Ltd., Manchester, UK) in a room with 12-h light/dark cycle, and controlled humidity (55 ±5%) and temperature (20-24°C). Diet and water were given *ad libitium*.

The animal experiment was performed in conformity with the laws and regulations for animal experiments in Norway and was approved by the National Experimental Animal Board in Norway.

3.1.2 Experimental diets and treatments of mice

The dams were normal weight before mating. The experimental litters were given two types of diets from Research Diets Inc. (New Brunswick, NJ, USA): A HFD, D12451 diet, containing 20%, 35% and 45% kcal from protein, carbohydrates, and fat, respectively, and a matching control low fat diet, D12450H diet, containing 20%, 70% and 10% kcal from protein, carbohydrates and fat, respectively. The amount of sucrose was 17% of the calories in both diets. The HFD had 4.73 kcal/g, whereas the low fat diet had 3.85 kcal/g. The HFD contained 22.9% more kcal per gram diet. To spread out evenly dietary treatment groups, mice were randomly assigned to the experimental groups; the first dam was given 10% fat diet, the second dam was given 45% fat diet, the third dam 10% fat diet, and so on. Similarly, the litters were given either of the two diets after birth alternately, and after weaning in turns until the necessary numbers in all experimental groups were obtained.

Blood was collected by cardiac puncture under anesthesia with ZRF cocktail (containing 3.3 mg zolazepam, 3.3 mg tiletamine, 0.5 mg xylazine and 2.6 µg fentanyl per mL 0.9% NaCl) into Microvette serum/clot activator tubes (Sarstedt AS, Ski, Norway), and serum was collected for protein analysis (in this thesis, mainly IGF-1). Thereafter, the mice were sacrificed by cervical dislocation. Mice livers were dissected, weighed, rapidly frozen on dry ice and then stored at -80°C until use. In total, six treatment groups were included in this experiment, and each group consisted of 12 mice, except the lactation (LA) group with 11 mice due to loss of one liver sample during RNA isolation.

The experiment was designed in order to determine the most susceptible exposure period for development, and the design and treatment groups are presented in Figure 3.1. The mice were exposed to a 45% HFD in three different periods of their life: i) *in utero*, via the dams, then the offspring mice were given 10% control diet after the birth; ii) from birth to weaning, via milk during lactation, then they were given 10% control diet; or iii) from weaning at 3 weeks to termination at 23 weeks.

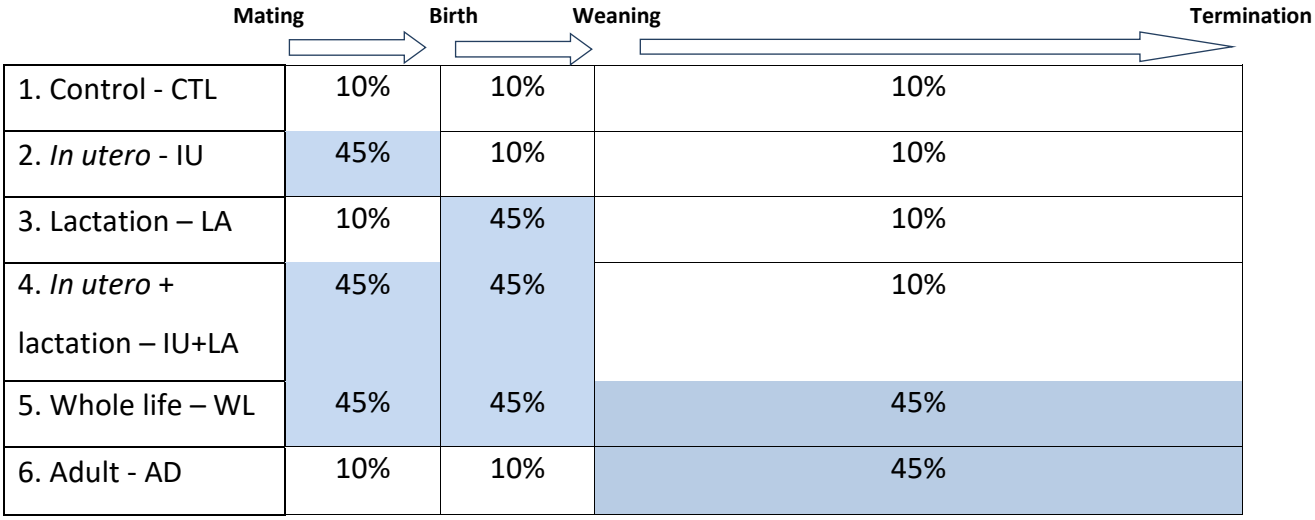

Figure 3.1: Experimental design with feed intake for the mice. Group 1: 10% fat throughout life (10%+10%+10%)-*CTL*; Group 2: 45% fat *in utero* (45%+10%+10%) – *IU*; Group 3: 45% fat during lactation (10%+45%+10%) - *LA*; Group 4: 45% fat *in utero* and during lactation (45%+45%+10%) – *IU+LA*; Group 5: 45% fat throughout life (45%+45%+45%) – *WL*; Group 6: 45% fat as adults (10%+10%+45%) – *AD*. n=12 for all groups except LA group n=11.

3.2 Recording of feed intake, body and liver weights

The body and liver weight data were recorded the Ngo and co-workers study, but only included only the results for the mice used in this thesis. Body weight of the dams was registered at mating and weekly during the pregnancy and lactation periods. Body weight of the offspring was recorded on day 3-4 after birth and thereafter weekly from weaning until termination at 23 weeks. The terminal BMI at 23 weeks was calculated based on the measured body weight and nasoanal length, recorded at termination: BMI (g/cm^2) = body weight (g) /nasoanal length (cm^2). The feed intake was monitored weekly by measuring the weight of feed in and out of the cages for the dams during pregnancy and lactation periods, and for the pups from weaning to termination. The liver was dissected and weighed at termination and stored at -80°C until use.

3.3 Protein expression analysis

There are numerous technologies to analyze protein expression levels, and the method of choice depends on the goal for the experiment. In this study, the protein levels were quantified by an immunoassay, where the proteins of interest bind to target specific antibodies and fluorescence was measured for quantification of protein levels. For

quantification of the protein expression levels a multiplex sandwich enzyme-linked immunosorbent assay (ELISA) based assay was used. The use of two different antibodies for detection of each protein of interest gives a good specificity. Luminex xMAP™ Technology (Luminex Corporation, Austin,Texas, USA) is a fast and advanced way to measure the level of several target proteins in the same assay (multiplexing). Each analyte (within the multiplex panel) is assessed individually without interference from the other analytes in the panel. This technology performs binding on the surface of color coded magnetic microparticles, which are then read in a compact analyzer. Figure 3.2 shows a Luminex assay principle using magnetic color coated beads.

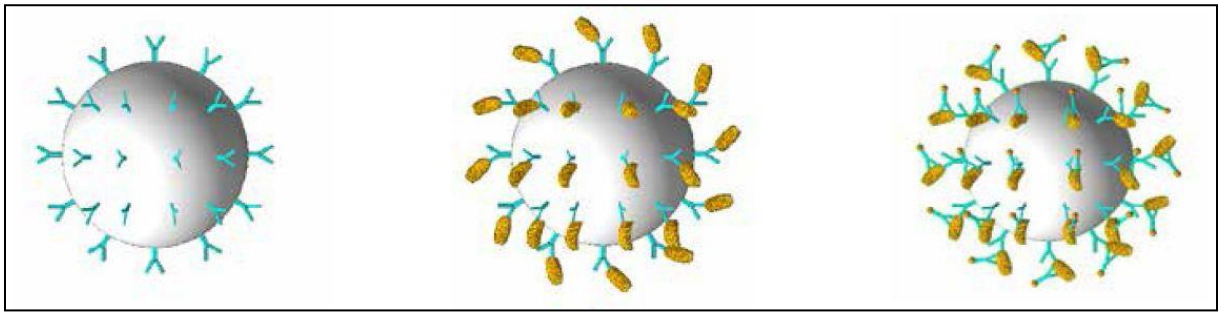

Figure 3.2: Protocol used with bead-based assay. Color-coded beads known as microspheres are pre-coated with analyte-specific capture antibodies. The beads are incubated with the samples, and antigen from the samples recognizes and binds to the capture antibodies. Captured analytes are afterwards detected using a mix of biotinylated detection antibodies and a streptavidin-phycoerythrin conjugate (Streptavidin-PE). An array reader with a dual laser system illuminates the microparticles. One laser excites the PE dye of the assay, and the second laser excites the dyes inside the beads to identify their color and which target is in on the specific microsphere. The intensity of the fluorescence- obtained signal is in direct proportion to the amount of analyte bound. This way the analyzer is capable of reading multiplex assay results by reporting the reactions occurring on each individual microsphere. Figure adapted from ThermoFisher.com. (97).

Regarding the selection of animals used in the different experiments in this study; there was not a complete overlap of animals used for protein analysis, due to lack of serum samples for some of the animals. Mice serum samples (n=78) from the five different HFD groups and the control group stored at -80°C were thawed overnight at -20°C, and then at 4°C the day of analysis. Mouse premixed multi-analyte kit (R&D Systems, Minneapolis, MN, USA) which contained seven biomarkers; IGF-1, Fatty acid binding protein 4/A, (FABP4/A), Lipocalin 2, Plasminogen activator inhibitor-1/Serpin E1 (PDGF-BB), Chitinase 3-like 1, PAI-1/Serpin E1 and Osteopontin were used. The procedure was performed according to the manufacturer protocol (see Appendix A1 for details). In brief, polypropylene test tubes, 0.6 ml microtubes, from Axygen Inc. (Union City, CA, USA) were used for dilutions of samples and standards. Serum samples were diluted 1:50 (10 µL sample + 490 µL calibrator diluent). The standards provided in the kit were aliquoted in four vials of standard cocktails and standards were

reconstituted by calibrator diluent with appropriate volumes according to the kit protocol. The reconstituted standards were combined in one single tube with 100 µl of each standard and 600 µl calibrator diluent. This added up to 1000 µL standard solution. The standard solution was used to produce a 3-fold dilution series were 100 µl was pipetted from one standard vial to the next vial. This resulted in seven standards with decreasing concentrations. The diluent was used as blank. The pipetting of samples, standards, blanks, reagents and microparticles were performed in the same 96-well microplate. The standards and blanks in the first two rows were run as duplicates. In the matter of replicates; biological replicates (high number of samples) where chosen instead of technical replicates. The samples were not analyzed with technical replicates, parallels due to priority of biological. After completion of the assay procedure, the 96-well plate was read on Bio-Rad Bio-Plex 200 dual laser flow based system (Bio-Rad Laboratories Inc., Hercules, CA, USA) detecting fluorescence intensity. Plex Manager 6.1 software (Bio-Rad Laboratories Inc., Hercules, CA, USA) was used to generate standard curves for analyzing concentrations of unknown samples.

3.4 Lipid class analysis

To assess the lipid levels in the mice livers, the concentration of four lipid classes; FC, Cholesterol esters (CE), TAG and FFA were measured. The mice liver samples were shipped to and analyzed at Vitas AS, Oslo, Norway (www.vitas.no). The samples were analyzed by normal phase high-performance liquid chromatography (NP-HPLC). The different lipids classes were chromatographic separated over time as a function of their polarity. An evaporative light scattering detector (ELSD) was used for detection of the different lipid classes.

To secure an adequate statistical power for the detection of potential differences in TAG concentrations in liver between treatment groups, a power-calculation to find minimum number of samples was performed using the G*power software (98). The coefficient of variation in % (CV %) of the analysis was below 5% for the TAG analysis and below 15% for the other three lipid classes; FC, CE and FFA, as stated by the performing laboratory. Due to limited resources, the analysis was scaled to the measurements of TAG with a (alpha) of 0.05

and b (beta) of 0.80. The data output showed a requirement of eight samples per group to be able to detect an increase compared to control of 50% or more.

Mice liver tissue was stored in -80°C at NIPH. The stored (-80°C at NIPH) liver tissue was weighed and ~ 100 mg liver tissue were sent for analysis. Tissue weight over 100 mg was needed to perform the analysis. The weighed samples were transferred into 2 mL Eppendorf® Safe-Lock microcentrifuge tubes with round bottom (Eppendorf, Hamburg, Germany) and packed in a Styrofoam box covered with dry ice. The samples were shipped by car to Vitas AS in Oslo. All weighing procedure was performed on dry ice.

At Vitas AS, the samples were homogenized and the lipid classes FC, CE, TAG and FFA were extracted by Folch extraction (10 vol of chloroform:methanol 2:1 v/v) (Folch et al., 1957). The organic fraction was subsequently analyzed by a 1260 Agilent chromatographic system (Agilent Technologies, Santa Clara, CA, USA) comprising an auto-sampler, a binary pump and a TCC column heater unit coupled to an ELSD (BÜCHI Labortechnik AG, Flawil, Switzerland). The lipid classes were separated using a normal-phase Silica monolithic column (Chromolith-performance, Merck, Darmstadt, Germany) with dimensions 4.6x100 mm. The lipid class separation was achieved by isocratic elution at 1.5 mL/min with a mobile phase consisting of Hexane:MTBE:Acetic acid (1000 ml; 50 mL; 250 mL). An injection volume of 5 uL was used. A drift tube temperature of 40°C and a gas pressure of 3.5 bar (N2) was used by the ELSD (99).

3.5 Gene expression analysis

Gene expression analysis was performed on mice livers to assess which signaling pathways involved in development of NAFLD are affected after exposure to a HFD during various life stages. The complete overview of analyzed genes is enclosed in Appendix A4 Table A.1 and overview of all samples is listed in appendix C2 Table A.2.

3.5.1 RNA isolation

Compared with DNA, RNA is susceptible to digestion by a wide variety of endogenous and exogenous RNases which are present on human skin and the surroundings. The overall objective was to keep the liver sample RNA integrity and purity intact for downstream applications. Precautions were taken to limit sample contamination and RNA degradation during liver preparation, isolation, purification, storage, and handling. All RNA-work was

done in an RNase-free environment in a laminar flow cabinet cleaned with water and 70% ethanol. RNase away (Molecular BioProducts, San Diego, CA, USA), an RNase inhibitor was used to clean benches, pipettes and other items used in the RNA isolation procedure. UV-light was applied in the laminar flow cabinet for 30 minutes before use to sterilize the workplace to prevent sample contamination. Gloves were changed frequently as a part of the RNA work routine.

Total RNA from mice livers was isolated using Quick-RNA™ MiniPrep kit (Zymo Reasearch Corp, Irvine, USA) according to the manufacturer protocol (see Appendix A2 for details). The kit uses a silica membrane in a column to facilitate binding of RNA (see Figure 3.3) (100). RNase-free stainless steel grinding 5 mm beads (Qiagen, Hilden, Germany) and RNA lysis buffer from the RNA isolation kit were added into 2 ml Eppendorf® Safe-Lock microcentrifuge tubes with round bottom (Eppendorf, Hamburg, Germany). Mice livers from 72 animals were taken out of the freezer at -80°C, and the samples were kept on dry ice during the liver slicing procedure into smaller pieces. Liver samples were transferred into 2 ml Eppendorf® Safe-Lock microcentrifuge tubes and weighed. The recommended RNA lysis buffer for tissue below 50 mg was 600 µL RNA lysis buffer. Four samples had weights above 50 mg, and for these samples, the RNA lysis buffer was adjusted to 900 µL. Samples were homogenized at 20 Hz for 2 minutes using the TissueLyser II instrument (Qiagen, Hilden, Germany). The homogenized samples were visually inspected after 2 minutes homogenization. If the samples were not homogenized completely, the procedure was repeated once more for complete lysis. The homogenized samples were stored at -80°C until RNA isolation. The work process until lysis completion of the liver samples was done as quickly as possible to avoid RNA degradation. The frozen lysates were thawed at 4°C, and RNA isolation was performed as twelve samples series. After completion of RNA isolation, the RNA was eluted in 50 µL DNase/RNase free water. Five µL was aliquoted for measuring of RNA yield, purity and integrity. Isolated RNA samples were stored at -80°C until use.

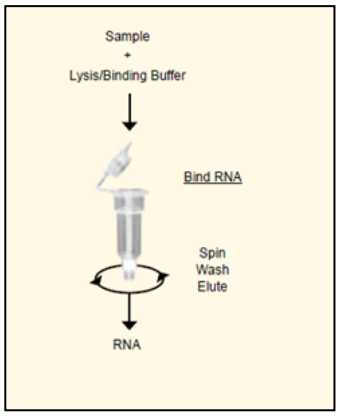

Figure 3.3: Overview of RNA isolation using column technology. Figure used with permission from Zymo Research (100).

3.5.2 RNA quality control

RNA quality encompasses both its purity (absence of protein, DNA, carbohydrates, lipids, and other compounds) and its integrity. Determining the purity and integrity of RNA are critical elements for the overall success of RNA-based analyses, because low quality RNA may strongly compromise the results of downstream applications. Following isolation, the RNA yield and purity were determined by use of a NanoDrop™ 1000 Spectrophotometer (ThermoFisher Scientific, Waltham, USA). NanoDrop™ 1000 is a full-spectrum (220-750 nm) spectrophotometer that measures 1 µL samples with accuracy and reproducibility. The recommendation by the producer was followed and the protocol in detail is described in Appendix A2. NanoDrop measures the absorbance of light to find the quality and quantity of nucleic acid in a sample. When assessing nucleic acids purity, there are two ratios of importance: 260/280 nm and 260/230 nm. Nucleic acids absorb light at 260 nm, proteins and phenols at 280 nm and carbohydrates, aromatic compounds and salts at 230 nm. The NanoDrop software calculates the ratios of these different wavelengths; thereby giving an estimation of the purity. Pure RNA should have an $A_{260/280}$ ratio of around 2.0, and RNA ratio above 1.8 is usually considered as RNA with good quality (101). The $A_{260/230}$ ratio is a secondary measure of nucleic acid of purity. Ratios are commonly in the rates of 1.8-2.2. Lower ratio may indicate the presence of organic contaminants, such as (but not limited to): phenol, TRIzol, chaotropic salts and other aromatic compounds. All samples of isolated RNA were analyzed using NanoDrop. As blank the elution solution from the isolation kit was used. The RNA integrity was measured using the Agilent 2100 Bioanalyzer system (Agilent Technologies, Santa Clara, USA) together with RNA 6000 Nano LabChip Assay kit (Agilent Technologies, Santa Clara, USA) using the Eukaryote Total RNA Nano protocol in the instrument. RNA samples are separated by traditional gel electrophoresis principles converted to a chip format. The chip contains samples wells, gel wells and wells for an external standard (ladder). Small molecules will pass through fast while larger fragments need longer time. The ladder facilitates plotting of a standard curve where migration time versus fragments size is plotted. From the migration time measured for each fragment in the sample the size is calculated. Dye molecules intercalate into RNA strands, and are detected by laser-induced fluorescence (102). Agilent Technologies has created a standardized and objective method to check for RNA integrity by introducing the ribonucleic acid integrity number (RIN), which is automatically calculated by the Expert 2100 software (Agilent

Technologies, Santa Clara, USA). The data output includes graphs, RNA concentrations, 28S ribosomal RNA (rRNA) and 18S rRNA ratios and the RIN. An elevated threshold baseline and a decreased 28S:18S ratio indicates RNA degradation (103). The score given (RIN) is in the range of 1 to 10. Ten is the maximum and indicates highly conserved RNA material. To perform qPCR on RNA the RIN number should be at least 5 and preferably 8 (103-105). Figure 3.4 shows an example of RNA with high and low RNA integrity analyzed in this study.

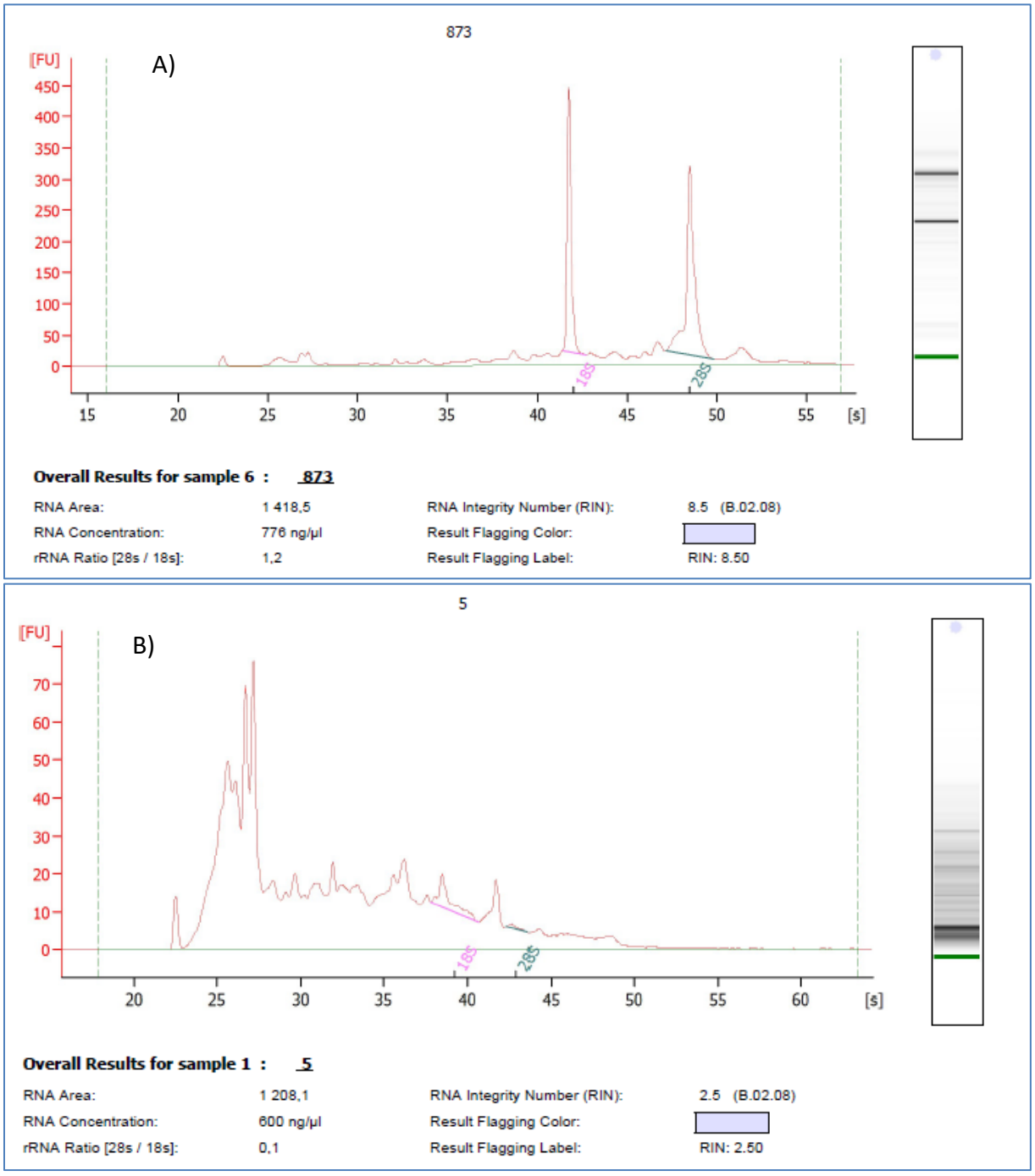

Figure 3.4: Liver samples from mice showing different output from integrity analysis. A) Sample with high integrity, RIN=8.5. B) Sample with degraded RNA; RIN=2.5.

3.5.3 cDNA synthesis

RNA molecules cannot serve as templates in PCR. To perform a gene expression measurement by qPCR, the mRNA in the sample must be copied into cDNA by reverse transcription reaction PCR. In order to produce cDNA, deoxynucleotides triphosphates (dNTPs), buffer containing magnesium, and primers are also needed in addition to mRNA and the RT enzyme. There are three different primer categories available for this purpose. Sequence/gene specific primers targeted to a specific sequence. Oligo deoxythymine (dT) primers binds to the poly (A) tails of mammalian mRNA and are suitable for transcribing the whole RNA template to cDNA. Finally, the random primers contain bases of all possible combinations, and bind randomly to multiple complementary sequences of the mRNA template. The kit used in this master project, the High-Capacity cDNA Reverse Transcription Kit (Applied Biosystems, Foster City, USA) utilizes the random primer scheme for cDNA synthesis. The package insert states the random primers facilitate that the first strand synthesis occurs efficiently with RNA molecules present. Afterwards, the RT-reaction is completed in a thermo cycler.

The RNA extracted from the mice liver samples was thawed and diluted using RNase-free water to contain 100 ng/µL as input for reverse transcription reaction. The 20 µL diluted RNA was then reverse transcribed to cDNA with 20 µL master mix containing random primers, dNTPs, buffered magnesium and Multiscribe™ Reverse Transcriptase enzyme. Hence, the total reaction volume for one sample was 40 µL. The mastermix and RNA template volumes, and the thermo cycler program in the Eppendorf Mastercycler (Eppendorf, Hamburg, Germany) used are shown in Tables 3.1 and 3.2 respectively.

Table 3.1: Mastermix and RNA template volumes in the reverse transcriptase PCR

10 X RT buffer	4.0 µL
dNTP mix	1.6 µL
Random primers	4.0 µL
Multiscribe™ Reverse Transcriptase	2.0 µL
Nuclease-free H_20	8.4µL
100 ng/ µL	20 µL

Table 3.2: Thermo cycler program in the RT-PCR reaction

Step 1	25°C	10 minutes
Step 2	37°C	120 minutes
Step 3	85°C	5 minutes
Step 4	4°C	∞

After cDNA synthesis was completed on the PCR instrument, the cDNA concentration and purity were measured using NanoDrop™ 1000 Spectrophotometer (see Appendix C1 for results).

3.5.4 Quantitative real time polymerase chain reaction (qPCR)

The real-time qPCR monitors the amplification of targeted DNA molecule during the PCR in real time. In order to detect and quantify gene expression from RNA, the same methodology is used as in conventional PCR using DNA as a template. The reaction mix used contains the fluorescent dye SYBR Green, a thermo-stable DNA polymerase, dNTPs, magnesium salts, selected gene-specific primers and sample cDNA (template). It is important to dilute the cDNA to prevent inhibition of the PCR reaction caused by leftovers of salts and other reagents from the RNA isolation procedure. To find the optimal cDNA concentration to ensure efficient qPCR runs a dilution series with pooled cDNA sample were analyzed. A 1:200 dilution was found to be the most efficient cDNA concentration for each run of the mice liver samples in this experiment. When dilutions were analyzed, the PCR efficiency was also evaluated to secure adequate PCR efficiency (E) obtained. A perfect PCR would theoretically double the amplicon amount from cycle to cycle which could give E=2. This is rarely the case, and studies have shown the efficiency to vary between 1.65 and 1.9. Factors like phenol, ethanol, hemoglobin, heparin, and even reverse transcription are known to alter the PCR efficiency (106). Seven reference genes and three target genes were analyzed in the dilution series and a simple regression analysis was performed to confirm acceptable PCR efficiency.

In the PCR reaction, for each gene of interest, a primer set (forward and reverse primers) contains the sequences complementary to the target gene sequence of interest. The specificity of the reaction depends on the primers used. The PCR process consists of thermal cycles (about 40 cycles are commonly used) and every cycle consists of three basic thermal steps. The first is denaturation to separate the DNA strands. The second is annealing that

facilitate binding of the primers to their complementary cDNA strands. Finally, the third is elongation by DNA polymerase to extend the new DNA fragments. Every cycle will ideally double the amount of target DNA. The fluorescence (in this case SYBR Green) intercalates to any double stranded DNA (included non-specific reaction products) and fluorescent light is emitted, which is measured after each cycle. When the fluorescence reaches a certain amplification threshold, which is the same for all samples in the run, it is registered how much time it took for each sample to reach this threshold. This time is reported in a value of Cq and is read on the X-axis as shown in Figure 3.5. The Y-axis shows relative fluorescence units (RFU). The threshold value must be chosen at the reaction's exponential phase. The Cq value found gives an quantification of amount RNA present in the tested sample tissue.

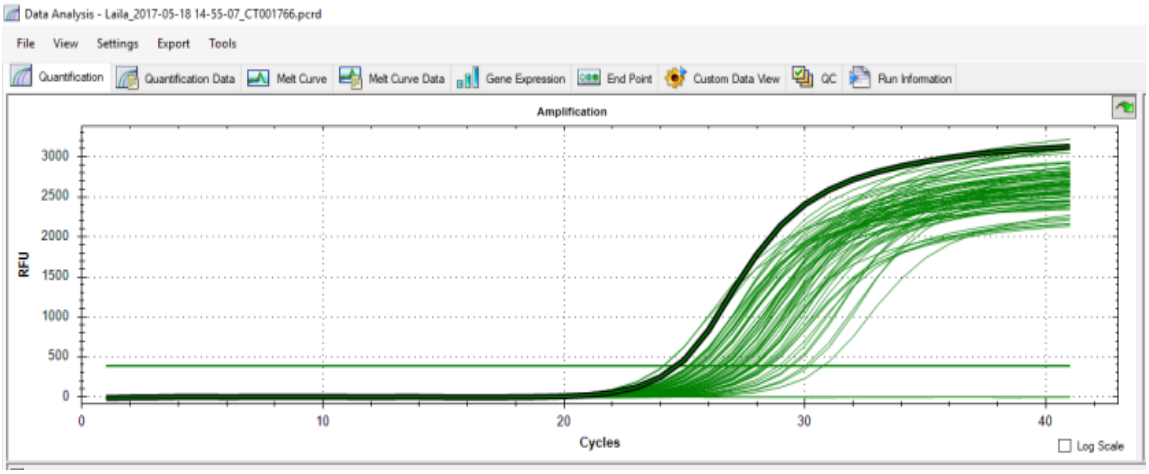

Figure 3.5: qPCR plot showing cycles on the X-axis and RFU (relative fluorescence units) on Y-axis for measuring of the *Srebf1* gene. The Cq value for the sample marked in green with black line in the graph gives Cq value of 24.63. This is the time for this sample to reach the threshold, and gives an estimate of the amount *Srebf1* gene present in this sample

qPCR reactions setups were prepared using the 4Lab™ Automated liquid handling robot (4titude Ltd., Surrey. UK). The associated Framestar 384-well PCR plates (4titude Ltd., Surrey, UK) were used. To minimize the number of freeze-thaw cycles, the cDNA were diluted 1:200 and pipetted in a number of 384-well plates and kept frozen at -20°C. The number of needed 384-well plates for one day of analysis was thawed at 4°C, centrifuged at 12000 x g at 4°C and loaded on the 4Lab™ liquid handling robot. Gene specific primers were purchased from Sigma Aldrich (St. Louis, USA). All primers were dissolved in Tris-EDTA (TE)-buffer (Invitrogen, ThermoFisher Scientific, Carlsbad, CA, USA) at a 100 µM concentration. The primers were then diluted 1:10 in TE buffer and aliquoted to appropriate volumes and stored in microtubes at -20°C. All primer sequences are listed in Appendix A4. Each 10 µL qPCR reaction was made of 4 µL diluted cDNA, 0.5 µL of each primerset (10 µM) and 5 µL KAPA

SYBR Fast qPCR Master mix kit (Kapa Biosystems, Wilmington, Massachusetts, USA).The KAPA SYBR Fast qPCR Master mix where mixed with gene-specific primers in a RNase-free environment in a laminar flow cabinet (equipped with UV light) and pipetted in a 96-well plate (Tear-A-Way non-skirted, 4titude Ltd., Surrey,UK) before loaded in the 4Lab™. Four µL 1:200 diluted cDNA sample and 6 µL ready-made mastermix where mixed in the appropriate wells for qPCR analysis. After pipetting the PCR plate was sealed with adhesive cover, centrifuged at 12 000 x g at 4°C for one minute before loaded on the PCR instrument.

The real time qPCR reactions were performed on Bio-Rad CFX384 Real-Time PCR System (Bio-Rad Laboratories Inc., Hercules, CA, USA) with a protocol shown Table 3.3.

Table 3.3: qPCR profile run on BioRad CFX384 Real-Time PCR System

Step	**Temperatur (°C)**	**Duration (min/sec)**	**Cycles**
Enzyme activation	95°C	3:00	Hold
Denaturation	95°C	0:03	40
Primer annealing	60°C	0:20	
Elongation	72°C	0:20 + late read	
Melt curve	0°C to 95 °C, increment 0.5°C	0:05 + late read	End

Five genes were analyzed on one 384-well plate. A screening strategy was decided for the possibility of in-depth experiments as a response to this study. Therefore; biological replicates (high number of samples) were chosen instead of technical replicates in the gene expression analysis. To verify that the PCR runs where valid; without contaminations, all qPCR runs had included No Template Controls (NTC) and No Reverse Transcriptase controls (NRT) for each gene analyzed. To confirm the presence of a single target a melting curve analysis was included in each run, which is a very important quality control step ensuring the detection of the gene of interest. At the end of each cycle the change of fluorescence due to gradual change in temperature can be measured by its melting temperature (Tm). At the melting point, the two DNA strands dissociate and the fluorescence intensity decreases as shown in Figure 3.6.

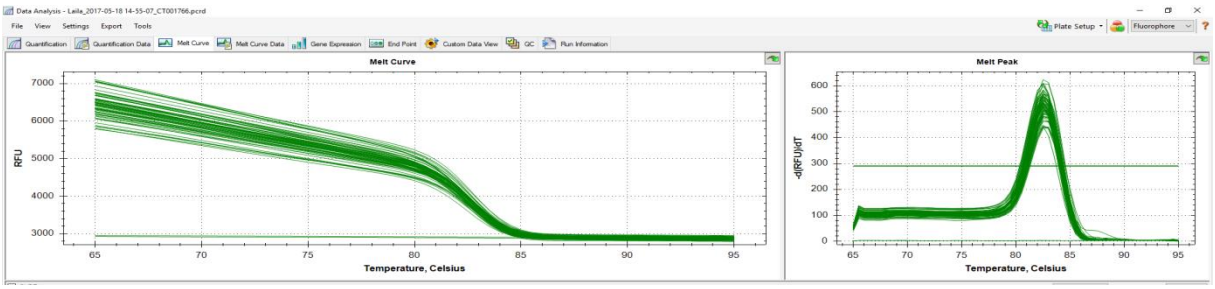

Figure 3.6: A melting curve from a qPCR run for detection of the gene *Srebf1*. The left curve represents raw data, and the right curve represents the derivate. The sudden decrease in fluorescence at around 82.50°C constitutes the melting point. The melting curve verifies identification of correct gene based on the knowledge that Tm°C for *Srebf1* primers is 82.50°C.

The temperature detected for the dissociation depends on base composition and length of the amplicons, and this can be used to identify contamination, mispriming and primer-dimer artifacts. This is especially important when using SYBR Green as a reporter dye, because of its willingness to bind to all double stranded DNA present in a sample. In few cases, the primers displayed a degree of self-complementarities and formed primer-dimers seen as a melting curve peak in the NTC control. Furthermore, any sample assay data point must be detected with 5 Cq values less than the corresponding NTC assay data point, and if the Cq values were lower than 5 Cq values the assay was defined as invalid and removed.

3.5.5 Gene expression analysis

Quantitative RT-qPCR was used to analyze the transcriptional response of mouse liver on control diet compared to HFD given in different life stages. The data was interpreted using CFX Manager Software version 3.1 (Bio-Rad Laboratories, Hercules, USA) and Microsoft Excel 2013. The level/intensity of fluorescence was read after each cycle in the qPCR run and a Cq value was calculated by the CFX Manager Software. Eleven samples that showed non-acceptable integrity (RIN) and purity were taken out of the study. The raw data Cq-values were pre-processed and outliers were excluded. Target genes with Cq-values above cycle 37 were considered beyond the LOD and replaced by Cq (LOD) (i.e. 37+1=38). Other missing values were imputed by k-nearest neighbors (knn) where k=10 (the nearest 10 non-missing values) algorithm.

The comparative $2^{-\Delta\Delta Cq}$ method described by Livak and Schmittgen (88) was used to analyze all gene expression data by relative quantification. Relative quantification indicates the relative difference between two samples from two different treatment groups. In this study the aim was to find differences between mice fed normal diet versus mice fed HFD. Prior to

normalization, the best fit of reference genes expressed at a constant level in the liver needed to be established for accurate and reliable gene expression results. Six known reference genes were included in the study. These were, *Hptr1, Ywahz, Tubβ5, Rpl13a, Actβ and Gusβ*. The reference genes *Hptr1, Tubβ5, Rpl13a and Actβ* were chosen as the most stably expressed reference genes. They were chosen based on stability and lowest CV% and the software NormFinder was used to calculate the stability of the reference genes (107). Figure 3.7 shows an overview of the results of the best combination of reference genes when the software NormFinder was used.

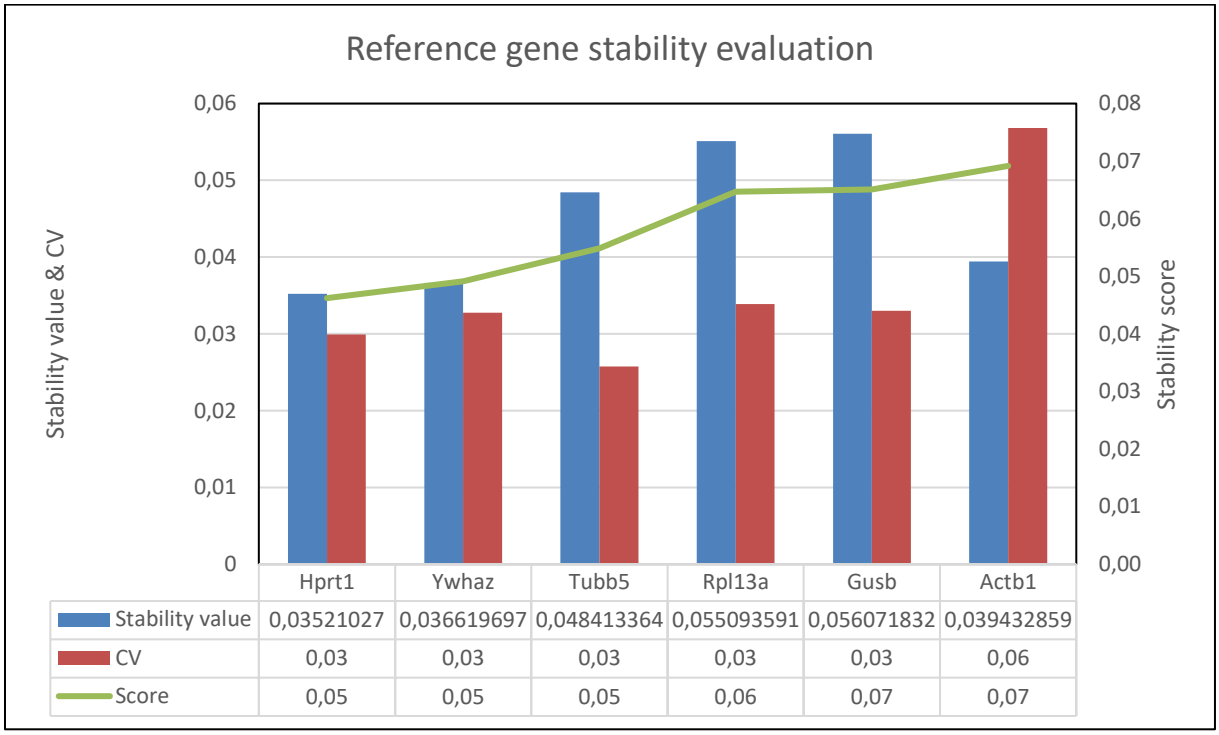

	Hprt1	Ywhaz	Tubb5	Rpl13a	Gusb	Actb1
Stability value	0,03521027	0,036619697	0,048413364	0,055093591	0,056071832	0,039432859
CV	0,03	0,03	0,03	0,03	0,03	0,06
Score	0,05	0,05	0,05	0,06	0,07	0,07

Figure 3.7: Overview of stability and CV data for normalization genes. Actβ and Hprt1 were found to be the best combination of two genes. Rpl13a and Tubβ5 were also included to cover a broad specter of the normalization genes; i.e., high and low abundant transcripts. Gusβ and Ywhaz were not chosen due to their high Cq-values

The raw Cq-values were imported to Microsoft Excel and normalized by subtracting the geometric mean of four reference genes from the Cq values of the target genes generating the ΔCq-value for the samples (88, 91, 95). The Cq-values were transformed to linear scale relative quantities (NRQ) as shown in the equation below.

$$NRQ = 2^{-\Delta Cq\ (sample)}$$

Where $\Delta Cq_{(sample)} = Cq_{(target\ gene)} - Cq_{(geometric\ mean\ of\ four\ reference\ genes)}$

The fold difference (FD) between high fat diet samples (HFD) and control diet samples(CD) were then calculated by dividing the normalized NRQ of the HFD samples by the normalized NRQ of the CD samples as shown below:

$FD=NRQ_{(HFD)}/NRQ_{(CD)}$

All gene expression results were reported as FD between the HFD and CD samples.

3.6 Statistical analysis of the results

Data were expressed as mean ± standard error (SE). Statistical analysis was performed using SPSS version 24 software (SPSS Inc, Chicago, IL, USA), and results with $p < 0.05$ were accepted as statistically significant. Normal distribution and equality of variances were evaluated using the Shapiro-Wilk normality test and the Levene's test of homogeneity of variance, respectively, before the data was analyzed further. The data that were not normally distributed were log2 transformed in an attempt to achieve normal distribution. If the data were still not normally distributed and/or showed lack of equal variance, non-parametric tests were applied. For assays with data with normal distribution the one-way analysis of variance (ANOVA) test followed by the post hoc tests Tukey's Honest Significant Difference test, Least Significant Difference test and Dunnett's two-sided test were applied. For the not normally distributed data, the Kruska-Wallis test was used. When significant results appeared from the Kruska-Wallis test, the Mann Whitney U test was used for comparing the significance level between groups.

In addition, for analyzing of mean between two groups for normal distributed data, the independent t-test was applied.

Body weight, BMI, absolute and relative liver weight

Relative liver weight (RLW) was analyzed by ANOVA and post hoc tests. Terminal body weight (TBW), absolute liver weight (ALW) and BMI were analyzed by Kruska-Wallis test. The data were presented as mean ± SE. For correlation of BMI and other results non-parametric Spearman Rank Order correlation was used.

Protein expression analysis

IGF-1, FABP4/A, Lipocalin 2, Chitinase 3-like 1, PAI-1/Serpin E1 and Osteopontin were analyzed by ANOVA. Platelet derived growth factor-BB (PDGF-BB) was analyzed by Kruska-

Wallis test. The two groups WL and AD were analyzed also separately to compare the mean only between these two groups. All proteins except PDGF-BB were analyzed by Independent t-test, and for PDGF-BB Mann Whitney U test was applied. The data were presented as mean ± SE.

Lipid level analysis

CE was analyzed by ANOVA and post hoc tests. FC, TAG and FFA were analyzed by Kruska Wallis test. The two groups WL and AD were analyzed also separately to compare the mean only between these two groups. CE, FC and TAG were analyzed using Independent t-test, and for FFA Mann Whitney U test was applied. Statistical analyses were also performed by rearranging the grouping in three groups with control group versus early phase exposure to HFD diet and later phases. ANOVA was applied for CE and FC, and for FFA and TAG the Kruska-Wallis test was used. The data were presented as mean ± SE. The TAG boxplot in Figure 4.3 was visualized in JMP Pr Statistical Database Software (Cary, NC, USA) due to possibility of viewing each individual TAG value in a boxplot.

Gene expression

In the RNA liver integrity chapter the data were expressed as mean ± SE. The statistical analyses of the qPCR data were carried out by ANOVA with post hoc tests. ΔCq-values were compared for each gene. For samples not normally distributed or that showed lack of equal variance, the non-parametric option Kruska-Wallis test followed by Mann Whitney U test was used. The data were presented as mean ± SE. For overview of the statistical results for gene expression analyzed in SPSS, the p-values are listed in Appendix C3 Table A.3.

Analyzing of litters:

The results from the mice from the same litter were calculated as the mean of these results to give one result as the result from the one litter.

4 Results

4.1 Body weight, BMI, absolute and relative liver weight

The published study by Ngo, et al. (2015) provided body and organ weight data for the selection of adult male C57BL/6J-Apc $^{+}/^{+}$mice included in this master thesis. The data were analyzed to determine potential effect between the treatments (Table 4.1).

Table 4.1: Effects of high fat diet. Effects of exposure to a HFD during different life stages on terminal bodyweight (TBW), absolute liver weight (ALW), relative liver weight (RLW) and BMI in male wild-type mice terminated at 23 weeks of age (mean of the group ±SE). RLW (%) =ALW/TBW x 100. n = number of offspring. There were no significant differences in TBW, ALW and BMI. * RLW of the IU group was significantly higher compared to the control group with a significance level $p<0.05$.

Groups	n	TBW (g)	ALW (g)	RLW (%)	BMI (g/ cm^2)
Control group – CTL	9	34.88 ±1.60	1.37 ±0.22	3.87 ±0.22	0.34 ±0.01
In utero – IU	10	36.96 ±1.03	1.70 ±0.08	4.60 ±0.12*	0.35 ±0.01
Lactation – LA	10	37.10 ±1.47	1.42 ±0.07	3.83 ±0.13	0.35 ±0.01
In utero+Lactation – IU+LA	10	35.77 ±1.19	1.43 ±0.07	4.07 ±0.12	0.34 ±0.01
Whole life – WL	10	40.98 ±2.65	1.58 ±0.18	3.78 ±0.26	0.38 ±0.02
Adult - AD	9	40.11 ±2.20	1.55 ±0.23	3.75 ±0.32	0.38 ±0.02
Average of all groups	58	37.63 ±0.75	1.51 ±0.05	3.99 ±0.09	0.36 ±0.05

Using the offspring as the statistical unit, all HFD treated groups showed a tendency of a higher terminal body weight (TBW) and a higher absolute liver weight (ALW) compared to the control group. However the findings were not statistically significant in any groups. The relative liver weight (RLW) was significantly higher for the IU group compared to the control and also compared with the other HFD treated groups except the IU+LA group ($p<0.05$). The body mass index (BMI) displayed a moderate increase for the groups WL and AD, but the data did not reach significance.

Using litters as the statistical units gave similar results with a significant difference in RLW for the IU group. Number of litters: n=38. CTL=6; IU=6; LA=7; IU+LA=6; WL=7; AD=6.

4.2 Protein expression analysis using Luminex assay

Protein analysis was run in mice serum by the use of Luminex xMAP™ Technology and Magnetic Luminex® Assay in a multiplex sandwich ELISA-based assay. Seven mouse biomarkers in serum were screened; IGF-1, FABP4/A, Lipocalin 2, PDGF-BB, Chitinase 3-like 1, PAI-1/Serpin E1 and Osteopontin. The main interest for this study was IGF-1.The total number of serum samples included in the study series was 78 samples. Due to a pipetting mistake by pipetting seven samples in duplicates in the microtiterplate, the available wells were reduced by seven. In addition a wrongly selected serum sample from another study was pipetted in one well in the microtiterplate. These eight wells with erroneous pipetted samples were removed from the study, hence the total number was 70 samples.

The protein expression levels are shown as FD between the HFD groups and the control group in Figure 4.1. IGF-1 showed an overall borderline difference between the groups ($p=0.054$). The IU group had borderline significant ($p=0.073$) and WL group had significant higher serum concentration of IGF-1 compared to the control ($p=0.039$).

Only slight and non-significant differences were observed for PDGF-BB, Lipocalin 2 and Chitinase 3-like 1. Several of the values for FABP4/A were above the range of the standard curve and should thus be interpreted with care.

In addition, the difference in expression of the serum biomarkers between the WL and AD groups for the biomarkers were analyzed by pair-wise testing. The data showed significant differences between the two groups for Lipocalin 2 and PAI-1/Serpin E1 ($p<0.05$). The difference in IGF-1 was not significant.

In addition, the difference in level only between the WL and AD groups for the biomarkers were analyzed statistically. The data showed significant differences between the two groups for Lipocalin 2 and PAI-1/Serpin E1 ($p<0.05$). The statistical result for IGF-1 gave no significant result ($p<0.05$).

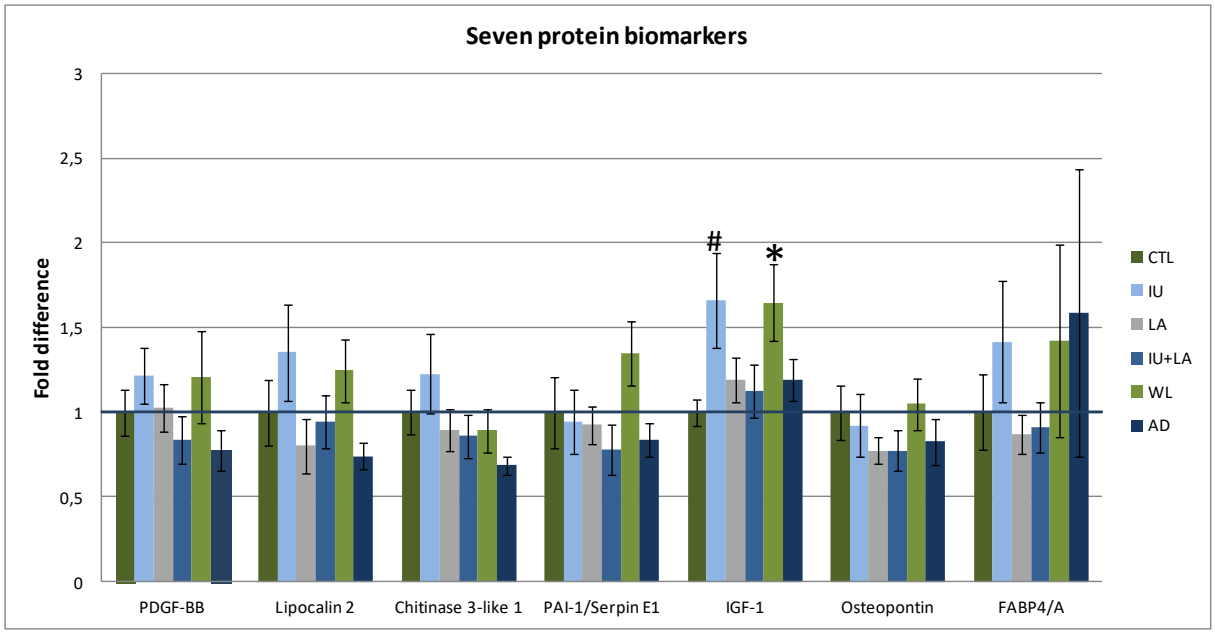

Figure 4.1: **Fold difference as protein expression levels for seven serum biomarkers**. The concentration of IGF-1, FABP4/A, PDGF-BB, Lipocalin 2, Chitinase 3-like 1, PAI-1/Serpin E1 and Ostepontin in serum in the different HFD groups were compared with the control group. Total number of samples from offspring=70. Control group (CTL), n=14; *In utero* (IU), n=10; Lactation (LA), n=12; In utero+Lactation (IU+LA), n=12; Whole life (WL), n=11; Adult (AD), n=11. Each value of the groups represents mean of the group ±SE. * Significantly different from control group ($p \leq 0.05$). # Borderline significantly different from control group ($p = 0.073$). Significance level $p<0.05$

Using litters as the statistical unit, significant differences in IGF-1 expression between groups were observed. The IU group showed significantly higher IGF-1 concentration compared to the control. The IU group had also a significant higher IGF-1 level than the groups IU+LA and AD. Differences in the levels of the other protein biomarkers compared to the controls did not reach significance. Number of litters: n=48. CTL=9; IU=6; LA=7; IU+LA=10; WL=8; AD=8.

4.3 Lipid analysis using normal-phase high-performance liquid chromatography

Liver lipid levels (TAG, FFA, FC and CE) were analyzed by Vitas AS, Oslo, Norway. The total number of samples included in the lipid assays was 48 samples for the assays divided in 8 samples per group. The differences in levels of TAG, FFA, FC or CE in HFD groups compared to the control group did not reach statistical significance ($p<0.05$) (Figure 4.2). In Figure 4.2, differences between the WL group and the AD group are suggested. To explore the data further, statistical analysis was performed where the WL group was compared to the AD group by pair-wise testing. This analysis showed that the level of FC ($p=0.036$) was significantly higher and TAG was not significantly higher ($p=0.385$). Statistical analyses were also performed by rearranging the grouping in three groups with control group versus early

phase exposure to HFD (IU, LA and IU+LA) and later phases (WL and AD). These differences did not reach statistical significance.

Using litters as the statistical unit, there were no significant differences in any HFD groups compared to the control ($p<0.05$). Number of litters: n=38. CTL=7; IU=5; LA=7; IU+LA=7; WL=5; AD=7.

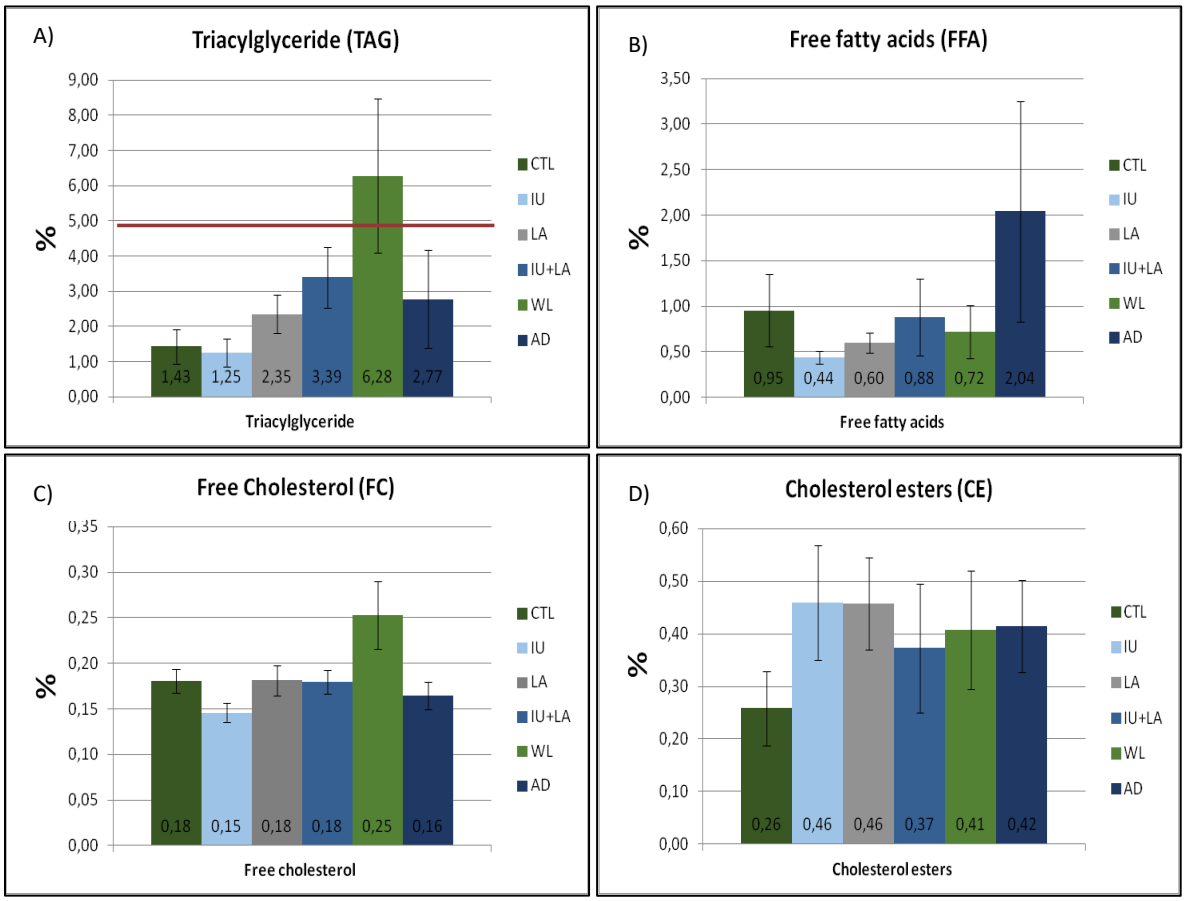

Figure 4.2: **Lipid levels in mouse livers**. The levels of triacylglyceride (TAG) (A), free fatty acids (FFA) (B), free cholesterol (FC) (C) and cholesterol esters (CE) (D) were measured in all HFD groups and control group. Total number of samples=48 (offspring). n=8 for all 6 groups. The results are expressed as mean ± SE. Analysis performed by Vitas AS, Norway. There were no significant differences in lipid levels present in the HFD groups compared to control group ($p<0.05$).

As mentioned in the introduction one definition of NAFLD is accumulation of TAG within hepatocytes that exceeds 5% of liver weight. This limit is shown as a red line in Figure 4.2 A. When looking at the mean result, the TAG concentration in the WL group was the only group to suggest liver steatosis. Figure 4.3 shows a TAG boxplot with individual results given within each group. This figure shows the occurrence of mice with liver steatosis in the groups LA, IU+LA, WL and AD. Percentages of animals with steatosis defined as >5% TAG were 8.3%

(1 of 8 animals), 37.5% (3 of 8 animals), 37.5% (3 of 8 animals) and 8.3% (1 of 8 animals) respectively.

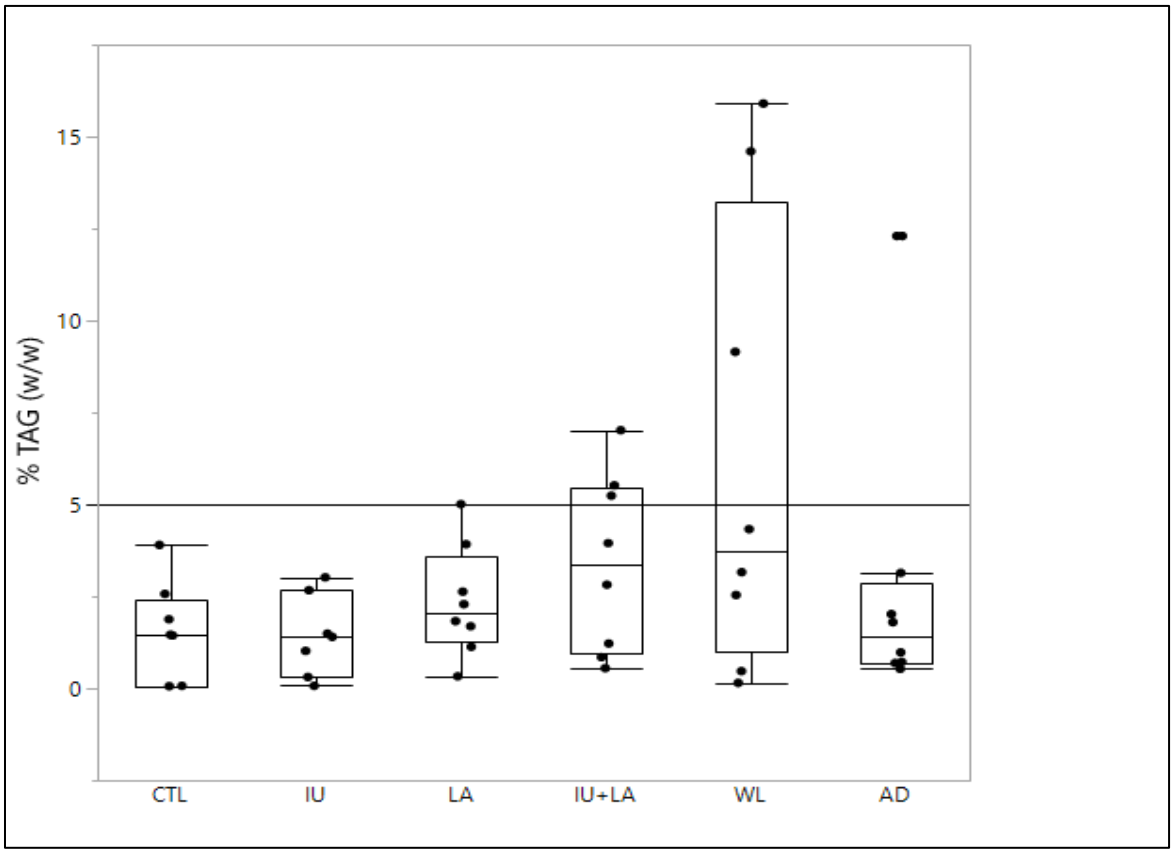

Figure 4.3: **Boxplot for triacylglyceride (TAG) levels in different treatment groups**. TAG concentrations (g TAG/100g liver) in liver for each individual mouse in each group are shown. Total number of samples=48 (offspring) for the TAG assay. n=8 for all 6 groups. Eight mice had TAG levels above 5%. Analysis performed by Vitas AS, Norway.

4.4 Gene expression RT-qPCR

In this master thesis, the transcriptional responses of a panel of 69 genes were studied. The genes were selected and examined based on their role in liver NAFLD. The KEGG pathway database was used to select genes involved in different signaling pathways (PPAR, insulin, Tnfα, Adipocytokine, NF-κB, oxidative stress) associated with liver steatosis/NAFLD. In downstream analysis, only those genes that passed the quality assurance criteria described in the Materials and Methods section were used. After data preprocessing and filtering, we ended up with a matrix of 48 genes × 59 samples, and this matrix was used for downstream analysis. The overview of the 48 genes is presented in Table 4.2.

.

Table 4.2: Overview of 48 genes included in Results and Discussion. Genes were grouped according to their function. *Significantly differentially expressed genes ($p \leq 0.05$); # Genes with borderline significant differences in expression

Gene symbol	Full gene name	Function
Genes related to liver steatosis		
Cd36	cd36 antigen	PPAR signaling pathway; fatty acid transport
Cyp2e1	cytochrome P450, family 2, subfamily e, polypeptide 1	Fatty acid metabolism; xenobiotics metabolism; high level in liver
Fasn	fatty acid synthase	Fatty acid biosynthesis
Nr1h2	nuclear receptor subfamily 1, group H, member 2	PPAR signaling pathway
Nr1h3	nuclear receptor subfamily 1, group H, member 3	PPAR signaling pathway; cholesterol metabolism
Pparα	peroxisome proliferator activated receptor alpha	PPAR signaling pathway; response to lipid
Pparδ*	peroxisome proliferator activated receptor delta	PPAR signaling pathway; response to lipid
Pparγ	peroxisome proliferator activated receptor gamma	PPAR signaling pathway; response to lipid
Pparγc1β	peroxisome proliferator activated receptor gamma, coactivator 1 beta	PPAR signaling pathway; response to lipid
Rxrα	retinoid X receptor alpha	PPAR signaling pathway; fatty acid oxidation
Scd1	stearoyl –Coenzyme A desaturase 1	PPAR signaling pathway; lipogenese
Srebf1	sterol regulatory element binding transcription factor 1	Transcriptonal activator; lipidhomeostasis
Genes related to oxidative stress response		
Cat	catalase	Enzyme; protects the cell from oxidative damage
Gpx1	glutathione peroxidase 1	Glutathione peroxidase family; protects cell from oxidative damage
Neil 1	nei endonuclease VIII-like 1 (E. coli)	DNA glycosylases; DNA repair
Neil3	nei endonuclease VIII-like 3 (E. coli)	DNA glycosylases; DNA repair
Nfe2l2 #	nuclear factor, erythroid derived 2, like 2	Transcription activator; response to oxidative stress
Sod1	superoxide dismutase 1, soluble	Antioxidant activity; cellular response to stress
Sod2	superoxide dismutase 2, mitochondrial	Antioxidant activity; cellular response to stress
Sod3	superoxide dismutase 3, extracellular	Antioxidant activity; cellular response to stress
Genes related to general development/function		
Hnf4α #	hepatic nuclear factor 4, alpha	Transcription factor; development of liver, pancreas and intestines, maintain glucose homeostasis
Lepr	leptin receptor	Cytokine receptor; involved in energy metabolism and body weight through hypothalamus effect
Lipe	lipase, hormone sensitive	Insulin signaling pathway; regulation of lipolysis in adipocytes
Lpin1	lipin1	Key lipid metabolism regulator
Ulk1	unc-51 like kinase 1	Involved in metabolic stress signals to the autophagy machinery
Ulk2	unc-51 like kinase 2	Involved in metabolic stress signals to the autophagy machinery

Table 4.2 continued: Overview of 48 genes included in Results and Discussion. Genes were grouped according to their function. *Significantly differentially expressed genes ($p \leq 0.05$); # Genes with borderline significant differences in expression

Gene symbol	Full gene name	Function
Genes related to insulin response		
Cebpα	CCAAT/enhancer binding protein (C/EBP), alpha	Transcription factor; adipogenesis, lipogenesis and insulin sensitivity
Cebpβ	CCAAT/enhancer binding protein (C/EBP), beta	Transcription factor; adipogenesis, lipogenesis and insulin sensitivity
Grb2	growth factor receptor bound protein 2	Insulin signaling pathway; part of MAPK signaling pathway
Gsk3β	glycogen synthase kinase 3 beta	Insulin signaling pathway; glucose homeostase, insulin resistance
IGF-1	insulin-like growth factor 1	Promote growth and development during fetal and postnatal life; mainly expressed in the liver
Igf2	insulin-like growth factor 2	Promote growth and development during fetal and postnatal life; paternal imprinted gene
Insr #	insulin receptor	Insulin signaling pathway; receptor tyrosine kinase family
Irs1	insulin receptor substrate 1	insulin signaling pathway; roles in metabolic and mitogenic pathways
Genes related to glucose regulation		
Akt2	thymoma viral proto-oncogene 2	AKT kinase; regulation of glucose
Fgf21	fibroblast growth factor 21	Stimulates glucose uptake in adipocytes
G6pc	glucose-6-phosphatase, catalytic	Insulin signaling pathway
Mlxip	MLX interacting protein	Insulin resistance; response to cellular glucose levels
Slc2a2 *	solute carrier family 2, member 2	Insulin signaling pathway; transfer glucose between liver and blood
Slc2a4	solute carrier family 2, member 4	Insulin signaling pathway; insulin-regulated glucose transport in adipose tissue
Genes related to inflammation		
Il4	interleukin 4	Cytokine; cell signaling; humoral and adaptive immunity
Il6rα	interleukin 6 receptor, alpha	Part of Il6 receptor complex; role in immunological response
Il10 *	interleukin 10	Anti-inflammatory cytokine; both innate and adaptive immune system
Il33	interleukin 33	Cytokine; cell signaling; humoral immune reponse
Nfκb1	nuclear factor kappa b subunit 1	Tnf signaling pathway; immunological response to infections
Socs3	suppressor of cytokine signaling 3	Tnf signaling pathway; regulates cytokine signal transduction
Tnfα	tumor necrosis factor alpha	Tnf signaling pathway; cytokine –cytokine receptor interaction. Also known as Tnf-alpha
Tnfrsf1a #	tumor necrosis factor receptor superfamily, member 1a	Tnf signaling pathway; cytokine –cytokine receptor interaction

4.4.1 RNA quality assessments

RNA with high quality is essential for downstream gene expression analysis. To ensure acceptable RNA quality of the samples, we analyzed the RNA samples with NanoDrop and Agilent 2100 Bioanalyzer to estimate their concentration and evaluate their purity and integrity.

RNA with high quality is essential for downstream gene expression analysis. To ensure acceptable RNA quality of the samples, we analyzed the RNA samples with NanoDrop and Agilent 2100 Bioanalyzer to estimate their concentration and evaluate their purity and integrity.

The liver samples varied in size due to technical performance of cutting the liver, and this resulted in total RNA concentrations from 285 ng/µL to 1885 ng/µL measured at NanoDrop. The RNA y**ie**ld (µg/mg) ranged from 0.36 µg/mg to 2.90 µg/mg liver weight in all 71 samples. The 59 samples that passed quality assurance, all of them ha $A_{260}/_{280}$-ratio greater than 1.8 indicating RNA with acceptable purity for downstream applications. However, the $A_{260}/_{230}$ ratios were more varying. Sixteen samples had $A_{260}/_{230}$ ratios below 1.8. The RNA integrity for the mice liver samples was checked by assessing the RIN numbers, where 10 is the top score and suggests the least degraded RNA, and 5 is viewed as the lowest acceptable RIN number. Twelve RNA samples had RIN numbers lower than 5, and these samples were removed from downstream analysis. This made the number of accepted mice liver samples in the study to be 59 samples in total. The grouped mean and SE for the results are provided in Table 4.3.

A chapter of RNA quality assessments and what to reflect on is found in chapter 5.6.2. Appendix C2 Table A.2 gives an overview of all samples and results from isolation and measurements by NanoDrop and Agilent 2100 Bioanalyzer.

Table 4.3: Liver total RNA yield, purity and integrity for all mice groups. The results are expressed as mean ± SE. Some groups showed lower RIN values than the total sample numbers due to not available (NA) RIN numbers.

Group	Treatment	RNA yield µg/mg liverweight	OD 260/280 ratio	OD 260/230 ratio	RIN value
CTL	10% fat throughout life - control group n=12/11 (RIN value)	0.93 ±0.15	2.09 ±0.03	1.82 ±0.09	5.83 ±0.54
IU	45% fat *in utero* n=12	1.32 ±0.18	2.08 ±0.01	1.87 ±0.05	6.04 ±0.46
LA	45% fat during lactation n=11/10 (RIN value)	0.93 ± 0.11	2.10 ±0.02	1.89 ±0.05	6.73 ±0.11
IU+LA	45% fat *in utero* and during lactation n=12/10 (RIN value)	1.16 ±0.22	2.06 ±0.02	1.81 ±0.08	6.60 ±0.35
WL	45% fat throughout life n=12	1.52 ±0.20	2.12 ±0.01	2.00 ±0.07	6.14 ±0.52
AD	45% fat as adults n=12	1.41 ±0.21	2.09 ±0.03	2.04 ±0.0	6.54 ±0.43
Average of all groups	All n=71/67(RIN value)	1.21 ±0.08	2.09 ±0.0)	1.91 ±0.03	6.30 ±0.18

4.4.2 Relative gene expression

The transcript level of some of the genes studied displayed alteration by the HFD exposure. Out of 48 target genes analyzed, three genes had a significant change in gene expression compared to the control group, and four genes showed borderline significant differences in expression compared to the control group. Due to high within-treatment group variability, few genes were found to have significantly different expression when compared to the control group. Then, the genes of interest were grouped based on their involvement in the various signaling pathways. The results are presented in Figures 4.4-4.9.

Genes related to liver steatosis

Twelve genes were analyzed to explore the potential impact on HFD for gene expression connected to liver steatosis. Figure 4.4 shows a statistically significantly up-regulated *peroxisome proliferator activated receptor* δ (*Pparδ)* gene in the LA group compared to control group (p=0.046). Further, regarding the Pparδ gene, the groups IU and IU+LA also showed up-regulated expression compared to the control group, although these differences were not statistically significant. None of the other genes in the group related to hepatic lipid metabolism were significant up- or down-regulated compared to the control group. For other similar genes analyzed belonging to the PPAR signaling pathway; such as *Pparγ* and *Pparγc1β*, there were suggested similar patterns in expression, although the difference were not significant. In Figure 4.4, the results indicated up-regulations of the *Cd36* gene in the following groups compared to the control: IU, LA and WL. The results indicated down-regulations of the *Scd1* gene in the following groups compared to control: LA, IU+LA and AD.

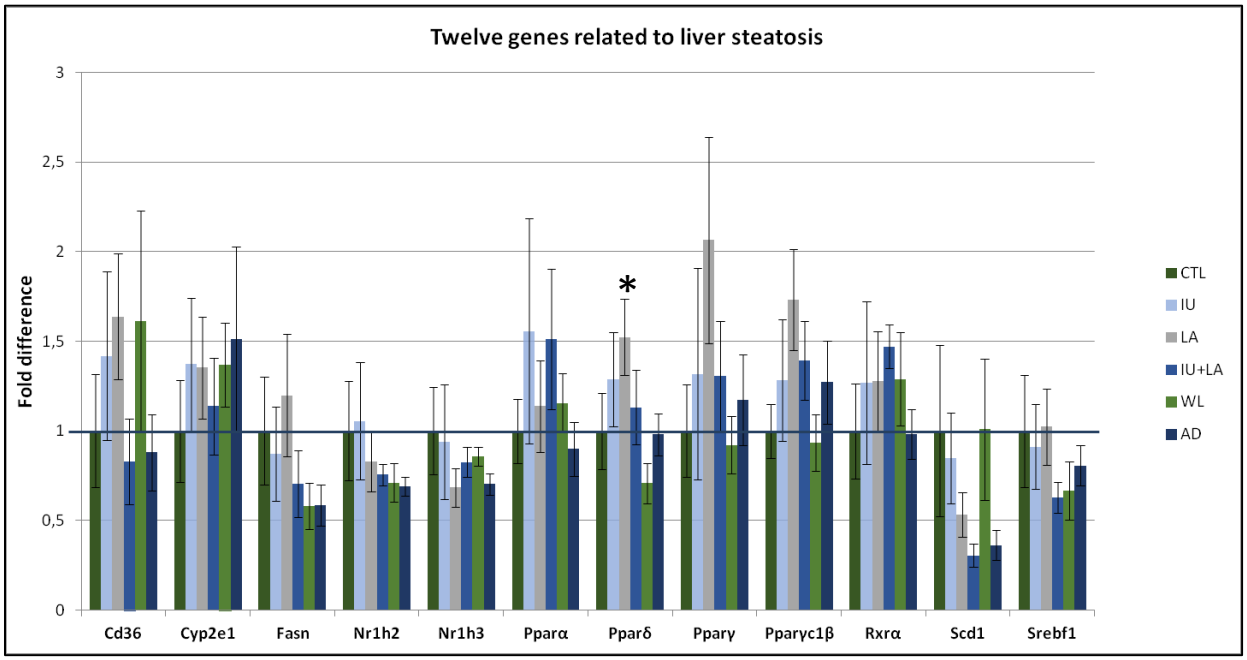

Figure 4.4: High fat diet (HFD) exposure effect on transcriptional levels of a selection of 12 genes related to liver steatosis in mice livers during different life stages covering *in utero* to adult life. Each value represents mean of the group ±SE. Total number of samples = 59 (offspring). CTL, n = 9; IU, n = 10; LA, n =10; IU+LA, n =9; WL, n =10; AD, n =11. * Significantly different from control group with a significance level p <0.05.

Genes related to inflammation

Eight genes were analyzed to explore the potential impact on HFD for gene expression connected to inflammation (Figure 4.5). Figure 4.5 shows a statistically significantly up-regulated *interleukin Il10* (*Il10)* gene in the IU group compared to control group (p=0.035). This significant result was reported only in the Dunnett 2-sided test. In addition, the *tumor necrosis factor receptor superfamily, member 1a* (*Tnfrsf1a)* gene, showed borderline significant differences in expression in the IU+LA group compared to the control group (p=0.063). None of the other genes in the HFD groups were statistically significantly up- or down-regulated compared to the control group. The bars in Figure 4.5 showed up-regulations in especially the early developmental phases for the different genes involved in inflammation processes, even though the findings were not significant.

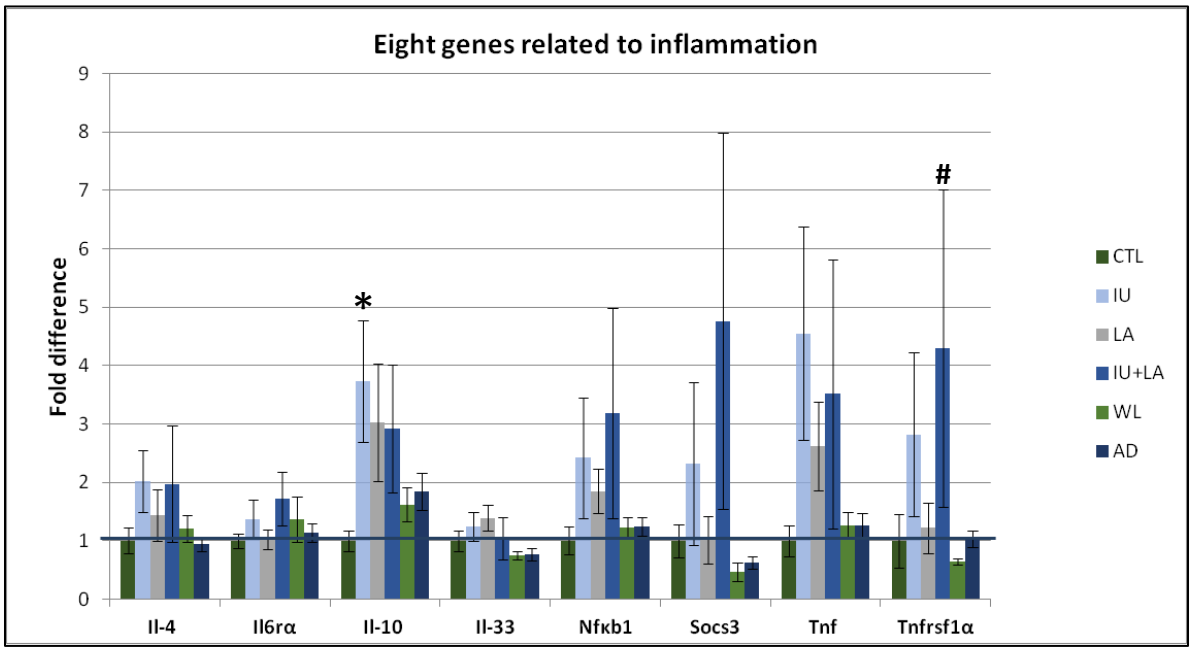

Figure 4.5: High fat diet (HFD) exposure effect on transcriptional levels of a selection of 8 genes related to inflammation in mice livers during different life stages covering *in utero* to adult life. Each value represents mean of the group ±SE. Total number of samples = 59 (offspring). CTL, n = 9; IU, n = 10; LA, n =10; IU+LA, n =9; WL, n =10; AD, n =11. # Borderline significantly different from control group with a significance level p=<0.05. The significantly difference in the *Il10* gene was reported only in the Dunnett 2 sided test.

Genes related to oxidative stress response

Eight genes were analyzed to explore the potential impact on HFD for gene expression connected to oxidative stress response (Figure 4.6). The *nuclear factor erythroid derived 2 like 2* (*Nfe2l2)* gene in the LA group showed borderline significant differences in expression compared to control group (p=0.053). None of the other genes were statistically significant up- or down-regulated in the HFD groups compared to the control group. In figure 4.6 the results indicates down-regulations of the *Cat* gene in the following groups compared to control: IU+LA, WL and AD, but the differences were not statistically significant.

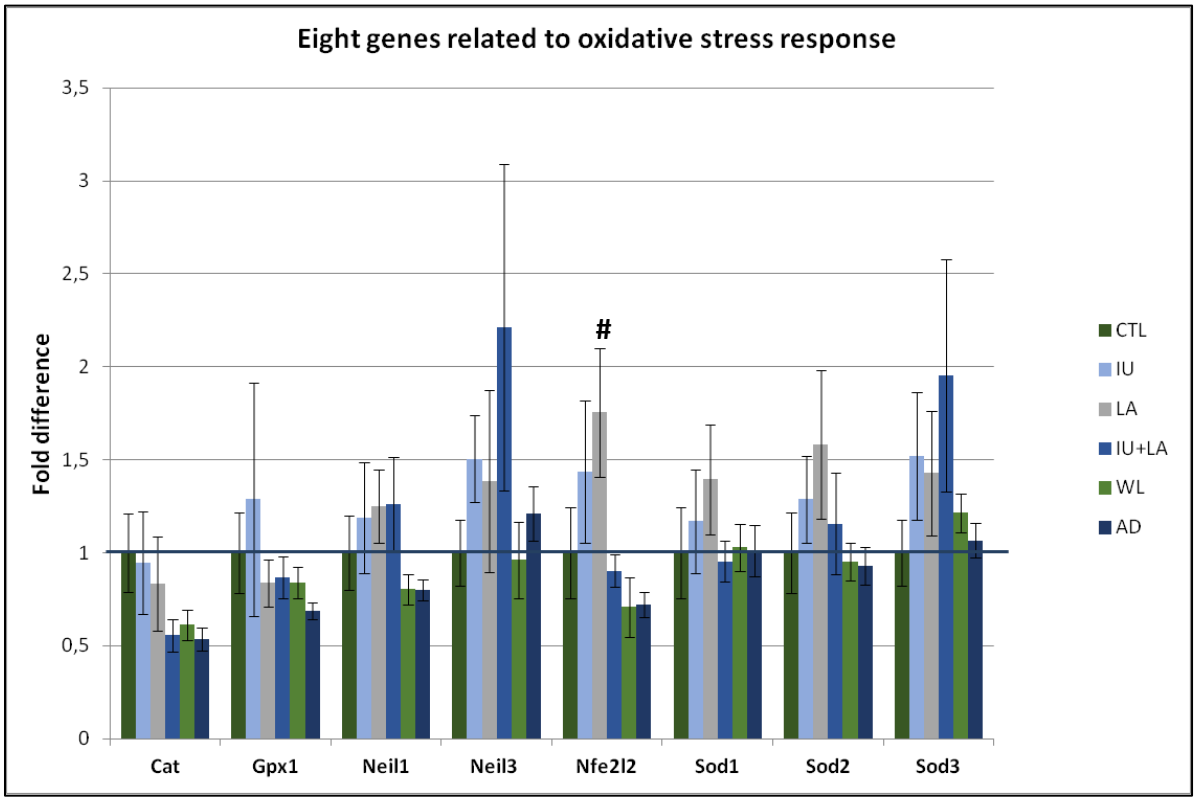

Figure 4.6: High fat diet (HFD) exposure effect on transcriptional levels of a selection of eight genes related to oxidative stress response in mice livers during different life stages covering *in utero* to adult life. Each value represents mean of the group ±SE. Total number of samples = 59 (offspring). CTL, n = 9; IU, n = 10; LA, n =10; IU+LA, n =9; WL, n =10; AD, n =11. # Significantly different from control group with a significance level p <0.05.

Genes related to general development/function

Six genes were analyzed to explore the potential impact on HFD for gene expression connected to general development/function (Figure 4.7). The *hepatic nuclear factor 4 alpha* (*Hnf4α)* gene in the LA group showed borderline significant increased expression compared to the control group (p=0.073). None of the other genes were statistically significant up- or down-regulated in the HFD groups compared to the control group.

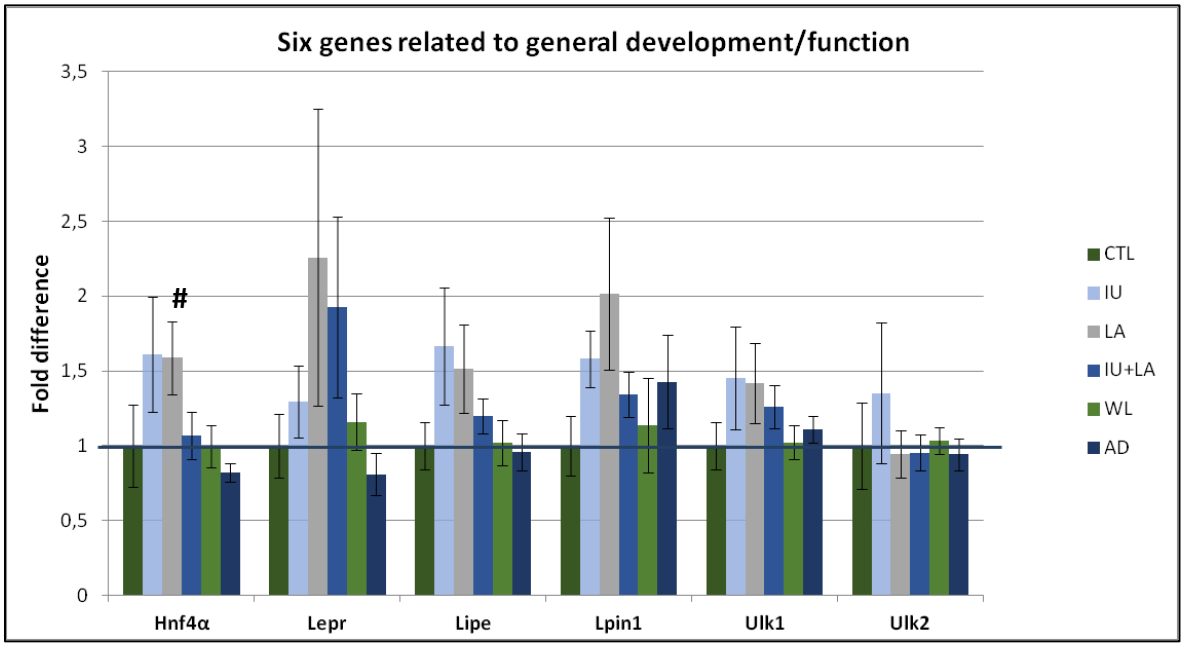

Figure 4.7: High fat diet (HFD) exposure effect on transcriptional levels of a selection of six genes related to general development/function in mice livers during different life stages covering *in utero* to adult life. Each value represents mean of the group ±SE. Total number of samples = 59 (offspring). CTL, n = 9; IU, n = 10; LA, n =10; IU+LA, n =9; WL, n =10; AD, n =11. # Borderline significantly different from control group with a significance level p <0.05

Genes related to insulin response

Eight genes were analyzed to explore the potential impact on HFD for gene expression connected to insulin response (Figure 4.8). The *insulin receptor* (*Insr)* gene in the IU and IU+LA group showed borderline significant differences in expression compared to the control group (p=0.097 and p=0.103 respectively). The results in the groups IU, LA and AD also suggested a major up-regulated expression of *Insr* compared to the control group, although these differences were not significant. None of the other genes in the groups were statistically significant up- or down-regulated compared to the control group. In Figure 4.8 the *Irs1* gene showed the same patterns of non-significant up-regulations as for the *Insr* gene in the following groups compared to the control: IU, LA, IU+LA and AD. The results also indicated a non-significant up-regulation of the *Igf1* gene in the LA group.

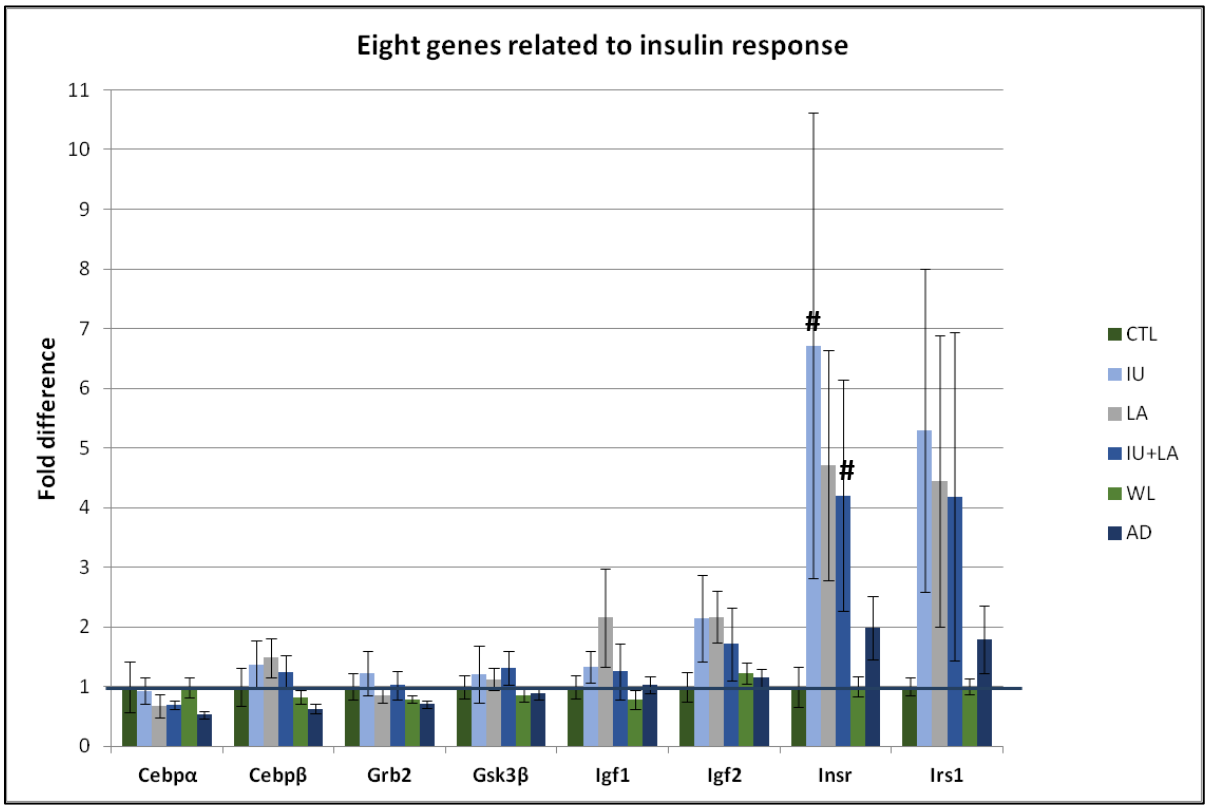

Figure 4.8: High fat diet (HFD) exposure effect on transcriptional levels of a selection of eight genes related to insulin response in mice livers during different life stages covering *in utero* to adult life. Each value represents mean of the group ±SE. Total number of samples = 59 (offspring). CTL, n = 9; IU, n = 10; LA, n =10; IU+LA, n =9; WL, n =10; AD, n =11. # Borderline significantly different from control group with a significance level p <0.05

Genes related to glucose regulation

Six genes were analyzed to explore the potential impact on HFD for gene expression connected to glucose regulation (Figure 4.9). Figure 4.9 shows a statistically significantly up-regulated *solute carrier family 2 member 2* (*Slc2a2)* gene in the IU+LA group compared to control group (p=0.040). The results in the groups IU and LA also suggested a up-regulated expression of *Slc2a2* compared to the control group, although these differences were not significant. The *Slc2a2* gene which is also involved in the insulin-pathway, suggested similar patterns for up-regulations as for the *Insr* and *Irs1* genes (Figure 4.8).

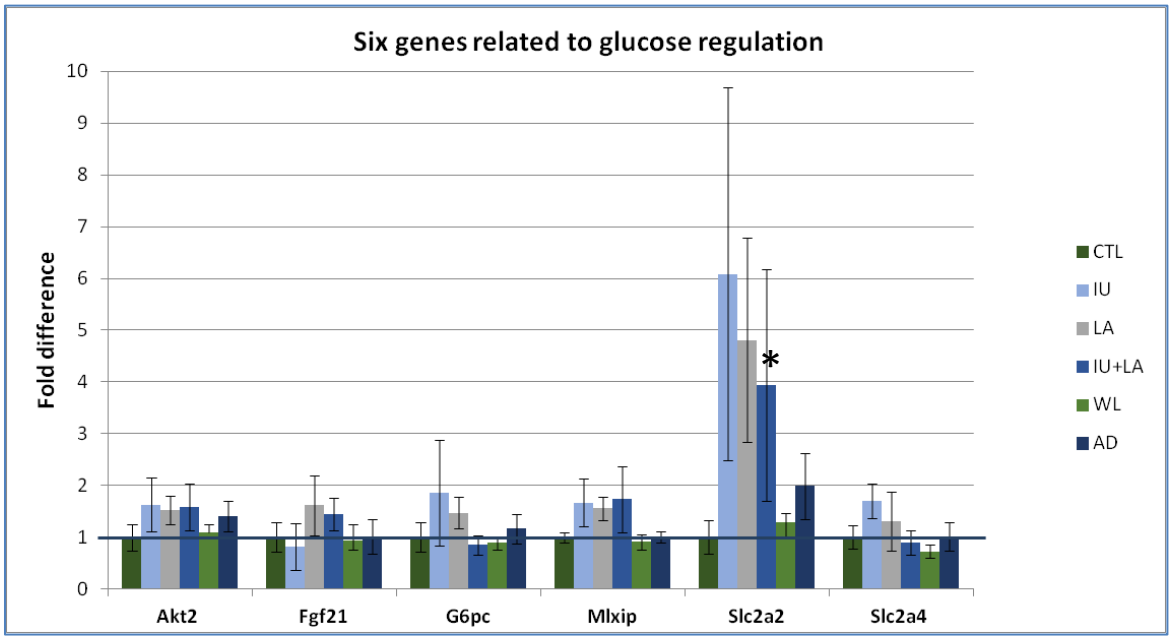

Figure 4.9: High fat diet (HFD) exposure effect on transcriptional levels of a selection of six genes related to glucose regulation in mice livers during different life stages covering *in utero* to adult life. Each value represents mean of the group ±SE. Total number of samples = 59 (offspring). CTL, n = 9; IU, n = 10; LA, n = 10; IU+LA, n = 9; WL, n = 10; AD, n = 11.

Statistics were also run based on litters as the statistical unit. In the IU+LA group, the *Insr* gene showed borderline significant differences in expression compared to the control group (p=0.054). The *Nfe2l2* gene came up as a weak borderline result (p=0.080). The other genes gave no significant results of the HFD groups compared to the control (p≤0.05). Compared to the results using the mean of the offspring in each group with two significant and three borderline statistically significant results on gene expression, the data evaluated with litter as the statistical unit had one significant and one borderline result. Number of litters: n=42. CTL=7; IU=6; LA=7; IU+LA=7; WL=7; AD=8.

4.5 Correlation data

Statistical analysis was performed to investigate potential correlations between BMI and liver lipids or mRNA expression (Table 4.4). Table 4.4 show a relatively high correlation between BMI and liver TAG, and moderate correlations between BMI and mRNA expression levels of *Igf1*, *Socs3* and *Tnfα*.

Table 4.4: Spearman's Rank order correlation for BMI data compared to liver TAG and mRNA expression levels. Only statistical significant correlations are shown.

Variable 1	Variable 2	Spearman's correlation coefficient (rho)	Significance level (p)
BMI	*Igf1*	0.36	0.0070
BMI	TAG (lipid)	0.54	0.0002
BMI	*Socs3*	0.35	0.0096
BMI	*Tnfα*	0.29	0.0303

5 Discussion

Accumulating evidence points to overeating as one of the major reasons for the high prevalence of liver steatosis worldwide appearing at increasingly younger age. The spectrum of NAFLD ranges from isolated steatosis to NASH with accompanying complications (71). The liver steatosis as an isolated condition is usually viewed as a benign condition, but in 20-30% of the of cases, simple steatosis develops to NASH (33). The primary goal of this study was to assess which cell signaling pathways may contribute to the development of liver steatosis and NAFLD following HFD exposure during various life stages. The signaling pathways contributing to NAFLD are connected in a complex network. Activation or inhibition of these signaling pathways depends on the exposure and the developmental life stage. In this thesis, candidate genes involved in NAFLD associated signaling pathways were selected, and then, categorized into several functional groups (Table 4.2). The transcriptional levels of this gene panel were examined in liver samples from mice exposed to HFD during different life stages and compared with samples from mice on CD by qPCR analysis. Moreover, to be able to link potential changes in signaling pathways to physiological differences, body weight, liver lipid levels and serum IGF-1, were also evaluated.

5.1 Analysis of weight data after HFD exposure

Animal models showed that exposure to maternal obesity and HFD intake caused greater post-natal weight gain, TBW and adiposity in offspring compared to animals fed standard chow (55, 56, 108, 109). All groups showed a higher TBW compared to the control group, though the results were not significant higher. All HFD groups showed a tendency of a higher ALW compared to the control group and in the IU group the RLW was significantly higher compared to the control group. Increased liver weight in the IU group was also observed in the main study in which a significantly higher ALW was observed in the IU and UL groups compared the mice given a HFD as adults or throughout life (3). As discussed below, there was no increase in lipid accumulation in the IU group. There must consequently be other explanations for the increase in liver weight observed, as e.g. liver hypertrophy, but this has not been examined in the current study.

5.2 Analysis of lipids in liver after HFD exposure

5.2.1 TAG measurement

TAG is the most abundant type of fat in fatty livers, and lipid accumulation within hepatocytes that exceeds 5% of liver weight is one definition of simple liver steatosis (24, 29, 110).

TAG level in liver from the different treatment groups suggest an increasing degree of liver accumulation of TAG in the LA period, with further increases in the IU+LA and WL groups. The WL was the group with highest TAG concentration in the liver; however the results did not reach statistical significance which may be explained by the large variability of TAG accumulation between animals within this group. Further, the results showed that the LA, IU+LA, WL and AD groups all had mice represented in their groups that met the criteria of liver steatosis. In the WL group three mice had TAG levels between 9% and 16%; which means a mild steatosis if compared to grading of steatosis in humans proposed in Table 1.1 in the introduction chapter. Percentages of animals with steatosis defined as >5% TAG were 8.3% (1 of 8 animals), 37.5% (3 of 8 animals), 37.5% (3 of 8 animals) and 8.3% (1 of 8 animals) in LA, UL, WL, AD respectively. These findings are supported by other studies were HFD increased levels of TAG with development of liver steatosis in mice as adults (69, 111, 112). Even though the IU group demonstrated the same TAG mean level as the control group, a study of nonhuman primates suggested that prenatal HFD disturbed the lipid metabolism in a way that gave rise to a lifelong pre-disposition for NAFLD (93, 113). This might suggest an altered lipid metabolism in the liver for offspring fed HFD through the diet of the dam. This is also underpinned by studies showing that mice offspring of dams exposed to HFD during IU and LA developed hypercholesterolemia, adiposity, IR and hepatosteatosis (56, 114). Of note, the WL group had a higher TAG liver content than the AD group, supporting the notion that in utero exposure predispose the mice to liver steatosis. A study by Ashino et al indicated that in 82-day old mice offspring of dams fed a 45% HFD, there was an increase in the level of the lipogenic protein acetyl-CoA carboxylase which through a chain of interactions leads to decreased β-oxidation capacity (46). This finding suggests an increased susceptibility of offspring exposed to HFD *in utero* to NAFLD through reduced FFA oxidation capacity. We observed a moderate positive correlation between liver TAG and BMI

(rho=0.54). This likely reflects an increased level of circulating lipids in the obese animals leading to higher FFA uptake up by the liver, and increased liver TAG production and storage (111).

5.2.2 FFA measurement

FFA in liver is rapidly converted to TAG for storage in lipid droplets or eliminated via β-oxidation or secreted by VLDL (71, 93). Several studies in humans supported this by results suggesting that FFA levels were not altered in the liver in patients with NAFLD (115, 116). No significant differences in FFA results compared to the control group were observed in the present study. The AD group showed a higher mean level of FFA compared to the other groups. However, the results for this group revealed a high within-group variation due to a markedly elevated FFA concentration in one single animal.

5.2.3 Cholesterol measurement

Liver Free Cholesterol (FC) accumulation is relevant to the pathogenesis of NAFLD/NASH (71). FC and CE were analyzed in our study to see if the levels were affected due to HFD exposure. There were no significant differences between the groups, but one animal had increased level of FC in the WL group compared to the other overall results. Due to one single observation it is difficult to suggest whether this is representative for a HFD treatment throughout life. Thus, the pairwise comparison between the WL group and the AD group that revealed significantly higher levels in the WL group should be interpreted with care. FC is considered to be an essential lipotoxic molecule crucial in the development of experimental and human NASH, and increased FC levels have been seen in NASH but not simple steatosis (116). A study in humans found that FC showed a stepwise increase from the control group to NAFLD and to NASH (115). A study in mice linked hepatic accumulation of FC rather than TAG towards hepatocyte death and liver damage (111). FC is suggested to be an important factor for disease progression from simple liver steatosis to NASH (71). Ioannou and co-workers have suggested that many mechanisms protects against excessive FC rise in liver, and one suggested solution was esterification of FC to a more inert Cholesterol ester (CE) by Acetyl-co-enzyme A acetyltransferase 2 (116). Our results suggested a slight increase in CE levels in all HFD treated groups compared to the control, but the difference between the diet groups did not reach statistical significance. Studies

suggested that the CE concentration in liver do not appear to be increased in human NAFLD (115, 117).

5.3 Analysis of IGF-1 in serum after HFD exposure

Most of the circulating IGF-1 is synthesized by the liver and is regulated by GH (74). In our study the IU group showed a borderline significant increase and the WL group a significantly increase of serum IGF-1 compared to the control, whereas the other HFD groups showed only modest increases. This suggests an impact of HFD treatment on systemic IGF-1, which may depend on both pre- and post-natal exposure conditions. A study proposes that HFD in itself, regardless of overweight, increases systemic IGF-1 levels (118). A study in humans showed that lower serum IGF-1 was associated with NASH, but not with liver steatosis. The distinction could be related to whether inflammation was present or not (74). A humans study suggested that IGF-1 has an anti-inflammatory impact on hepatocytes (76). A study in mice reported that IGF-1 has an protective effect on steatosis and inflammation and improves oxidative stress and mitochondrial function in the liver (77). However, as reviewed by Lewitt and co-workers, there are conflicting results from different studies whether obesity caused by HFD increases or decreases the IGF-1 level (119).

5.4 Gene expression changes after HFD exposure

In this thesis, the transcriptional response of a panel of 69 genes following exposure to HFD in different life stages was evaluated by qPCR. The genes were selected based on their role in NAFLD associated signaling pathways. There are many variables in a RT-qPCR set-up that can influence the qPCR assays, and it is important to have in mind what other factors can impact the results. After quality assessment of the qPCR analysis of the 69 genes; 48 genes were included for result evaluation. There was relatively high within-treatment group variability in the analysis performed. Later in this discussion chapter the technical and biological variables to consider when evaluating the gene expression results will be mentioned. The gene expression analysis showed three genes with significantly higher expression (*Il10*, *Pparδ* and *Slc2a2*) and four genes with a borderline significantly higher expression (*Hnf4α*, *Insr, Nfe2l2* and *Tnfrsf1α*) compared to the control group. In addition, the FD results showed some tendencies that are included in a wider discussion on which signaling pathways in liver are changed due to HFD exposure during various life stages.

5.4.1 Genes related to liver steatosis

Liver steatosis is often referred to as the first hit in the two hit and multi hit hypotheses of development of NAFLD (31, 34). Twelve genes that were grouped under liver steatosis were analyzed. Of these, the expression of the *Pparδ* gene was significantly higher in the LA group compared to the control. Dietary lipids regulate activity of PPAR transcription factors and induce an increase in the expression of their target genes (120). All genes belonging to the PPAR signaling pathway (including *Rxrα* that encodes the retinoid X receptor alpha that form heterodimers with all PPARs) and the Pparγ co activator *Pparγc1β* showed up-regulation in the early life stages (IU, LA and IU+LA). A study proposes that high expression of *Pparδ* in the liver can be a reaction to excessive accumulation of lipids, and/or products of oxidative stress, and/or pro-inflammatory mediators, to prevent hepatic IR and to limit further *de novo* lipogenesis (121, 122). None of the other eleven genes grouped under liver steatosis showed significant differences.

5.4.2 Genes related to oxidative stress response and inflammation

Proposed hits involved in NAFLD progression include oxidative stress and inflammation (31, 111, 123). We analyzed eight genes related to oxidative stress response and eight genes related to inflammation. The *Nfe2l2* gene, also known by the name *Nrf2*, showed a borderline significantly increased expression in the LA group compared to the control. The *Nfe2l2* gene is a transcription factor that binds to antioxidant-responsive elements (ARE) and have shown to activate transcription of several anti-oxidative genes and involvement of reducing the concentration of ROS (124-127). Several studies have suggested the *Nfe2l2* gene to protect hepatic cell from oxidative damage during development of NAFLD (124, 127).

Our results also showed a borderline significant higher difference in expression for the *Tnfrsf1a* gene in the IU+LA group compared to the control. The pro-inflammatory cytokine Tumor necrosis factor (Tnf-α) exerts its biological responses by binding to cell surface receptors, including Tnfrsf1a, and studies have suggested that cytokines like Tnf-α and its receptors are higher in liver in NASH patients (68). It has been proposed that FFA induces the production of Tnf-α (67). A study argued that it might be dietary factors like HFD, which initiated inflammatory response in the liver (111). A suggestion of disturbance in the

cytokine-balance can be implied by the miRNA project at NIPH (personal communication) which suggest moderate increased levels of serum Tnf-α in mice from all HFD groups involving *in utero* exposure, but not in the LA and AD groups.

In addition the results revealed a significant higher difference in expression of the *Il10* gene in the IU group compared to the control. This result (p=0.035) was only shown in the Dunnett 2 sided test, and the ANOVA result provided p=0.160. We decided to report this result given the Dunnett 2 sided test functions as a stand-alone test regardless of ANOVA results. Il-10 is an anti-inflammatory cytokine that dampens inflammations (128). The Il-10 serum level have been seen decreased in a human study with NAFLD, and a proposed cause was a chronic low-grade of inflammation in the patients (129). Another study of adipose tissue in mice observed decreased level of the *Il10* gene in diet-induced obesity together with high levels of genes encoding TNF-α (130). They also showed high expression of the *Il10* gene in the lean mice. The study proposed that Il-10 protects against inflammation in the adipose tissue. In our study the high level of the *Il10* gene indicates a protective effect

5.4.3 Genes related to liver insulin response

Excessive accumulation of TAG in hepatocytes has been shown to be strongly associated with IR (131) and IR is an important feature for developing liver steatosis (30). We analyzed eight genes involved in insulin signaling. Of these, the insulin receptor (*Insr*) gene in the IU+LA group showed borderline significant increased expression compared to the control group, and the other early developmental groups also showed a tendency of up-regulation. The insulin receptor (INSR) interacts with the insulin receptor substrate 1 (IRS-1) in the insulin signaling pathway (132). The *Irs1* gene showed similar pattern as the *Insr* gene, supporting a modification of the insulin signaling pathway in response to HFD. This suggestion can be supported by results from the adipose tissue study at NIPH (personal communication) which showed increased level of serum insulin in the HFD exposed mice (significant positive trend in relation to number of days exposed to a HFD).

5.4.4 Genes related to glucose regulation

In an insulin resistant liver gluconeogenesis is increased due to impaired insulin signaling which normally inhibits gluconeogenesis. This may lead to hyperglycemia and

hyperinsulinemia (30). Six genes were analyzed to assess potential changes in glucose regulation in the different life stages due to HFD exposure. Of these, the *Slc2a2* gene in the IU+LA group showed significant increased expression compared to the control group (p=0.040), and the other early life stages also showed a tendency of up-regulation (p=0.211 for both IU and LA groups). A study in mice revealed increased level of *Slc2a2*/GLUT2 in mice liver showing IR (133). In addition to increased gluconeogenesis, the HFD mice offspring might also be prone to impaired glucose tolerance as suggested in the main obesity study at NIPH (3). The *Slc2a2* gene, with the protein product known as GLUT2, plays an important role in liver glucose flux (133). The GLUT2 protein has shown to transport glucose bidirectionally in the hepatocytes (134). Several studies have suggested that the transport direction of glucose was dependent on the substrate concentration gradient that changes according to food-intake. Hence, the indirect connection between insulin and glucose levels (133, 135) Our results may indicate the same phenomena as the *Slc2a2* gene showed the same expression as the *Insr* gene with increased expression following HFD exposure in the early life stages (Figure 4.8).

5.4.5 Genes related to general development/function

The genes in this group have various functions related to a general liver development and function. Of the six genes analyzed, the Hnf4α gene in the LA group showed a borderline significant increase in expression compared to the control group. The IU group also showed similar up-regulation, but this was not a statistical significant result (p=0.108). A few studies suggested that Hnf4α regulated the transcription of genes involved in the NAFLD progression through lipid metabolism and oxidative stress (123, 136). Hnf4α regulates the gene *Hnf1α*, which is an additional transcription regulator involved in lipid metabolism, but the expression of this gene was not examined in the present study.

5.5 Differences in susceptibility for development of liver steatosis dependent on life stages of exposure to HFD

Included in the main goal was to assess which of the various life periods could be more susceptible for development of liver steatosis due to the HFD treatment. Fetal programming is a known phenomena from years of research, and the research involved around DOHaD hypothesis have generated strong support for the notion that the earliest period of a life is

crucial for further development regarding health (39, 40, 42, 137). However, the contribution of dietary stress in different life stages to NAFLD susceptibility of the adult is less clear.

The TAG measurements showed higher mean level in the IU+LA and WL groups compared to the AD group. Also, a higher number of animals showed liver steatosis; 37.5% in the IU+LA ant the WL versus 8.3% in AD. This suggests that the *in utero* exposure period is especially important for the susceptible to develop steatosis as an adult. Also it seems that a period of post-natal exposure is required for the phenotype to be revealed as the IU group did not show an increased accumulation of liver lipids.

In some cases, the response in the IU+LA groups appeared to lower than in the IU group, as observed for serum Igf-1 (and also glucose tolerance data as presented by Ngo and co-workers (3). If correct, this finding suggests that exposure during lactation may protect against some of the changes observed after *in utero* exposures.

For the mRNA analysis, the significant and borderline significant genes showed an overall more marked increased in expression in the early developmental life stages compared to animals exposed throughout life or as adults. These observations underline the complexities of fetal programming and the importance also of post-natal conditions for modulation of gene expression and physiological adaptations.

5.6 Overall considerations regarding this study

This study has involved liver and serum samples from mice, different laboratory workflows and data processing. Here, we review some technical and biological variables to consider when evaluating the results.

5.6.1 Mice as an animal obesity model

Mice do not imitate completely the true human situation, and this is a limitation of animal studies in general. DIO is one of the most used models in rodents to explore obesity related questions. However, DIO is not a standardized model, thus different DIO studies vary e.g. in regards to fat percentage in the diet which is usually between 45% and 60% (as kcal from fat). The 60% diet is likely to be significantly more severe than the 45% diet. Furthermore, increasing the total percentage of lipids in the diet leads to a decrease of other nutrients,

hence there may be difficulties in interpreting if experimental results can be ascribed to an increase of one or a decrease of another macronutritient (93). Interpretation may be further challenged due to the fact that many DIO protocols do not used matched control and HFD diets, thus introducing further experimental variability.

In most maternal exposure studies, dams are put on HFD to build obesity before mating which might give different results from studies in which HFD exposure starts at mating (94, 138). In our study, the HFD contained 45% fat, and the dams were on regular diet (with approximately 10% fat) before mating. The HFD diet contained 45% kcal from fat and was matched to the control diet with an exchange of carbohydrates with fat. In addition, the HFD and the control diet were matched on protein, vitamin and minerals.

We observed marked biological variability, not only between but also within each treatment group. Biological variability was high for TAG accumulation (shown in Figure 4.3), especially in the WL and AD groups that appeared to have some "high response" animals. The social structures between the animals in one cage may influence dietary intake and thus contribute to variability in such feeding experiments.

5.6.2 Methodological aspects in gene expression

In the gene expression analysis data a high intra-group variability was also observed and this variability may have both biological and technical origin. In this project, variability that may originate from technical sources has been thoroughly evaluated. RNA is a highly sensitive molecules and easily exposed to degradation through RNases, and caution in every step of the gene expression analysis need to be taken (139). In 2009 the guidelines "Minimum information for publication of quantitative real-time PCR experiments" (MIQE) were published as an aid to document all the important steps in a study using real-time PCR experiments (140). The MIQE guidelines can be a good tool to provide the important conditions in a study for the public readers (141).

Pre-analytical steps are important to consider when evaluating the qPCR data. Tissues are more vulnerable for RNA degradation through the sampling and extraction procedure. A suggested reason can be the solid and rough structure of the tissue, the RNase enzymatic activity and problems during thawing, cutting and lysis process. Tissue-matrix effect is also relevant in RT-qPCR. Hemoglobin, fat, glycogen and DNA-binding proteins can inhibit the

reverse transcriptase as well as the PCR (103). Tissues like liver are rich in nucleases which may degrade RNA faster and more comprehensively than tissues like heart or muscle (142).

In relative quantification studies, the focus is often to compare the difference in expression of a particular gene between different conditions. A sample maximization method is suggested as the proper strategy, where as many samples as possible are analyzed in the same setup and qPCR run in order to reduce run-to-run variations (87). In this study, all of the 71 samples were run in a one 384-well PCR-plate to avoid plate-to-plate variability for each gene.

Both RNA purity and RNA integrity are important for qPCR analysis. The MIQE guidelines suggest that RNA samples with an $OD_{260/280}$ above 1.8 and $OD_{260/230}$ ratio between 1.8 – 2.2 as pure RNA, and samples with lower values usually contain higher levels of contaminants that can inhibit both the RT and qPCR reactions (143). All of the 71 samples analyzed had an $OD_{260/280}$ ratio above 1.8 and complied with the guideline. Of the 71 RNA samples, 22 samples had an $OD_{260/230}$ ratio below 1.8. Lower $OD_{260/230}$ ratio may indicate the presence of organic contaminant present, such as chaotropic salts. However, there is no consensus for what is the acceptable lower limit for the $OD_{260/230}$ (144). The reason for the observed low $OD_{260/230}$ ratios might be salt leftovers from the extraction procedure. It has been shown that trace amounts of guanidine thiocyanate in the lysis buffer influence the $OD_{260/230}$ ratio, but it is not likely to inhibit downstream applications (144, 145). Further, the $OD_{260/230}$ ratio also depends on RNA concentration in the sample. Trace amounts of contaminants can have a major impact if the RNA concentration is low. However, the most important focus is the amount of contaminant that is transferred to the cDNA synthesis, rather than the $OD_{260/230}$ ratio (144).

Comparison of a partially degraded RNA sample to an intact sample can artificially show some genes as being more highly expressed in the better quality sample (87). In addition, studies in humans suggest that degraded RNA sample can give significantly higher Cq values than a sample with high integrity (87, 143, 146). RNA integrity is measured by the instrument Agilent Bioanalyzer. RIN of 10 is viewed as perfectly intact and RIN of 1 as almost fragmented and degraded RNA (139). Several studies suggest that RNA samples with RIN below 5 should not be used for downstream applications (87, 103, 139). The RIN value for

the most of mice liver samples was over five; however, twelve samples had RIN numbers below than five. These samples were removed from downstream analysis. Table 4.3 in the result chapter shows the mean RIN values for the different developmental groups ranging from 5.83 (CTL) to 6.73 (LA). This is in concordance with a study that suggests that the average RIN for solid tissues (calf) was between six and eight (103).

Some of the technical variability can partly be reduced by a suitable normalization method, and the geometric mean of multiple reference genes is commonly accepted (89, 139). The purpose of normalization is to remove the technical variations as much as possible so the difference in gene expression is biologically related. Normalization against three or more validated reference genes has established itself as a standard (87). In this study, we observed a high variability within treatment group. The SE of the mean of the normalized relative gene expression values of several samples was high. The reason for this is unclear, but the Cq values in general was high, several of the liver samples showed RIN values close to five, and sixteen samples had a low $OD_{260/230}$ ratio, which can inhibit the assays and give high Cq values. We speculate that the observed intra-group variability could be reduced by increasing the cDNA amount in the qPCR reaction, but the timeline did not give this opportunity.

5.6.3 Methodological aspects in protein expression

Multiplex protein expression analysis in a suspension format was performed using a ready-made multiplex kit. The focus of the analysis was serum IGF-1. However, as serum material is a limited resource, we included some additional biomarkers of potential interest in the analysis. All samples were measured on the same microtiter plate to avoid plate-to-plate variability. Due to limited economical resources, we prioritized maximizing the number of biological parallel samples and only use one technical replicate per sample. The manual pipetting steps, especially the pipetting of serum, is considered the largest source of variability in such multiplex experiments and it was crucial for correct results to have a detailed work list. Even though the worklist was in place; erroneous pipetting in this study revealed during sample application led to removal of seven samples due to reduced available wells in the microtiterplate. The quantifications of the proteins are measured against standard curves with a certain dynamic range. The FABP4/A analysis gave results outside the dynamic range, and the software extrapolated the protein concentration. In this

case, these results would need to be diluted and re-analyzed to give reliable results. This was not performed.

5.6.4 Methodological aspects in lipid class measurements

The lipid analysis was performed by Vita AS, Oslo, Norway.

TAG was the main focus for lipid class measurements, and the correlation of variant was stated to be 5%. The high variability in the TAG assay, especially in the WL group, is considered most likely to be treatment related, and not technical variation.

5.7 Conclusion and suggestions for further studies

The main objective of this master thesis was to determine potential changes in signaling pathways involved in NAFLD after exposure to HFD during different life stages, covering *in utero* to adult life.

The findings from this study suggest that HFD exposure leads to disturbed fat metabolism with mild liver steatosis observed in the following percentages of animals: CTL (0%), IU (0%) LA (8.3%), IU+LA (37.5%), WL (37.5%) and AD (8.3%). Differences in mean TAG levels compared to the control group did not reach statistical significance, reflecting the marked variability in response within the HFD exposed groups.

We found that HFD exposure during different life stages increased hepatic secretion of IGF-1 protein expression in the IU and WL groups, and not increase in the LA, IU+LA and AD groups. This finding indicates a modification in the IGF-1 regulation and signaling for these groups with potential implications for organ growth.

Further, the gene expression data did reveal changes in several of the signaling pathways related to NAFLD due to HFD exposure in different life stages. The results showed three significantly (*Il10*, *Pparδ* and *Slc2a2;* $p<0.05$) and four borderline significantly (*Hnf4α*, *Nfe2l2*, *Insr* and *Tnfrsf1a;* $p<0.1$) differentially expressed genes in some of the HFD groups compared to the control group. These results suggest that HFD during early development may induce persistent changes in liver expression of genes involved in lipid metabolism, oxidative stress response, inflammation, insulin response and glucose homeostasis.

Finally, our results indicated that HFD exposure in early life stages is important for programming of risk of NAFLD as an adult. The data suggested that gestation to adulthood is associated with a greater risk of liver steatosis than exposure from weaning to adulthood. However, analyzing additional liver samples for TAG concentration would be necessary to strengthen this observation.

A suggestion for further studies can be a study for confirmation of the gene expression data with a focus on one or two signaling pathways combined with determination of the related protein expression in liver. In particular, the suggested increase in NAFLD in mice exposed to HFD at early life stages and throughout life compared to those exposed only as adult should be confirmed and the underlying differences in cell signaling should be explored in more depth.

References

1. Le MH, Devaki P, Ha NB, Jun DW, Te HS, Cheung RC, et al. Prevalence of non-alcoholic fatty liver disease and risk factors for advanced fibrosis and mortality in the United States. PloS one. 2017;12(3):e0173499.
2. El-Kader SMA, El-Den Ashmawy EMS. Non-alcoholic fatty liver disease: The diagnosis and management. World journal of hepatology. 2015;7(6):846.
3. Ngo HT, Hetland RB, Steffensen I-L. The Intrauterine and Nursing Period Is a Window of Susceptibility for Development of Obesity and Intestinal Tumorigenesis by a High Fat Diet in Min/+ Mice as Adults. Journal of Obesity. 2015;2015:25.
4. Rinella ME. Nonalcoholic fatty liver disease: a systematic review. Jama. 2015;313(22):2263-73.
5. Ludwig J, Viggiano TR, Mcgill DB, Oh B. Nonalcoholic steatohepatitis: Mayo Clinic experiences with a hitherto unnamed disease. Mayo Clinic Proceedings. 1980;55(7):434-8.
6. Glastras SJ, Chen H, Pollock CA, Saad S. Maternal obesity increases the risk of metabolic disease and impacts renal health in offspring. Bioscience Reports. 2018.
7. OECD. Health at a glance 2017: OECD indicators: OECD publishing; 2017 [cited 2018 20.05.]. Available from: http://www.oecd.org/health/health-systems/health-at-a-glance-19991312.htm.
8. Norwegian Institute of Public Health. Overweight and obesity in Norway 2017 [cited 2018 16.04.2018]. Available from: https://www.fhi.no/en/op/hin/risk--protective-factors/overweight-and-obesity-in-norway.
9. Stewart ST, Cutler DM, Rosen AB. Forecasting the effects of obesity and smoking on US life expectancy. New England Journal of Medicine. 2009;361(23):2252-60.
10. The Global Burden of Disease Obesity Collaborators. Health Effects of Overweight and Obesity in 195 Countries over 25 Years. New England Journal of Medicine. 2017;377(1):13-27.
11. Furukawa S, Fujita T, Shimabukuro M, Iwaki M, Yamada Y, Nakajima Y, et al. Increased oxidative stress in obesity and its impact on metabolic syndrome. The Journal of clinical investigation. 2017;114(12):1752-61.
12. Grundy SM. Obesity, metabolic syndrome, and cardiovascular disease. The Journal of Clinical Endocrinology & Metabolism. 2004;89(6):2595-600.
13. World Health Organization. Body Mass Index - BMI 2018 [cited 2018 20.05.]. Available from: http://www.euro.who.int/en/health-topics/disease-prevention/nutrition/a-healthy-lifestyle/body-mass-index-bmi.
14. Hruby A, Manson JE, Qi L, Malik VS, Rimm EB, Sun Q, et al. Determinants and consequences of obesity. American journal of public health. 2016;106(9):1656-62.
15. O'reilly JR, Reynolds RM. The risk of maternal obesity to the long-term health of the offspring. Clinical endocrinology. 2013;78(1):9-16.
16. Leibowitz KL, Moore RH, Ahima RS, Stunkard AJ, Stallings VA, Berkowitz RI, et al. Maternal obesity associated with inflammation in their children. World Journal of Pediatrics. 2012;8(1):76-9.
17. Visscher PM, Brown MA, McCarthy MI, Yang J. Five years of GWAS discovery. The American Journal of Human Genetics. 2012;90(1):7-24.
18. Visscher PM, Wray NR, Zhang Q, Sklar P, McCarthy MI, Brown MA, et al. 10 years of GWAS discovery: biology, function, and translation. The American Journal of Human Genetics. 2017;101(1):5-22.
19. Zaitlen N, Kraft P, Patterson N, Pasaniuc B, Bhatia G, Pollack S, et al. Using extended genealogy to estimate components of heritability for 23 quantitative and dichotomous traits. PLoS genetics. 2013;9(5):e1003520.
20. Zillikens MC, Yazdanpanah M, Pardo LM, Rivadeneira F, Aulchenko YS, Oostra BA, et al. Sex-specific genetic effects influence variation in body composition. Diabetologia. 2008;51(12):2233-41.
21. Levy E, Saenger A, Steffes M, Delvin E. Pediatric obesity and cardiometabolic disorders: risk factors and biomarkers. EJIFCC. 2017;28(1):6.

22. World Health Organization. Childhood overweight and obesity 2018 [cited 2018 May 20 2018]. Available from: http://www.who.int/dietphysicalactivity/childhood.
23. Llewellyn A, Simmonds M, Owen C, Woolacott N. Childhood obesity as a predictor of morbidity in adulthood: a systematic review and meta-analysis. Obesity reviews. 2016;17(1):56-67.
24. Kneeman JM, Misdraji J, Corey KE. Secondary causes of nonalcoholic fatty liver disease. Therapeutic advances in gastroenterology. 2012;5(3):199-207.
25. Anderson EL, Howe LD, Jones HE, Higgins JP, Lawlor DA, Fraser A. The prevalence of non-alcoholic fatty liver disease in children and adolescents: a systematic review and meta-analysis. PloS one. 2015;10(10):e0140908.
26. Das K, Das K, Mukherjee PS, Ghosh A, Ghosh S, Mridha AR, et al. Nonobese population in a developing country has a high prevalence of nonalcoholic fatty liver and significant liver disease. Hepatology. 2010;51(5):1593-602.
27. McPherson S, Hardy T, Henderson E, Burt AD, Day CP, Anstee QM. Evidence of NAFLD progression from steatosis to fibrosing-steatohepatitis using paired biopsies: implications for prognosis and clinical management. Journal of hepatology. 2015;62(5):1148-55.
28. Zhu J-Z, Hollis-Hansen K, Wan X-Y, Fei S-J, Pang X-L, Meng F-D, et al. Clinical guidelines of non-alcoholic fatty liver disease: A systematic review. World journal of gastroenterology. 2016;22(36):8226.
29. European Association for the Study of the Liver, European Association for the Study of Diabetes. EASL-EASD-EASO Clinical Practice Guidelines for the management of non-alcoholic fatty liver disease. Obesity facts. 2016;9(2):65-90.
30. Ahmed M. Non-alcoholic fatty liver disease in 2015. World journal of hepatology. 2015;7(11):1450.
31. Day CP, James OF. Steatohepatitis: a tale of two “hits”? Gastroenterology. 1998;114(4):842-5.
32. James O, Day C. Non-alcoholic steatohepatitis: another disease of affluence. The Lancet. 1999;353(9165):1634-6.
33. Yu J, Marsh S, Hu J, Feng W, Wu C. The pathogenesis of nonalcoholic fatty liver disease: interplay between diet, gut microbiota, and genetic background. Gastroenterology research and practice. 2016;2016.
34. Tilg H, Moschen AR. Evolution of inflammation in nonalcoholic fatty liver disease: the multiple parallel hits hypothesis. Hepatology. 2010;52(5):1836-46.
35. Alam S, Mustafa G, Alam M, Ahmad N. Insulin resistance in development and progression of nonalcoholic fatty liver disease. World journal of gastrointestinal pathophysiology. 2016;7(2):211.
36. Welsh JA, Karpen S, Vos MB. Increasing prevalence of nonalcoholic fatty liver disease among United States adolescents, 1988-1994 to 2007-2010. The Journal of pediatrics. 2013;162(3):496-500. e1.
37. Wankhade UD, Zhong Y, Kang P, Alfaro M, Chintapalli SV, Thakali KM, et al. Enhanced offspring predisposition to steatohepatitis with maternal high-fat diet is associated with epigenetic and microbiome alterations. PloS one. 2017;12(4):e0175675.
38. Walsh JM, McAuliffe FM. Impact of maternal nutrition on pregnancy outcome–Does it matter what pregnant women eat? Best Practice & Research Clinical Obstetrics & Gynaecology. 2015;29(1):63-78.
39. Barker DJ. The origins of the developmental origins theory. Journal of internal medicine. 2007;261(5):412-7.
40. Ekamper P, van Poppel F, Stein AD, Bijwaard GE, Lumey L. Prenatal famine exposure and adult mortality from cancer, cardiovascular disease, and other causes through age 63 years. American journal of epidemiology. 2015;181(4):271-9.
41. Lukaszewski M-A, Eberlé D, Vieau D, Breton C. Nutritional manipulations in the perinatal period program adipose tissue in offspring. American Journal of Physiology-Endocrinology and Metabolism. 2013;305(10):E1195-E207.
42. Heindel JJ, Vandenberg LN. Developmental origins of health and disease: a paradigm for understanding disease etiology and prevention. Current opinion in pediatrics. 2015;27(2):248.

43. Bernal AJ, Jirtle RL. Epigenomic disruption: the effects of early developmental exposures. Birth defects research Part A: Clinical and molecular teratology. 2010;88(10):938-44.
44. McKay J, Mathers J. Diet induced epigenetic changes and their implications for health. Acta physiologica. 2011;202(2):103-18.
45. Brumbaugh DE, Friedman JE. Developmental origins of nonalcoholic fatty liver disease. Pediatric research. 2014;75:140.
46. Ashino NG, Saito KN, Souza FD, Nakutz FS, Roman EA, Velloso LA, et al. Maternal high-fat feeding through pregnancy and lactation predisposes mouse offspring to molecular insulin resistance and fatty liver. The Journal of nutritional biochemistry. 2012;23(4):341-8.
47. Alfaradhi MZ, Fernandez-Twinn DS, Martin-Gronert MS, Musial B, Fowden A, Ozanne SE. Oxidative stress and altered lipid homeostasis in the programming of offspring fatty liver by maternal obesity. American Journal of Physiology-Regulatory, Integrative and Comparative Physiology. 2014;307(1):R26-R34.
48. Wang C-Y, Liao JK. A mouse model of diet-induced obesity and insulin resistance. mTOR: Springer; 2012. p. 421-33.
49. Mouse Genome Sequencing Consortium. Initial sequencing and comparative analysis of the mouse genome. Nature. 2002;420:520.
50. Justice MJ, Siracusa LD, Stewart AF. Technical approaches for mouse models of human disease. Disease models & mechanisms. 2011;4(3):305-10.
51. Parekh PI, Petro AE, Tiller JM, Feinglos MN, Surwit RS. Reversal of diet-induced obesity and diabetes in C57BL/6J mice. Metabolism. 1998;47(9):1089-96.
52. Wilson RM, Messaoudi I. The impact of maternal obesity during pregnancy on offspring immunity. Molecular and cellular endocrinology. 2015;418:134-42.
53. Kim J, Kim J, Kwon YH. Effects of disturbed liver growth and oxidative stress of high-fat diet-fed dams on cholesterol metabolism in offspring mice. Nutrition research and practice. 2016;10(4):386-92.
54. de Paula Simino LA, de Fante T, Fontana MF, Borges FO, Torsoni MA, Milanski M, et al. Lipid overload during gestation and lactation can independently alter lipid homeostasis in offspring and promote metabolic impairment after new challenge to high-fat diet. Nutrition & Metabolism. 2017;14(1):16.
55. de Fante T, Simino LA, Reginato A, Payolla TB, Vitoréli DCG, de Souza M, et al. Diet-induced maternal obesity alters insulin signalling in male mice offspring rechallenged with a high-fat diet in adulthood. PloS one. 2016;11(8):e0160184.
56. Kruse M, Seki Y, Vuguin PM, Du XQ, Fiallo A, Glenn AS, et al. High-fat intake during pregnancy and lactation exacerbates high-fat diet-induced complications in male offspring in mice. Endocrinology. 2013;154(10):3565-76.
57. Elahi MM, Cagampang FR, Mukhtar D, Anthony FW, Ohri SK, Hanson MA. Long-term maternal high-fat feeding from weaning through pregnancy and lactation predisposes offspring to hypertension, raised plasma lipids and fatty liver in mice. British Journal of Nutrition. 2009;102(4):514-9.
58. Thakali KM, Saben J, Faske JB, Lindsey F, Gomez-Acevedo H, Lowery Jr CL, et al. Maternal pregravid obesity changes gene expression profiles toward greater inflammation and reduced insulin sensitivity in umbilical cord. Pediatric research. 2014;76(2):202.
59. Zhou D, Pan Y-X. Pathophysiological basis for compromised health beyond generations: role of maternal high-fat diet and low-grade chronic inflammation. The Journal of nutritional biochemistry. 2015;26(1):1-8.
60. Chen Y, Wang J, Yang S, Utturkar S, Crodian J, Cummings S, et al. Effect of high-fat diet on secreted milk transcriptome in midlactation mice. Physiological genomics. 2017;49(12):747-62.
61. de los Ríos EA, Ruiz-Herrera X, Tinoco-Pantoja V, López-Barrera F, Martínez de la Escalera G, Clapp C, et al. Impaired prolactin actions mediate altered offspring metabolism induced by maternal high-fat feeding during lactation. The FASEB Journal. 2018:fj. 201701154R.

62. Pfeifer A. PVAT and Its Relation to Brown, Beige, and White Adipose Tissue in Development and Function. Frontiers in Physiology. 2018;9:70.
63. Shaik AA, Qiu B, Wee S, Choi H, Gunaratne J, Tergaonkar V. Phosphoprotein network analysis of white adipose tissues unveils deregulated pathways in response to high-fat diet. Scientific reports. 2016;6:25844.
64. Bugianesi E, McCullough AJ, Marchesini G. Insulin resistance: a metabolic pathway to chronic liver disease. Hepatology. 2005;42(5):987-1000.
65. Cui H, López M, Rahmouni K. The cellular and molecular bases of leptin and ghrelin resistance in obesity. Nature Reviews Endocrinology. 2017;13(6):338-51.
66. Yki-Järvinen H. Non-alcoholic fatty liver disease as a cause and a consequence of metabolic syndrome. The lancet Diabetes & endocrinology. 2014;2(11):901-10.
67. Berlanga A, Guiu-Jurado E, Porras JA, Auguet T. Molecular pathways in non-alcoholic fatty liver disease. Clinical and experimental gastroenterology. 2014;7:221.
68. Petta S, Muratore C, Craxi A. Non-alcoholic fatty liver disease pathogenesis: the present and the future. Digestive and Liver Disease. 2009;41(9):615-25.
69. Gregorio BM, Souza-Mello V, Carvalho JJ, Mandarim-de-Lacerda CA, Aguila MB. Maternal high-fat intake predisposes nonalcoholic fatty liver disease in C57BL/6 offspring. American Journal of Obstetrics & Gynecology. 2010;203(5):495. e1-. e8.
70. Yamaguchi K, Yang L, McCall S, Huang J, Yu XX, Pandey SK, et al. Inhibiting triglyceride synthesis improves hepatic steatosis but exacerbates liver damage and fibrosis in obese mice with nonalcoholic steatohepatitis. Hepatology. 2007;45(6):1366-74.
71. Arguello G, Balboa E, Arrese M, Zanlungo S. Recent insights on the role of cholesterol in non-alcoholic fatty liver disease. Biochimica et Biophysica Acta (BBA)-Molecular Basis of Disease. 2015;1852(9):1765-78.
72. Barrera F, George J. Non-alcoholic fatty liver disease: more than just ectopic fat accumulation. Drug Discovery Today: Disease Mechanisms. 2013;10(1-2):e47-e54.
73. Adamek A, Kasprzak A. Insulin-Like Growth Factor (IGF) System in Liver Diseases. International journal of molecular sciences. 2018;19(5).
74. Dichtel LE, Corey KE, Misdraji J, Bredella MA, Schorr M, Osganian SA, et al. The association between IGF-1 levels and the histologic severity of nonalcoholic fatty liver disease. Clinical and translational gastroenterology. 2017;8(1):e217.
75. Ita JR, Castilla-Cortázar I, Aguirre G, Sanchez-Yago C, Santos-Ruiz MO, Guerra-Menendez L, et al. Altered liver expression of genes involved in lipid and glucose metabolism in mice with partial IGF-1 deficiency: an experimental approach to metabolic syndrome. Journal of translational medicine. 2015;13(1):326.
76. Hribal ML, Procopio T, Petta S, Sciacqua A, Grimaudo S, Pipitone RM, et al. Insulin-like growth factor-I, inflammatory proteins, and fibrosis in subjects with nonalcoholic fatty liver disease. The Journal of Clinical Endocrinology & Metabolism. 2013;98(2):E304-E8.
77. Nishizawa H, Iguchi G, Fukuoka H, Takahashi M, Suda K, Bando H, et al. IGF-I induces senescence of hepatic stellate cells and limits fibrosis in a p53-dependent manner. Scientific reports. 2016;6:34605.
78. Clemmons DR. The relative roles of growth hormone and IGF-1 in controlling insulin sensitivity. The Journal of clinical investigation. 2004;113(1):25-7.
79. Villeneuve DL, Crump D, Garcia-Reyero N, Hecker M, Hutchinson TH, LaLone CA, et al. Adverse outcome pathway (AOP) development I: strategies and principles. Toxicological Sciences. 2014;142(2):312-20.
80. Slenter DN, Kutmon M, Hanspers K, Riutta A, Windsor J, Nunes N, et al. WikiPathways: a multifaceted pathway database bridging metabolomics to other omics research. Nucleic Acids Research. 2018;46(D1):D661-D7.
81. Bader GD, Cary MP, Sander C. Pathguide: a Pathway Resource List. Nucleic Acids Research. 2006;34(suppl_1):D504-D6.

82. Lodish H KC, Bretscher A, Amon A, Berk A, Krieger M, Ploegh H, Scott M. Molecular Cell Biology. 7 ed. New York: W.H.Freeman and Company; 2013. 1154 p.
83. Mantione KJ, Kream RM, Kuzelova H, Ptacek R, Raboch J, Samuel JM, et al. Comparing bioinformatic gene expression profiling methods: microarray and RNA-Seq. Medical science monitor basic research. 2014;20:138.
84. Schena M, Shalon D, Davis RW, Brown PO. Quantitative Monitoring of Gene Expression Patterns with a Complementary DNA Microarray. Science. 1995;270(5235):467-70.
85. VanGuilder HD, Vrana KE, Freeman WM. Twenty-five years of quantitative PCR for gene expression analysis. Biotechniques. 2008;44(5):619.
86. Metzker ML. Sequencing technologies—the next generation. Nature reviews genetics. 2010;11(1):31.
87. Derveaux S, Vandesompele J, Hellemans J. How to do successful gene expression analysis using real-time PCR. Methods. 2010;50(4):227-30.
88. Livak KJ, Schmittgen TD. Analysis of relative gene expression data using real-time quantitative PCR and the 2− ΔΔCT method. methods. 2001;25(4):402-8.
89. Vandesompele J, De Preter K, Pattyn F, Poppe B, Van Roy N, De Paepe A, et al. Accurate normalization of real-time quantitative RT-PCR data by geometric averaging of multiple internal control genes. Genome biology. 2002;3(7):research0034. 1.
90. Tatsumi K, Ohashi K, Taminishi S, Okano T, Yoshioka A, Shima M. Reference gene selection for real-time RT-PCR in regenerating mouse livers. Biochemical and biophysical research communications. 2008;374(1):106-10.
91. Schmittgen TD, Livak KJ. Analyzing real-time PCR data by the comparative CT method. Nature Protocols. 2008;3:1101.
92. Goni R, García P, Foissac S. The qPCR data statistical analysis. Integromics White Paper. 2009:1-9.
93. Hughes AN, Oxford JT. A lipid-rich gestational diet predisposes offspring to nonalcoholic fatty liver disease: a potential sequence of events. Hepatic medicine: evidence and research. 2014;6:15.
94. Williams L, Seki Y, Vuguin PM, Charron MJ. Animal models of in utero exposure to a high fat diet: a review. Biochimica et Biophysica Acta (BBA)-Molecular Basis of Disease. 2014;1842(3):507-19.
95. Duale N, Steffensen IL, Andersen J, Brevik A, Brunborg G, Lindeman B. Impaired sperm chromatin integrity in obese mice. Andrology. 2014;2(2):234-43.
96. Gutzkow K, Duale N, Danielsen T, Stedingk H, Shahzadi S, Instanes C, et al. Enhanced susceptibility of obese mice to glycidamide-induced sperm chromatin damage without increased oxidative stress. Andrology. 2016;4(6):1102-14.
97. ThermoFisher. How Luminex technology works 2018 [cited 2018 April 9]. Available from: https://www.thermofisher.com/no/en/home/references/protein-analysis-guide/multiplex-assays-luminex-assays/how-luminex-technology-works.html.
98. Faul F, Erdfelder E, Lang A-G, Buchner A. G* Power 3: A flexible statistical power analysis program for the social, behavioral, and biomedical sciences. Behavior research methods. 2007;39(2):175-91.
99. Folch J, Lees M, Sloane Stanley G. A simple method for the isolation and purification of total lipids from animal tissues. J biol Chem. 1957;226(1):497-509.
100. Zymo Research. Quick-RNA MiniPrep R1054 2018 [cited 2018 21.05.]. Available from: https://dwo0hlbtc3ypb.cloudfront.net/amasty/amfile/attach/_R1054_R1055_Quick-RNA_Miniprep_Kit_ver.3.2.2.pdf.
101. Sambrook J, Fritsch EF, Maniatis T. Molecular cloning: a laboratory manual: Cold spring harbor laboratory press; 1989.
102. Agilent Technologies. Agilent 2100 Bioanalyzer 2100 Experts's User guide May 2005 [cited 2018 April 07]. Available from: https://www.agilent.com/cs/library/usermanuals/Public/G2946-90004_Vespucci_UG_eBook_(NoSecPack).pdf.
103. Fleige S, Pfaffl MW. RNA integrity and the effect on the real-time qRT-PCR performance. Molecular aspects of medicine. 2006;27(2-3):126-39.

104. Fleige S, Walf V, Huch S, Prgomet C, Sehm J, Pfaffl MW. Comparison of relative mRNA quantification models and the impact of RNA integrity in quantitative real-time RT-PCR. Biotechnology letters. 2006;28(19):1601-13.
105. Duale N, Brunborg G, Rønningen KS, Briese T, Aarem J, Aas KK, et al. Human blood RNA stabilization in samples collected and transported for a large biobank. BMC research notes. 2012;5(1):510.
106. Schefe JH, Lehmann KE, Buschmann IR, Unger T, Funke-Kaiser H. Quantitative real-time RT-PCR data analysis: current concepts and the novel "gene expression's C T difference" formula. Journal of Molecular Medicine. 2006;84(11):901-10.
107. Andersen CL, Jensen JL, Ørntoft TF. Normalization of real-time quantitative reverse transcription-PCR data: a model-based variance estimation approach to identify genes suited for normalization, applied to bladder and colon cancer data sets. Cancer research. 2004;64(15):5245-50.
108. Howie G, Sloboda D, Kamal T, Vickers M. Maternal nutritional history predicts obesity in adult offspring independent of postnatal diet. The Journal of physiology. 2009;587(4):905-15.
109. Borengasser SJ, Kang P, Faske J, Gomez-Acevedo H, Blackburn ML, Badger TM, et al. High fat diet and in utero exposure to maternal obesity disrupts circadian rhythm and leads to metabolic programming of liver in rat offspring. PloS one. 2014;9(1):e84209.
110. Machado MV, Diehl AM. Pathogenesis of nonalcoholic steatohepatitis. Gastroenterology. 2016;150(8):1769-77.
111. Li S, Zeng X-Y, Zhou X, Wang H, Jo E, Robinson SR, et al. Dietary cholesterol induces hepatic inflammation and blunts mitochondrial function in the liver of high-fat-fed mice. The Journal of nutritional biochemistry. 2016;27:96-103.
112. Oben JA, Mouralidarane A, Samuelsson AM, Matthews PJ, Morgan ML, McKee C, et al. Maternal obesity during pregnancy and lactation programs the development of offspring non-alcoholic fatty liver disease in mice. Journal of hepatology. 2010;52(6):913-20.
113. McCurdy CE, Bishop JM, Williams SM, Grayson BE, Smith MS, Friedman JE, et al. Maternal high-fat diet triggers lipotoxicity in the fetal livers of nonhuman primates. The Journal of clinical investigation. 2009;119(2):323-35.
114. Chechi K, Cheema SK. Maternal diet rich in saturated fats has deleterious effects on plasma lipids of mice. Experimental & Clinical Cardiology. 2006;11(2):129.
115. Puri P, Baillie RA, Wiest MM, Mirshahi F, Choudhury J, Cheung O, et al. A lipidomic analysis of nonalcoholic fatty liver disease. Hepatology. 2007;46(4):1081-90.
116. Ioannou GN. The role of cholesterol in the pathogenesis of NASH. Trends in Endocrinology & Metabolism. 2016;27(2):84-95.
117. Bellanti F, Villani R, Facciorusso A, Vendemiale G, Serviddio G. Lipid oxidation products in the pathogenesis of non-alcoholic steatohepatitis. Free Radical Biology and Medicine. 2017;111:173-85.
118. Memmott RM, Pearman K, Gills J, Tullot T, Wong V, Singer B, et al. Increased NSCLC tumorigenesis in mice fed a high fat diet is associated with increased plasma IGF-1 levels and PD-1 expression in CD4+ tumor-infiltrating lymphocytes. AACR; 2017.
119. Lewitt MS, Dent MS, Hall K. The insulin-like growth factor system in obesity, insulin resistance and type 2 diabetes mellitus. Journal of clinical medicine. 2014;3(4):1561-74.
120. Dubois V, Eeckhoute J, Lefebvre P, Staels B. Distinct but complementary contributions of PPAR isotypes to energy homeostasis. The Journal of Clinical Investigation. 2017;127(4):1202-14.
121. Vacca M, Allison M, Griffin JL, Vidal-Puig A. Fatty acid and glucose sensors in hepatic lipid metabolism: implications in NAFLD. Semin Liver Dis. 2015;35(3):250-61.
122. Vacca M, Degirolamo C, Massafra V, Polimeno L, Mariani-Costantini R, Palasciano G, et al. Nuclear receptors in regenerating liver and hepatocellular carcinoma. Molecular and cellular endocrinology. 2013;368(1-2):108-19.
123. Baciu C, Pasini E, Angeli M, Schwenger K, Afrin J, Humar A, et al. Systematic integrative analysis of gene expression identifies HNF4A as the central gene in pathogenesis of non-alcoholic steatohepatitis. PloS one. 2017;12(12):e0189223.

124. Zhang Z, Zhou S, Jiang X, Wang Y-H, Li F, Wang Y-G, et al. The role of the Nrf2/Keap1 pathway in obesity and metabolic syndrome. Reviews in Endocrine and Metabolic Disorders. 2015;16(1):35-45.
125. Ishii T, Itoh K, Yamamoto M. [18] Roles of Nrf2 in activation of antioxidant enzyme genes via antioxidant responsive elements. Methods in enzymology. 348: Elsevier; 2002. p. 182-90.
126. Wang C, Cui Y, Li C, Zhang Y, Xu S, Li X, et al. Nrf2 deletion causes "benign" simple steatosis to develop into nonalcoholic steatohepatitis in mice fed a high-fat diet. Lipids in health and disease. 2013;12(1):165.
127. Tang W, Jiang Y-F, Ponnusamy M, Diallo M. Role of Nrf2 in chronic liver disease. World Journal of Gastroenterology: WJG. 2014;20(36):13079.
128. Sharma DL, Lakhani HV, Klug RL, Snoad B, El-Hamdani R, Shapiro JI, et al. Investigating Molecular Connections of Non-alcoholic Fatty Liver Disease with Associated Pathological Conditions in West Virginia for Biomarker Analysis. Journal of clinical & cellular immunology. 2017;8(5).
129. Zahran WE, El-Dien KAS, Kamel PG, El-Sawaby AS. Efficacy of tumor necrosis factor and interleukin-10 analysis in the follow-up of nonalcoholic fatty liver disease progression. Indian Journal of Clinical Biochemistry. 2013;28(2):141-6.
130. Lumeng CN, Bodzin JL, Saltiel AR. Obesity induces a phenotypic switch in adipose tissue macrophage polarization. The Journal of clinical investigation. 2007;117(1):175-84.
131. Postic C, Girard J. Contribution of de novo fatty acid synthesis to hepatic steatosis and insulin resistance: lessons from genetically engineered mice. The Journal of clinical investigation. 2008;118(3):829-38.
132. Kanehisa M, Sato Y, Kawashima M, Furumichi M, Tanabe M. KEGG as a reference resource for gene and protein annotation. Nucleic acids research. 2015;44(D1):D457-D62.
133. Yonamine C, Pinheiro-Machado E, Michalani M, Alves-Wagner A, Esteves J, Freitas H, et al. Resveratrol Improves Glycemic Control in Type 2 Diabetic Obese Mice by Regulating Glucose Transporter Expression in Skeletal Muscle and Liver. Molecules. 2017;22(7):1180.
134. Thorens B, Mueckler M. Glucose transporters in the 21st Century. American Journal of Physiology-Endocrinology and Metabolism. 2009;298(2):E141-E5.
135. Thorens B. GLUT2, glucose sensing and glucose homeostasis. Diabetologia. 2015;58(2):221-32.
136. Yu D, Chen G, Pan M, Zhang J, He W, Liu Y, et al. High fat diet-induced oxidative stress blocks hepatocyte nuclear factor 4α and leads to hepatic steatosis in mice. Journal of cellular physiology. 2018;233(6):4770-82.
137. Catalano PM. Obesity and pregnancy—the propagation of a viscous cycle? : Oxford University Press; 2003.
138. Zheng J, Xiao X, Zhang Q, Yu M, Xu J, Wang Z. Maternal high-fat diet modulates hepatic glucose, lipid homeostasis and gene expression in the PPAR pathway in the early life of offspring. International journal of molecular sciences. 2014;15(9):14967-83.
139. Becker C, Hammerle-Fickinger A, Riedmaier I, Pfaffl M. mRNA and microRNA quality control for RT-qPCR analysis. Methods. 2010;50(4):237-43.
140. Bustin SA, Benes V, Garson JA, Hellemans J, Huggett J, Kubista M, et al. The MIQE guidelines: minimum information for publication of quantitative real-time PCR experiments. Clinical chemistry. 2009;55(4):611-22.
141. Bustin SA, Beaulieu J-F, Huggett J, Jaggi R, Kibenge FS, Olsvik PA, et al. MIQE precis: Practical implementation of minimum standard guidelines for fluorescence-based quantitative real-time PCR experiments. BioMed Central; 2010.
142. Sidova M, Tomankova S, Abaffy P, Kubista M, Sindelka R. Effects of post-mortem and physical degradation on RNA integrity and quality. Biomolecular detection and quantification. 2015;5:3-9.
143. Taylor SC, Mrkusich EM. The state of RT-quantitative PCR: firsthand observations of implementation of minimum information for the publication of quantitative real-time PCR experiments (MIQE). Journal of molecular microbiology and biotechnology. 2014;24(1):46-52.

144. Cicinnati VR, Shen Q, Sotiropoulos GC, Radtke A, Gerken G, Beckebaum S. Validation of putative reference genes for gene expression studies in human hepatocellular carcinoma using real-time quantitative RT-PCR. BMC cancer. 2008;8(1):350.
145. Qiagen. RNA preparation on downstream applications. 2018 [cited 2018 May 13]. Available from: https://www.qiagen.com/gb/resources/resourcedetail?id=11226191-0a82-4a9b-ba4a-99800b6f8595&lang=en.
146. Huang X, Baumann M, Nikitina L, Wenger F, Surbek D, Körner M, et al. RNA degradation differentially affects quantitative mRNA measurements of endogenous reference genes in human placenta. Placenta. 2013;34(7):544-7.

Appendix A: Detailed protocols/primer sequences

A1: Protocol for Luminex assay

1. To avoid cross-contamination, pipette tips were changed between additions of each standard level, between sample additions and between reagent additions. Separate reservoirs were used for each reagent.
2. Reagent preparation: All reagents were brought to room temperature before use. The wash buffer was made the day before. 20 mL of Wash Buffer Concentrate was added to 480 mL distilled water to prepare 500 mL of ready-to-use wash buffer. The ready work solution was stored in the refrigerator at 4°C in a glass container closed with a cork. All serum samples were thawed at 4°C and diluted 1:50 by 10 µL sample and 490 µL Calibrator diluent RD6-52 in 0.6 ml polypropylene test tubes.
3. Standard Cocktails B, C, E and F were provided in the kit. Each standard was reconstituted with the volumes 0.275 mL, 0.2 mL, 0.2 mL and 0.25 mL of Calibrator Diluent RD6-52, respectively. The standards were gentle agitated for 15 minutes prior to dilutions. 100 µL each of the standard cocktails was combined in one single polypropylene tube, and in addition 600 µL Calibrator diluent RD6-52 was added to the one tube. This tube was used to make the dilution series.
4. Microparticles were prepared within 30 minutes of use. The Microparticle Cocktail vial was centrifuged for 30 seconds at 1000 x g before removing the cap. The vial was gently vortexed to resuspend the microparticles. The Microparticle Cocktail was diluted using Assay Diluent RD1W (500 uL microparticles and 5 mL diluent) in the mixing bottle provided in the kit. Light was avoided for microparticles.
5. The Biotin Antibody Cocktail vial was centrifuged for 30 seconds at 1000 x g before removing the cap. The vial was gently vortexed. The Biotin Antibody Cocktail was diluted using Assay diluent RD1W (500 µL biotin antibody cocktail and 5 mL diluent). The vial was gently mixed.
6. Streptavidin-PE preparation was performed in a polypropylene test tube wrapped with aluminium foil to protect the Streptavidin-PE from light during handling and storage. The Streptavidin-PE vial was centrifuged for 30 seconds at 1000 x g before removing the cap. The vial was gently vortexed. The Streptavidin-PE concentrate was diluted to a 1X concentration by adding 220 µL of Streptavidin-PE concentrate to 5.35

mL of Wash Buffer. This provided enough Streptavidin-PE to assay one 96-well microplate.

7. The diluted microparticles were resuspended by vortexing, and 50 µL of microparticle cocktail was pipetted in each well of the microplate.
8. 50 µL of standard or sample was added to the assigned wells. The microplate was covered with a foil plate sealer. The microplate was incubated for two hours at room temperature on the horizontal orbital microplate shaker KS125 basic (IKA, Wilmington, NC, USA) set at 800 ± 50 rpm.
9. The wash procedure was performed using the Bio-Plex Pro Wash Station (Bio-Rad Laboratories Inc., Hercules, CA, USA) with a magnetic device designed to accommodate a microplate. The microplate was put on the washer. One minute was allowed before removing the liquid.The wells were filled with Wash buffer (100 µL), and one minute was allowed before removing the liquid again. This wash procedure was repeated three times.
10. 50 µL of diluted Biotin Antibody cocktail was added to each well. The microplate was covered with a foil plate sealer. The microplate was incubated for one hour at room temperature on a horizontal orbital microplate shaker set at 800 ± 50 rpm.
11. The wash procedure was repeated.
12. 50 µL of diluted Streptavidin-PE was added to each well. The microplate was covered with a foil plate sealer. The microplate was incubated for 30 minutes at room temperature on a horizontal orbital microplate shaker set at 800 ± 50 rpm.
13. The wash procedure was repeated.
14. The microparticles were resuspended by adding 100 µL of Wash buffer to each well. The microplate was incubated for two minutes on the shaker set at 800 ± 50 rpm.
15. The microplate was read in the Bio-Rad Bio-Plex 200 dual laser flow based instrument within 90 minutes.

A2: Protocols for isolation and quality controls

A2.1 Zymo Research Quick-RNA™ Mini Prep

1. Reagent preparation: Before starting, 96 mL 100% ethanol was added to the 24 mL RNA wash buffer concentrate. Already reconstituted, aliquoted and frozen DNase I was thawed, and prepared as DNase I reaction mix in a RNase-free tube. 5 µL DNase I

and 75 µL DNA Digestion buffer per sample to be isolated was added and mixed gently in an RNase-free Eppendorf-tube.

2. After thawing at 4°C, the lysates were cleared by centrifugation at 10 000 x for 30 seconds.
3. The supernatant was transferred to a filtration column and centrifuged at 10 000 x g for 1 minute for removing of the majority of gDNA. The flow-through was saved for RNA purification.
4. All centrifugation steps in the following procedure were performed at 14 000 x g.
5. To bind the RNA, equal volume of 95% ethanol was added to the sample in RNA lysis buffer (1:1). The tube was mixed well. The mixture was transferred to a new filtration column and centrifuged at for 30 seconds. The flow-through was discarded. As the columns only had capacity of 700 µL, the column had to be filled and centrifuged twice per sample.
6. The column was prewashed with 400 µL RNA wash buffer added and centrifuged for 30 seconds. The flow-through was discarded.
7. 80 µL DNase reaction mix was added directly to the column matrix. The column was incubated in room temperature for 15 minutes, and centrifuged for 30 seconds.
8. 400 µL RNA Prep buffer was added to the column and centrifuged for 30 seconds. The flow-through was discarded.
9. 700 µL RNA Wash buffer was added to the column and centrifuged for 30 seconds. The flow-through was discarded.
10. 400 µL RNA wash buffer was added to the column and centrifuged for 2 minutes to ensure complete removal of the wash buffer. The column was carefully transferred into an RNase-free Eppendorph tube.
11. 50 µL DNase/Rnase-free water was added directly to the column matrix and centrifuged for 30 seconds to elute the RNA.
12. The eluted sample RNA was stored immediately at -°80C.

A2.2 NanoDrop spectrophotometer for assessment of quality and quantity

1. The NanoDrop™ 1000 Spectrophotometer was initialized and as blank 1.5 µL Rnase/DNase-free H_2O was used.
2. The protocols RNA-40 and ss-DNA-33 were chosen for RNA and cDNA respectively.

3. Input volume for each sample was 1.5 µL.
4. The results gave purity measures as absorbance ratios of 260/280 and 260/230 and yield in ng/µL.
5. The instrument was cleaned between each measurement with lens-cleaning tissue on both upper and lower pedestals. After use the pedestals were cleaned with dH_20.

A2.3 RNA Nano 6000 Assay for RIN determination

1. RNA ladder preparation: The RNA ladder was spun down and pipetted into an RNase-free tube. The ladder was denatured for 2 minutes at 70°C and immediately cooled on ice. Aliquots required for daily use were prepared and stored at -70°C in 0.5 mL RNase-free vials. The frozen RNA ladder aliquots did not need additional heat denaturation.
2. All reagents were equilibrated to room temperature for 30 minutes before use.
3. The dye and dye mixtures were protected from light to avoid decomposing and hence reduction of signal intensity. The light covers were removed only when pipetting.
4. RNA samples were denatured for 2 minutes at 70°C and kept on ice afterwards before use.
5. The RNA ladder aliquot was thawed on ice before use.
6. 550 µL of RNA 6000 gel matrix was spun through a spin filter for 10 minutes in room temperature at 1500 x g. The filtered gel was aliquoted into 65 µL aliquots in RNase-free microcentrifuge tubes and stored at 4°C.
7. The RNA dye concentrate was vortexed for 10 seconds and spun down. 1 µL of dye concentrate was added to 65 µL of filtered gel, and the two were mixed well by vortexing. The gel-dye mix was spun down for 10 minutes in room temperature at 13 000 x g.
8. A RNA Nano Chip was put on the chip priming station.
9. 9 µL of the gel-dye mix was pipetted in the well marked G.
10. The plunger was positioned at 1 mL and the chip priming station was closed.
11. The plunger was pressed until it was held by the clip. After 30 seconds of wait, the clip was released. After a 5 seconds wait, the plunger was pulled back to the 1 mL position.

12. The chip priming station was opened, and 9 µL of gel-dye mix was pipetted into wells marked G.
13. 5 µL of RNA marker was pipetted in all 12 wells and the well marked with a ladder icon.
14. 1 µL of prepared and thawed ladder was pipetted in the well marked with a ladder icon.
15. 1 µL of RNA sample was pipetted in each of the 12 sample wells.
16. The chip was vortexed horizontally in the IKA vortexer for 1 minute at 2400 rpm.
17. The electrodes of the Agilent 2100 Bioanalyzer were decontaminated for a minute with 350 µL RNaseZAP followed by 350 µL RNase-free water for minimum 10 seconds.
18. The Eukaryote Total RNA Nano protocol was chosen in the Bioanalyzer software and the chip was run in the instrument within 5 minutes.

A3: Protocol for cDNA synthesis

A3.1 cDNA synthesis using High-Capacity cDNA Reverse Transcription Kit

1. The equipments (pipettes, tips, cooling block and more) and the laminar flow cabinet were cleaned with RNase away and ethanol before the procedure was carried out. In addition the cabinet was treated with UV light for 30 minutes
2. The RNA was thawed at 4°C and correct amount of RNA was transferred to a 96-well PCR plate where correct amount of dH_20 had been pipetted to achieve 100 ng/uL RNA as input concentration for the samples. The volume of RNA in each well was 20 µL in the PCR plate.
3. The kit components of the RT master mix were thawed on ice, and mixed according to the volumes stated in the package insert. 20 µL of RT master mix was pipetted manually in each well in the PCR plate. This gave equal amount of diluted sample RNA and RT mastermix; and the total reaction volume was 40 µL.
4. The PCR plate was sealed with adhesive cover and centrifuged for one minute at 13 000 x g before cDNA synthesis was performed in the Eppendorf Mastercycler.
5. cDNA was stored at -80°C until used.

A4: Primer sequences for reference genes and target genes

Table A.1: Overview of all genes analyzed (reference and target genes) with their primer sequences and melting point listed.

Gene symbol	Gene name	Forward/reverse primers (F/R)	Primer sequence (5'→3')	Tm°
Reference genes				
Actβ	actin, beta (	F	CCCGCGAGTACAACCTTCT	64.0
		R	CGTCATCCATGGCGAACT	65.0
Gusβ	glucuronidase beta	F	CTCTGGTGGCCTTACCTGAT	62.0
		R	CAGACTCAGGTGTTGTCATCG	63.0
Hprt1	hypoxanthine guanine phosphoribosyl transferase	F	GACCGGTTCTGTCATGTCG	63.0
		R	ACCTGGTTCATCATCACTAATCAC	63.0
RpL13a	ribosomal protein L13a	F	ATCCCTCCACCCTATGACAA	59.0
		R	GCCCCAGGTAAGCAAACTT	59.0
Tubβ5	Tubulin beta 5 class 1	F	CTGAGTACCAGCAGTACCAGGAT	51.0
		R	CTCTCTGCCTTAGGCCTCCT	58.0
Ywhaz	tyrosine 3-monooxygenase/tryptophan 5-monooxygenase activation protein, zeta polypeptide	F	CTTCCTGCAGCCAGAAGC	59.0
		R	GGTTTCCTCCAATCACTAGCC	59.0
Target genes				
Adipor1	adiponectin receptor 1	F	GCTTGGTTTTGTGCTATTTC	59.0
		R	TTCTCTGAATGACAGTAGACAG	56.0
Adipor 2	adiponectin receptor 2	F	ATGTCATCTCAGAAGGGTTC	58.1
		R	GATGAGAGTGAAACCAGATG	57.1
Akt2	thymoma viral proto-oncogene 2	F	GAAAGGAGACTGTAAAAAGTGG	58.0
		R	ATACAGTATCGTCTTGGGTC	56.0
Cat	catalase	F	CTCCATCAGGTTTCTTTCTTG	60.3
		R	CAACAGGCAAGTTTTTGATG	60.8
Cd36	cd36 antigen	F	CATTTGCAGGTCTATCTACG	57.0
		R	CAATGTCTAGCACACCATAAG	57.0
Cebpα	CCAAT/enhancer binding protein (C/EBP), alpha	F	AAGGGTGTATGTAGTAGTGG	53.0
		R	AAAAAGAAGAGAAGGAAGCG	59.3
Cebpβ	CCAAT/enhancer binding protein (C/EBP), beta	F	ATCACTTAAAGATGTTCCTGC	57.0
		R	TGTCTTCACTTTAATGCTCG	58.0
Cyp2e1	cytochrome P450, family 2, subfamily e, polypeptide 1	F	GATGGAGAAGGAAAAACACAG	60.2
		R	GGTATTTCATGAGAATCAGGAG	59.1
Ephb2	Eph receptor B2 (alias Erk)	F	CAGCATCAAGGAAAAGCTAC	59.1
		R	CTATATAGATCTTCATGCCTGG	57.0
Fasn	fatty acid synthase	F	GATTCAGGGAGTGGATATTG	58.0
		R	CATTCAGAATCGTGGCATAG	61.0
Fgf21	fibroblast growth factor 21	F	CAGTCCAGAAAGTCTCCTG	57.4
		R	AGAAACCTAGAGGCTTTGAC	56.7

Table A.1 continued: Overview of all genes analyzed (reference genes and target genes) with their primer sequences and melting point listed.

Gene symbol	Gene name	Forward/reverse primers (F/R)	Primer sequence (5'→3')	Tm°
Target genes				
G6pc	glucose-6-phosphatase, catalytic	F	TTCAAGTGGATTCTGTTTGG	60.1
		R	AGATAGCAAGAGTAGAAGTGAC	53.6
Gpx1	glutathione peroxidase 1	F	CGACATCGAACCCGATATAGA	64.0
		R	ATGCCTTAGGGGTTGCTAGG	64.0
Gpx2	glutathione peroxidase 2	F	TCCCTTGCAACCAGTTCG	65.0
		R	CTTGAGGCTGTTCAGGATCTC	63.0
Grb2	growth factor receptor bound protein 2	F	AGAAGAAATGCTCAGCAAAC	58.7
		R	ATCATTTCCAAACTTGACGG	61.4
Grb10	growth factor receptor bound protein 10	F	CTTGGAAGAAGCTGTATGTG	57.5
		R	GTGTCTGGGTTCTTTTGAAG	58.8
Gsk3α	glycogen synthase kinase 3 alpha	F	GGAGATCATCAAGGTACTAGG	56.8
		R	AGATTTGAACACCTTTGTCC	58.1
Gsk3β	glycogen synthase kinase 3 beta	F	CACTCTTCAACTTTACCACTC	55.5
		R	ATTAGTATCTGAGGCTGCTG	56.2
Hmox1	heme oxygenase 1	F	CATGAAGAACTTTCAGAAGGG	60.0
		R	TAGATATGGTACAAGGAAGCC	57.0
Hmox2	heme oxygenase 2	F	TACGGCACCAGAAAAGGAAA	64.0
		R	GTGCTTCCTTGGTCCCTTC	64.0
Hnf4α	hepatic nuclear factor 4, alpha	F	TCCTAGGCAATGACTACATC	57.0
		R	CTGGATCAAAGAAGATGATGG	61.0
Igf1	insulin-like growth factor 1	F	GACAAACAAGAAAACGAAGC	59.0
		R	ATTTGGTAGGTGTTTCGATG	59.0
Igf1r	insulin-like growth factor 1 receptor	F	AGAACCGAATCATCATAACG	59.0
		R	TTTTAAATGGTGCCTCCTTG	61.0
Igf2	insulin-like growth factor 2	F	GTACTTCCGGACGACTTC	57.1
		R	CTGAACTCTTTGAGCTCTTTG	58.5
Il4	interleukin 4	F	CTGGATTCATCGATAAGCTG	60.0
		R	TTTGCATGATGCTCTTTAGG	60.0
Il6	interleukin 6	F	TGATGGATGCTACCAAACTGG	60.0
		R	TTCATGTACTCCAGGTAGCTATGG	60.0
Il6rα	interleukin 6 receptor, alpha	F	AAAGTTCTACAGAAGCAACG	56.3
		R	TTGAGTCTCAGGATGATGAAG	59.4
Il10	interleukin 10	F	CAGGACTTTAAGGGTTACTTG	57.0
		R	ATTTTCACAGGGGAGAAATC	59.0
Il13	interleukin 13	F	GGTCCTGTAGATGGCATTGCA	62.0
		R	GGAGCTGAGCAACATCACACA	63.0
Il33	interleukin 33	F	GCTACTACGCTACTATGAGTC	53.0
		R	CAGATGTCTGTGTCTTTGATG	58.0
Ins1	insulin 1	F	GAGGTACTTTGGACTATAAAGC	55.0
		R	TTGAAACAATGACCTGCTTG	61.0

Table A.1 continued: Overview of all genes analyzed (reference and target genes) with their primer sequences and melting point listed.

Gene symbol	Gene name	Forward/reverse primers (F/R)	Primer sequence (5'→3')	Tm°
Target genes				
Ins2	insulin II	F	AGCAGGAAGGTTATTGTTTC	57.0
		R	ACATGGGTGTGTAGAAGAAG	57.0
Insr	insulin receptor	F	AAGACCTTGGTTACCTTCTC	56.0
		R	GGATTAGTGGCATCTGTTTG	60.0
Irs1	insulin receptor substrate 1	F	GATCGTCAATAGCGTAACTG	57.0
		R	ATCGTACCATCTACTGAAGAG	55.0
Irs2	insulin receptor substrate 2	F	CCAGGAGACAAGAACTCC	57.1
		R	GCTTCACTCTTTCACGAC	55.7
Lep	leptin	F	CTTTGGTCCTATCTGTCTTATG	57.0
		R	TCTTGGACAAACTCAGAATG	57.8
Lepr	leptin receptor	F	CTGAGATACAGTACAGCATTG	55.0
		R	TGATATTGACATCGATCACG	60.0
Lipe	lipase, hormone sensitive	F	AACTCCTTCCTGGAACTAAG	57.0
		R	CTTCTTCAAGGTATCTGTGC	57.0
Lpin1	lipin1	F	CAGGAAGAAAGATAAACGGAG	59.0
		R	CATTCTTGGGGAAATACAGG	61.0
Mlxip	MLX interacting protein	F	CCTTTCCAGGATCTCTTCTC	59.4
		R	AGATGTAATGAGGCTATTGGG	59.5
Mlxipl	MLX interacting protein-like (alias ChREBP)	F	ATATCTCCGACACACTCTTC	55.6
		R	CAACATAAGCATCTTCTGGG	59.7
Neil1	nei endonuclease VIII-like 1 (E. coli)	F	ATCTACGTTTTTACACAGCC	56.0
		R	AAGTACGTTCTCTCTGAACC	55.0
Neil2	nei like 2 (E. coli)	F	TTGTCTGAAAAGTTCCATCG	60.0
		R	ATGTTCCCTAATCCTGAGAAG	59.0
Neil 3	nei like 3 (E. coli	F	GACTTTCTAACAGTGAACTCC	55.0
		R	CCTTGTTTTCTCCATCTTTCC	61.0
Nfe2l2	nuclear factor, erythroid derived 2, like 2 (alias Nrf2)	F	AGCATGATGGACTTGGAATTG	64.0
		R	CCTCCAAAGGATGTCAATCAA	64.0
Nfκb1	nuclear factor of kappa light polypeptide gene enhancer in B cells 1, p105	F	ATCTATGATAGCAAAGCCCC	59.6
		R	TGGATGTCATCTTTCTGAAC	57.6
Nr1h2	nuclear receptor subfamily 1, group H, member 2	F	TCACCCACTATTAAGGAAGAG	57.4
		R	TCTAAGATGACCACGATGTAG	56.8
Nr1h3	nuclear receptor subfamily 1, group H, member 3(alias Lxrα)	F	GATGTTTCTCCTGATTCTGC	58.8
		R	CTCCAACCCTATCCCTAAAG	59.1
Ogg1	8-oxoguanine DNA-glycosylase 1	F	CAGAAATTCCAAGGTGTGAG	60.0
		R	AATGTTGTTGTTGGAGGAAC	59.0
Pcsk9	proprotein convertase subtilisin/kexin type 9	F	GAGATTATGAAGAGCTGATGC	58.1
		R	GTTTGTTCAATCTGTAGCCTC	57.9

Table A.1 continued: Overview of all genes analyzed (reference and target genes) with their primer sequences and melting point listed.

Gene symbol	Gene name	Forward/reverse primers (F/R)	Primer sequence (5'→3')	Tm°
Target genes				
Pklr	pyruvate kinase liver and red blood cell	F	GTGAAGAAGTTTGATGAGATCC	59.2
		R	CAAGAAAACCTTCTCTCTGCTG	59.2
Pparα	peroxisome proliferator activator receptor alpha	F	GATGTCACACAATGCAATTC	59.0
		R	CAGTTTCCGAATCTTTCAGG	61.0
Pparδ	peroxisome proliferator activator receptor delta	F	CTGACAGATGAAGACAAACC	57.0
		R	CTTCCTCTTTCTCCTCTTCC	59.0
Pparγ	peroxisome proliferator activated receptor gamma	F	AAAGACAACGGACAAATCAC	59.0
		R	GGGATATTTTTGGCATACTCTG	61.0
Pparγc1β	peroxisome proliferative activated receptor, gamma, coactivator 1 beta	F	AAGAACTTCAGACGTGAGAG	56.0
		R	TCAAAGCGCTTCTTTAGTTC	59.0
Rxrα	retinoid X receptor alpha	F	TAACAGAGCTGGTGTCTAAG	54.6
		R	TTAGAGTCAGGGTTGAACAG	56.9
Scd1	stearoyl-Coenzyme A desaturase 1	F	GTGGGGTAATTATTTGTGACC	59.5
		R	TTTTTCCCAGACAGTACAAC	56.7
Slc2a2	solute carrier family 2 (facilitated glucose transporter), member 2	F	TTGTGCTGCTGGATAAATTC	60.0
		R	AAATTCAGCAACCATGAACC	61.0
Slc2a4	solute carrier family 2 (facilitated glucose transporter), member 4	F	CAATGGTTGGGAAGGAAAAG	63.0
		R	AATGAGTATCTCATAGGAGGC	56.0
Socs3	suppressor of cytokine signaling 3	F	CCAAAGAAATAACCACTCCC	59.9
		R	GATCTGCGAGGTTTCATTAG	58.9
Sod1	superoxide dismutase 1, soluble	F	GGTCCAGCGGATGAAGAG	64.0
		R	GGACACATTGGCCACACC	65.0
Sod2	superoxide dismutase 2, mitochondrial	F	TGGACAAACCTGAGCCCTAA	65.0
		R	GACCCAAAGTCACGCTTGATA	64.0
Sod3	superoxide dismutase 3, extracellular	F	CTTGGGAGAGCTTGTCAGGT	63.0
		R	CACCAGTAGCAGGTTGCAGA	64.0
Srebf1	sterol regulatory element binding transcription factor 1	F	AATAAATCTGCTGTCTTGCG	59.5
		R	CCTTCAGTGATTTGCTTTTG	59.9
Tnfα	tumor necrosis factor alpha	F	TTGAGATCCATGCCGTTG	63.0
		R	CTGTAGCCCACGTCGTAGC	62.0
Tnfrsf1a	tumor necrosis factor receptor superfamily, member 1a	F	GGTTATCTTGCTAGGTCTTTG	57.1
		R	GATCCCTACAAATGATGGAG	58.4
Ulk1	Unc-51 like kinase 1	F	AGATTGCTGACTTTGGATTC	58.3
		R	AGCCATGTACATAGGAGAAC	55.6
Ulk2	unc-51 like kinase 2	F	GAGCTTAATGCCTAGTATTCC	56.3
		R	GATTTCTCTGAAGCAAACCC	60.3
Vldlr	very low density lipoprotein receptor	F	CTGTGGAGATATTGATGAATGC	60.9
		R	TTTCTCTCTAGGCCAATCTTC	59.1

A5: KEGG pathway for NAFLD

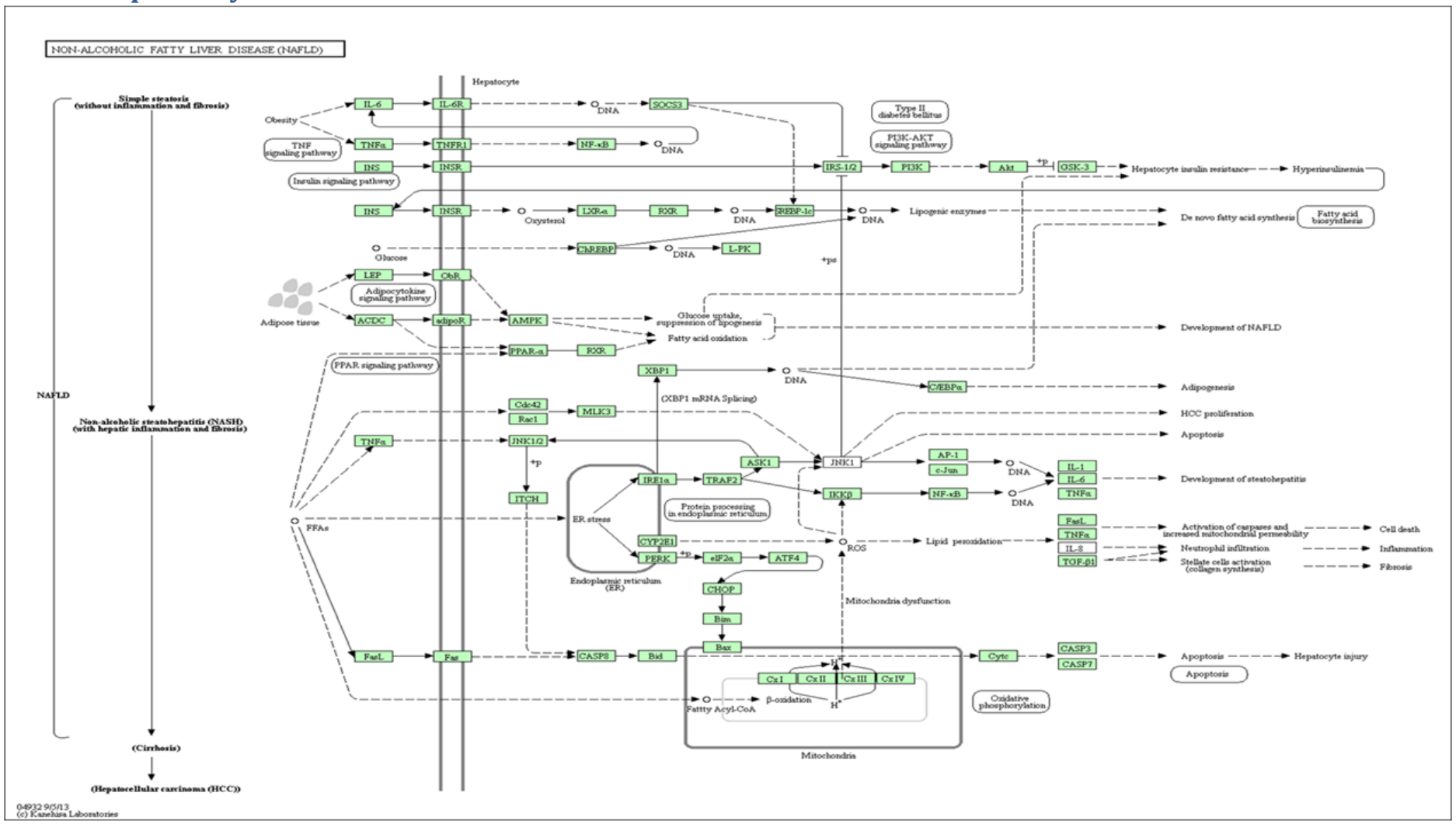

Figure A.1: NAFLD signaling pathway from KEGG database. Figure used with permission from KEGG Database (132).

Appendix B: Products and manufacturers

B1: Products and manufacturers

Product	Manufacturer	Country
2100 Bioanalyzer	Agilent Technologies	USA
4Lab™ Automated liquid handling robot	4titude	United Kingdom
Absolutt alkohol prima (100% (absolute) ethanol)	Kementyl Norge	Norway
Bio-Plex 200 dual laser flow system	Bio-Rad	USA
Bio-Plex Pro Wash Station	Bio-Rad	USA
CFX384 Real-Time PCR system	Bio-Rad	USA
Distilled water (dH_20)	Produced at NIPH	Norway
Eppendorf Master Cycler	Eppendorf	Germany
Eppendorf tubes (1.5 mL/2 mL)	Eppendorf	Germany
Framestar 384-well PCR plate	4titude	United Kingdom
Gene specific primers	Sigma Aldrich	USA
High-Capacity cDNA Reverse Transcription kit	Applied Biosystems	USA
KAPA SYBR Fast qPCR Master mix kit	Kapa Biosystems	USA
KS125 basic microplate shaker	IKA	USA
Mouse premixed multi-analyte kit	R&D Systems	USA
NanoDrop™ 1000 Spectrophotometer	ThermoFisher Scientific	USA
Polypropylene tubes 0.6 mL	Axygen	USA
Quick-RNA™ MiniPrep kit	Zymo Research	USA
RNA 6000 Nano LabChip Assay kit	Agilent Technologies	USA
RNase away	Molecular Bioproducts	USA
Rnase free stainless beads 5 mm	Qiagen	Germany
Tris EDTA (TE) buffer	Invitrogen, ThermoFisher Scientific	USA
Tear-A-Way 96-well PCR plate non-skirted	4titude	USA
TissueLyser II	Qiagen	Germany

Appendix C: Additional results

C1: Protein expression results for seven biomarkers

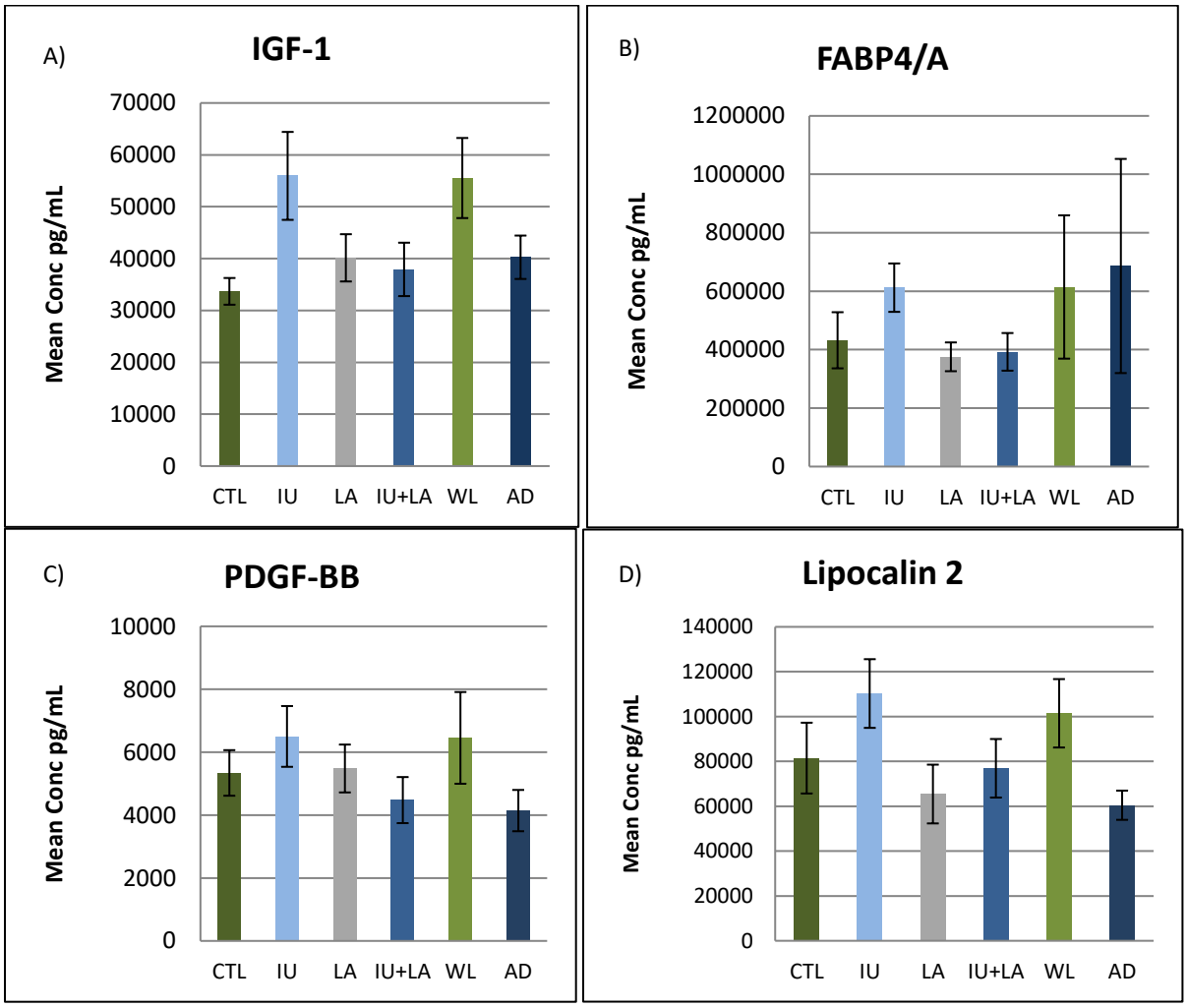

Figure A.2: **Effects of exposure to a high fat diet.** HFD exposure effect on the proteins IGF-1(A), FABP4/A (B), PDGF-BB (C) and Lipocalin 2 (D) expression levels during different periods of life. The concentrations of the above mentioned proteins were measured from all developmental groups. Total number of samples = 70. CTL, n = 14; IU, n =10; LA, n =12; IU+LA, n =12; WL, n =11; AD, n =11.

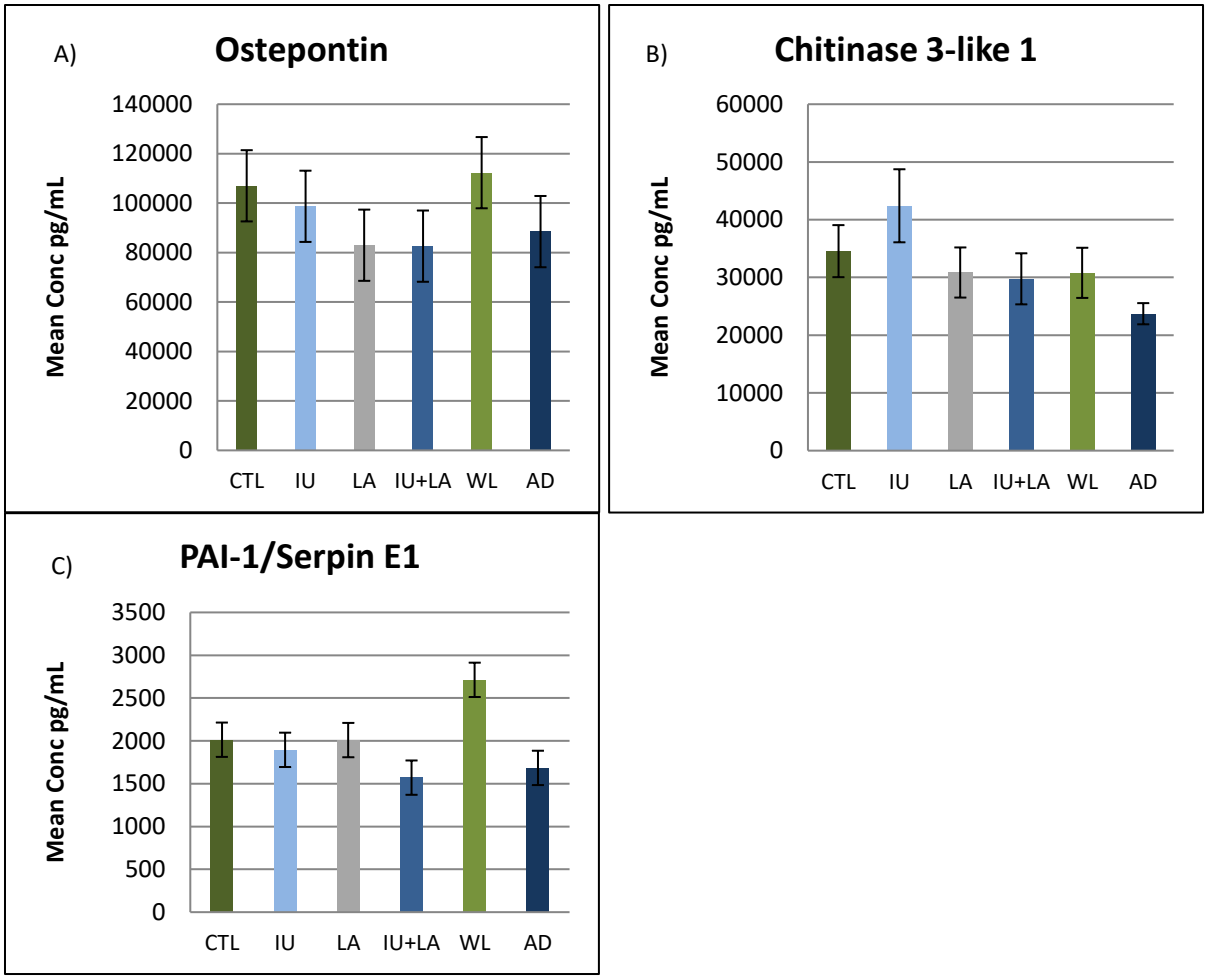

Figure A.3: Effects of exposure to a high fat diet. HFD exposure effect on the proteins Chitinase 3-like 1 (A), PAI-1/Serpin E1 (B) and Ostepontin (C) expression levels during different periods of life**.** The concentrations of the above mentioned proteins were measured from all developmental groups. Total number of samples = 70. CTL, n =14; IU, n =10; LA, n =12; IU+LA, n =12; WL, n =11; AD, n =11.

C2: Results for RNA yield, purity, integrity and cDNA yield and purity

Table A.2: An overview of all results involving RNA and cDNA yield and purity, and RNA integrity. Total number of samples; n=71. The samples with blue marked rows were taken out of the study due to high degree of degraded RNA (RIN # below 5).

Sample ID	Grouping	NanoDrop RNA yield ng/uL	OD 260/280 of RNA	OD 260/230 of RNA	Bioanalyzer RNA RIN#	NanoDrop cDNA yield ng/ul	OD 260/280 of cDNA	OD 260/230 of cDNA
566	CTL	417	2,06	1,58	6,2	1918	1,83	2,24
893	CTL	668	1,96	1,08	NA	1579	1,86	2,27
897	CTL	1010	2,09	1,58	6,7	1650	1,85	2,28
635	CTL	509	2,17	2,32	2,2	1836	1,85	2,28
285	CTL	1081	2,14	2,12	6,8	1844	1,85	2,27
286	CTL	876	2,14	2,05	6,7	1906	1,85	2,27
336	CTL	429	1,88	1,88	7,1	1854	1,86	2,27
69	CTL	1204	2,04	1,69	6,7	1815	1,84	2,3
135	CTL	517	2,14	1,80	2,4	1823	1,84	2,27
136	CTL	720	2,13	1,79	5,8	1915	1,84	2,27
137	CTL	472	2,16	1,87	6,5	1854	1,85	2,27
418	CTL	814	2,15	2,12	7	1940	1,85	2,28
273	IU	469	2,00	1,65	6,3	1810	1,85	2,28
291	IU	1253	2,06	1,87	6,3	1785	1,86	2,28
318	IU	441	2,13	2,21	2,6	1975	1,84	2,25
753	IU	693	2,09	1,65	3,1	1869	1,84	2,27
760	IU	628	2,13	1,84	6,5	1828	1,85	2,24
763	IU	1090	2,13	1,94	7,8	1873	1,85	2,26
601	IU	1268	2,04	1,89	7	1966	1,85	2,26
608	IU	371	2,02	1,59	6,3	1961	1,84	2,25
638	IU	910	2,08	1,86	6,8	1796	1,84	2,24
270	IU	1440	2,09	1,92	7,7	1602	1,86	2,26
271	IU	1126	2,09	2,04	6,2	1572	1,84	2,27
644	IU	538	2,09	2,03	5,9	1455	1,85	2,25
579	LA	463	2,11	1,73	7,1	1839	1,85	2,25
580	LA	576	2,19	2,23	6,3	1772	1,85	2,27
807	LA	1144	2,03	1,69	6,3	2115	1,83	2,24
809	LA	708	2,06	1,85	6,5	1577	1,85	2,24
822	LA	779	2,04	1,64	NA	1535	1,85	2,26
624	LA	600	2,16	1,91	6,5	1568	1,85	2,25
664	LA	930	2,15	2,04	7,3	1640	1,85	2,25
665	LA	585	2,15	2,01	6,8	1609	1,86	2,27
193	LA	323	2,08	1,86	6,6	1712	1,85	2,26

Table A.2 continued: An overview of all results involving RNA and cDNA yield and purity, and RNA integrity. Total number of samples; n=71. The samples with blue marked rows were taken out of the study due to high degree of degraded RNA (RIN # below 5).

Sample ID	Grouping	NanoDrop RNA yield ng/uL	OD 260/280 of RNA	OD 260/230 of RNA	Bioanalyzer RNA RIN#	NanoDrop cDNA yield ng/ul	OD 260/280 of cDNA	OD 260/230 of cDNA
201	LA	392	2,10	1,95	7,1	1822	1,84	2,26
238	LA	351	2,08	1,85	6,8	1861	1,84	2,26
261	IU+LA	458	2,05	1,67	6,2	1553	1,86	2,25
434	IU+LA	1115	2,06	1,59	6,8	1703	1,85	2,24
129	IU+LA	366	1,90	1,64	6,5	1811	1,85	2,23
890	IU+LA	390	2,18	2,41	8,4	1891	1,85	2,23
901	IU+LA	518	2,09	1,69	6,4	1881	1,85	2,22
902	IU+LA	680	2,12	1,74	4,2	1829	1,83	2,2
903	IU+LA	1102	2,02	1,71	6,2	1609	1,76	2
885	IU+LA	284	1,93	1,62	NA	1526	1,85	2,17
610	IU+LA	452	1,99	1,55	NA	1442	1,85	2,19
672	IU+LA	990	2,12	2,01	6,6	1818	1,83	2,24
673	IU+LA	859	2,11	2,10	6,9	1939	1,85	2,23
32	IU+LA	1795	2,09	2,04	7,8	1833	1,85	2,26
427	WL	797	2,11	1,80	6,3	1607	1,86	2,26
459	WL	589	2,18	2,10	2,5	1547	1,85	2,25
481	WL	454	2,04	2,08	5,5	1542	1,85	2,25
26	WL	907	2,18	2,21	7,3	1464	1,85	2,25
34	WL	1077	2,07	1,88	2,4	1438	1,86	2,25
101	WL	677	2,1	1,57	6,7	1694	1,85	2,24
115	WL	642	2,11	2,19	6,8	1874	1,84	2,24
743	WL	924	2,12	2,21	7,6	1801	1,85	2,25
744	WL	608	2,11	1,62	7,2	1597	1,85	2,25
23	WL	432	2,18	2,30	7,1	1657	1,85	2,25
25	WL	1885	2,09	2,02	7,5	1536	1,85	2,23
35	WL	1295	2,12	2,02	6,8	1349	1,86	2,26
126	AD	765	2,17	2,17	6,8	1703	1,85	2,26
878	AD	548	2,12	1,87	6,3	1582	1,85	2,25
124	AD	887	2,11	2,05	5,8	1433	1,85	2,27
372	AD	604	2,16	2,23	2,3	1490	1,86	2,28
381	AD	454	1,82	1,96	6,4	1582	1,86	2,26
873	AD	1051	2,19	2,06	8,5	1784	1,85	2,25
874	AD	382	2,1	1,73	6,8	1916	1,84	2,24
875	AD	843	2,15	2,12	6,9	1812	1,85	2,26
307	AD	788	2,09	1,97	7,2	1534	1,85	2,27
345	AD	346	1,96	1,98	6,8	1549	1,85	2,26
10	AD	1041	2,15	2,19	7,5	1528	1,85	2,26
63	AD	1336	2,11	2,10	7,2	1496	1,85	2,25

C3: Statistical p-values for gene expression analysis

Table A.3: p-values for gene expression analysis. The genes marked in bold is reviewed as statistical significant or borderline significant different compared to the control group. The p-values of each group for the significant genes are listed below the overall p-value for the gene. Total number of genes analyzed =48.

Gene	p-value	Statistical method	Gene	p-value	Statistical method
Akt2	0.526	ANOVA	Neil1	0.625	Kruska-Wallis
Cat	0.326	ANOVA	Neil3	0.341	Kruska-Wallis
Cd36	0.503	ANOVA	Nfκb1	0.554	Kruska-Wallis
Cebpα	0.316	ANOVA	Nr1h2	0.874	ANOVA
Cebpβ	0.310	Kruska-Wallis	Nr1h3	0.426	Kruska-Wallis
Cyp2e1	0.813	ANOVA	**Nfe2l2**	**0.031**	Kruska-Wallis
Fasn	0.431	ANOVA	IU group	0.400	Mann-Whitney U Test
Fgf21	0.248	ANOVA	LA group	**0.053**	Mann-Whitney U Test
G6pc	0.849	ANOVA	IU+LA group	0.666	Mann-Whitney U Test
Gpx1	0.759	Kruska-Wallis	WL group	0.720	Mann-Whitney U Test
Grb2	0.790	Kruska-Wallis	AD group	0.941	Mann-Whitney U Test
Gsk3β	0.651	ANOVA	Pparα	0.772	ANOVA
Hnf4α	**0.069**	ANOVA	**Pparδ**	**0.046**	ANOVA
IU group	0.108	Dunnett t (2 sided)	IU group	0.243	LSD
LA group	**0.073**	Dunnett t (2 sided)	LA group	**0.046**	LSD
IU+LA group	0.781	Dunnett t (2 sided)	IU+LA group	0.665	LSD
WL group	0.927	Dunnett t (2 sided)	WL group	0.258	LSD
AD group	1.000	Dunnett t (2 sided)	AD group	0.717	LSD
IGF-1	0.256	ANOVA	Pparγ	0.592	ANOVA
Igf2	0.246	ANOVA	Pparγc1β	0.406	ANOVA
Il4	0.795	Kruska-Wallis	Rxrα	0.348	Kruska-Wallis

Table A.3 continued: p-values for gene expression analysis. The genes marked in bold is reviewed as statistical significant or borderline significant different compared to the control group. The p-values of each group for the significant genes are listed below the overall p-value for the gene. Total number of genes analyzed =48.

Gene	p-value	Statistical method	Gene	p-value	Statistical method
Il6rα	0.689	ANOVA	Scd1	0.428	ANOVA
Il10	0.160	ANOVA	**Slc2a2**	**0.277**	Kruska-Wallis
IU group	**0.035**	Dunnett t (2 sided)	IU group	0.211	Mann-Whitney U Test
LA group	0.172	Dunnett t (2 sided)	LA group	0.211	Mann-Whitney U Test
IU+LA group	0.364	Dunnett t (2 sided)	IU+LA group	**0.040**	Mann-Whitney U Test
WL group	0.665	Dunnett t (2 sided)	Slc2a4	0.482	ANOVA
AD group	0.389	Dunnett t (2 sided)	Socs3	0.348	Kruska-Wallis
Il33	0.121	ANOVA	Sod1	0.903	ANOVA
Insr	**0.083**	ANOVA	Sod2	0.457	ANOVA
IU	**0.097**	Dunnett t (2 sided)	Sod3	0.737	Kruska-Wallis
LA	0.160	Dunnett t (2 sided)	Srebf1	0.510	ANOVA
IU+LA	**0.103**	Dunnett t (2 sided)	Tnfα	0.378	Kruska-Wallis
WL	0.997	Dunnett t (2 sided)	**Tnfrsf1a**	**0.093**	Kruska-Wallis
AD	0.337	Dunnett t (2 sided)	IU group	0.156	Mann-Whitney U Test
Irs1	0.359	Kruska-Wallis	LA group	0.905	Mann-Whitney U Test
Lepr	0.588	Kruska-Wallis	IU+LA group	**0.063**	Mann-Whitney U Test
Lipe	0.502	ANOVA	WL group	0.604	Mann-Whitney U Test
Lpin1	0.303	ANOVA	AD group	0.131	Mann-Whitney U Test
Mlxip	0.282	ANOVA	Ulk1	0.794	Kruska-Wallis